

**EFFICIENT ELECTRON ACCELERATION BY SHORT
PULSE LASER**

Thesis Submitted for the Award of the Degree of

DOCTOR OF PHILOSOPHY

in

Physics

By

Ashok Kumar Pramanik

Registration Number: 41900224

Supervised By

Dr. Jyoti Rajput (13751)

Physics (Associate Professor)

Department of Physics, Lovely Professional University



LOVELY PROFESSIONAL UNIVERSITY, PUNJAB

2024

This thesis is dedicated to my

Parents, wife, son, and my friends

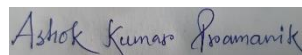
For their endless love...

DECLARATION BY THE CANDIDATE

I, Ashok Kumar Pramanik, hereby declare that the work done in the Ph.D. thesis entitled, “*Efficient electron acceleration by short pulse laser*” submitted to Lovely Professional University, Phagwara, Punjab, India by me in partial fulfilment of the requirements for the award of the degree of Doctor of Philosophy in Physics. To the best of my knowledge, no part of the thesis has been submitted for the award of any other degree by anybody in any other University/ Institution.

Place: Phagwara, Punjab, India

Date: 8/6/2023



Reg. No. - 41900224

Department of Physics

School of Chemical Engineering and Physical Sciences

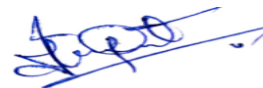
Lovely Professional University, Phagwara, Punjab

CERTIFICATE OF THE SUPERVISOR

This is to certify that the thesis entitled “**Efficient electron acceleration by short pulse laser**” submitted to the School of Chemical Engineering and Physical Sciences, Lovely Professional University, Phagwara, Punjab, India in requirement of partial fulfillment for the award of the degree of Doctor of Philosophy in Physics is a record of research work carried out by Mr. Ashok Kumar Pramanik under my supervision and guidance.

All help received from various sources have been duly acknowledged. No part of this thesis has been submitted elsewhere for award of any other degree.

Place: Phagwara, Punjab, India



Date: 8/6/2023

Associate Professor

Lovely Professional University

Phagwara, Punjab, India

ABSTRACT

The major objective of this thesis work is to present the theoretical and analytical study of short pulse laser interaction with electron in vacuum and plasma relevant to the particle acceleration. This field has a versatile application in not only Physics but also in Chemistry, Biology, and many other branches of Science. My intention is to enhance electrons energy in the order of GeV. For this purpose, I have chosen different laser envelope like: Sin^4 , Trapezoidal, Hermite-Cosh-Gaussian (HChG), Cos^2 . Out of two injection techniques: axial injection and sideways injection, I have considered axial injection throughout this research work. I have taken Newton-Lorentz equations of motion for analytical and numerical calculation of electron in the field of laser. In this thesis, the electron acceleration is analytically and numerically studied using a “Hermite-Cosh-Gaussian” shaped temporal profile for the first time.

Another way to increase electrons energy is by employing frequency chirp. It destroys symmetry in the laser pulse, as a result an apparently-static electric field is generated, which increases the drift velocity of electron and transverse momentum of electron. As a whole process, electron enhances up to higher energy and maintains the equal energy for larger time interval and path. After discovery of the Chirped Pulse Amplification technique in 1985 by two Nobel Laureates Gérard Mourou and Donna Strickland (2018) a dramatic change has been noticed in this research area. A little variation in chirp parameter very much affects the result of the process significantly, which has been reflected in this thesis.

Electron is accelerated with higher energies by the application of external magnetic field till betatron resonance is saturated. Also, it increases the $\mathbf{v} \times \mathbf{B}$ part of Newton-Lorentz force which results over all energy gain. This is the special feature of axial magnetic field.

In one part of my thesis, I have employed plasma ion channel on electron acceleration. Plasma ion channel produces an electrostatic field which captures the electron and not to escape from the interaction region and maintain betatron resonance. As a result, energy gain is much greater in plasma ion channel than in vacuum by employing same laser intensity. It is shown that for suitable choice of parameters, the scheme results in efficient acceleration of electron.

In the second part of my thesis, frequency chirp and axial magnetic field with prescribed laser envelopes jointly have been introduced to enhance electrons energy. I have noticed a significant results in the contest of electron acceleration which has been reflected in my thesis. I have also studied the polarization effect on electron acceleration. In a paper I have compared between LP and CP HChG laser pulse in vacuum. In case of CP laser pulse, electron enhances more energy gain than LP because CP laser is more efficient to energy transfer from laser pulse to electron. HChG laser pulse has two key parameters which control better trapping and self-focusing. The two parameters are decentered parameter (b) and hermite order (s). Better trapping has been investigated in case of radially polarized (RP) laser pulse which has been reflected in one of my paper.

GRAPHICAL ABSTRACT

Title of Graphical abstract: Efficient electron acceleration in vacuum and plasma.

Authors name: Ashok Kumar Pramanik, Dr. Jyoti Rajput

Name of Scholar: Ashok Kumar Pramanik Registration Number: 41900224

Program Name: PhD Physics Name/ UID of Supervisor: 13751

Name /UID of Co-supervisor (Wherever applicable):

Summary of graphical abstract: Laser driven electron acceleration has been analyzed theoretically in vacuum and plasma medium on the basis of “Capture and Acceleration Scenario” (CAS). The above mentioned acceleration follows two routes: 1. Direct Laser Acceleration (DLA) 2. Wakefield Acceleration. Throughout my research journey I have followed DLA route, I have concentrated myself to enhance electrons’ energy in the order of GeV. For that purpose I have taken different necessary steps which will fulfill my aim:

- I have employed different types of laser profile which includes: Trapezoidal laser pulse, Sin^4 laser pulse, Cos^2 laser pulse, Hermite-Cosh-Gaussian (HChG) laser pulse.
- I have employed different types of polarized radiation such as: Linearly Polarized (LP), Circularly Polarized (CP) and Radially Polarized (RP) radiation.
- Frequency chirp (linear) has been applied in my various papers.
- External Magnetic Field (Axial Magnetic Field) also has been used in enhancing electron acceleration in my papers.
- Vacuum as well as Ion Channel have been used as a medium of electron acceleration in my papers.

Various graphs including calibration graph has been analyzed in the contest of electron’s energy gain. Throughout my research journey I have successfully observed GeV order

energy gain. My study is very much effective for future research, producing X-Rays, radiation therapy and diminish the cost of radiation treatment.

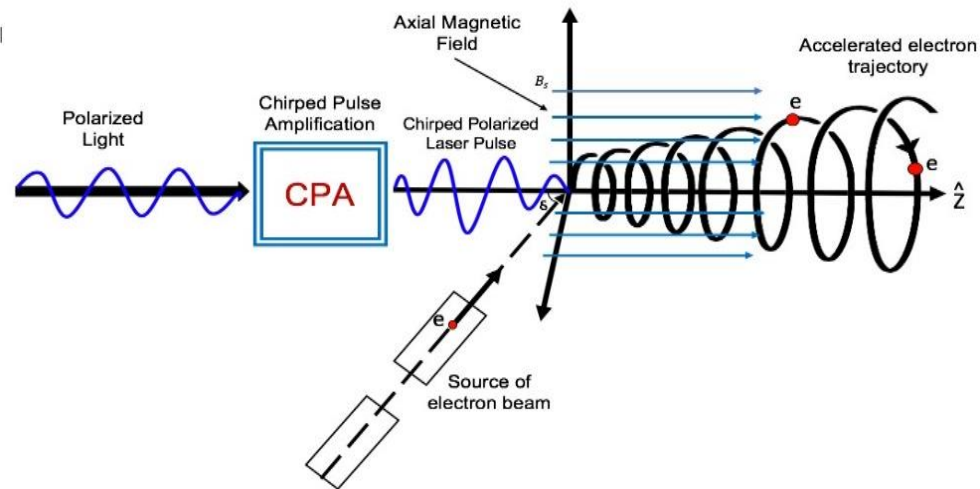


Figure 1: A schematic diagram showing electron acceleration by a Polarized chirped laser pulse in the presence of axial magnetic field in vacuum.

Novelty of work: We have noticed GeV order energy gain each of my every papers. This high energy is suitable for hard X-Ray generation. Also this GeV order energy may be used for radiation treatment for tumor/cancer cell which are situated deeper portion of our body.

Name and signature of all author: Ashok Kumar Pramanik

DR. Jyoti Rajput

ACKNOWLEDGEMENT

I would like to express my special and sincere gratitude to the University for letting me fulfill my dream of being a research scholar here. I would also like to thank the Physics department under School of Chemical Engineering and Physical Sciences, Lovely Professional University, Phagwara, Punjab.

I would like to express my deep and sincere gratitude to my research supervisor, Dr. Jyoti Rajput, M.Sc., M.Phil., Ph.D., Associate Professor, Department of Physics, School of Chemical Engineering and Physical Sciences, Lovely Professional University, Phagwara, Punjab for giving me this opportunity to do research and providing invaluable guidance, patience, motivation throughout the research. She has taught me the methodology to carry out the research and to present the research work as clearly as possible. Her dynamism, vision, and motivation has deeply inspired me. It was a great privilege and honor to work and study under her guidance.

I want to convey my deepest thanks to Dr. Niti Kant, Allahabad University and Dr. Harjit Singh Ghotra, Lovely Professional University, Co-authors of my research papers, for their technical support and guidance in each and every time. I'm lucky due to their friendly behavior.

I am also thankful to Dr. Nareshpal Singh Saini (Guru Nanak Dev University, Amritsar, India), expert of my SOTA; Dr. Mukesh Kumar (Lovely Professional University, Phagwara, Punjab, India), ETP panel member; Dr. Ajeet Kumar Srivastava (Lovely Professional University, Phagwara, Punjab, India), ETP panel member; and others panel members for their technical support.

I am also extremely grateful to my family: my parents for giving birth to me, my wife for full support, my son for encouraging and helping me from the beginning till the end of my research work.

TABLE OF CONTENTS

Subject	Page No.
Title Page	
Dedication	i
Declaration	ii
Certificate	iii
Abstract	iv-v
Graphical Abstract	vi-vii
Acknowledgement	viii
Table of Contents	ix-xiii
List of Figures	xiv-xviii
List of Tables	xix
List of Abbreviations	xx
List of Symbols	xxi-xxii

CHAPTER 1: INTRODUCTION	
Background	1-4
1.1 Electromagnetic waves	5
1.1.1 Characteristics	5
1.1.2 Mathematical representation	6
1.1.3 Electromagnetic spectrum	6
1.2 Maxwell's equations	7
1.3 Constitutive relation	7
1.4 Lorentz force	8

1.5 LASER	9
1.5.1 Properties	9
1.5.2 Working principle	9-10
1.5.3 Types of laser	10
1.5.4 Uses of laser	10
1.6 Beam Waist parameter and Rayleigh length	11
1.7 Ponderomotive force	12
1.8 Polarization	13
1.9 Chirped pulse amplification (CPA)	14-15
1.10 External Magnetic field	16
1.11 Plasma	17
1.11.1 Condition to be a plasma	17-18
1.11.2 Types of Plasma	18
1.11.3 Propagation of electromagnetic waves through plasma	18
1.11.4 How electron accelerates through plasma	19
1.11.5 Important phenomena when electron accelerates through plasma	19-23
1.12 Electron acceleration through plasma channel	23-24
1.13 Direct Laser Acceleration (DLA)	25-26
1.14 Importance of electron acceleration	27
CHAPTER 2 : LITERATURE REVIEW	28-36

Research Hypothesis	37
Objectives	38
Research Design/Methodology	39

CHAPTER 3: EFFICIENT ELECTRON ACCELERATION BY USING HERMITE-COSH-GAUSSIAN LASER BEAM IN VACUUM	
3.1 Introduction	40-43
3.1.1 Study of electron acceleration Phenomenon by Hermite Cosh Gaussian Laser Beam	
3.1.1.1. Electron dynamics	43-44
3.1.1.2 Result and Discussion	45-49
3.1.1.3 Conclusion	49
3.1.2 Effect of polarization on Hermite Cosh Gaussian laser beam	
3.1.2.1 Electron dynamics	50-51
3.1.2.2 Observation and Discussion	51-55
3.1.2.3 Conclusion	56
3.1.3 Combined influence of linear chirp and axial magnetic field	
3.1.3.1 Electron dynamics	57-59
3.1.3.2 Result and Discussion	59-66
3.1.3.3 Conclusion	67

CHAPTER 4 : STUDY OF ELECTRON ACCELERATION PHENOMENA BY EMPLOYING DIFFERENT LASER PULSE ENVELOPE IN VACUUM	
4.1 Introduction	68-70
4.1.1 Comparison of different laser pulse envelopes with frequency chirp	
4.1.1.1 Electromagnetic fields and electron dynamics	70-72
4.1.1.2 Results and discussion	72-76
4.1.1.3 Conclusion	77
4.1.2 Combined effect of frequency chirp and axial magnetic by trapezoidal laser pulse envelope	
4.1.2.1 Electron dynamics	77-79
4.1.2.2 Result and Discussion	79-83
4.1.2.3 Conclusion	83
4.1.3 Influence of frequency chirp and axial magnetic field by employing Cos^2 laser pulse envelope	
4.1.3.1 Electron Dynamics	84-85
4.1.3.2 Results and discussion	86-91
4.1.3.3 Conclusion	91

CHAPTER 5 : EFFICIENT ELECTRON ACCELERATION IN AN ION CHANNEL BY RADIALY POLARIZED HERMITE-COSH-GAUSSIAN LASER BEAM	
5.1 Introduction	92-94
5.1.1 Effect of intensity parameter on RP HChG laser beam	
5.1.1.1 Electromagnetic fields and electron dynamics	94-95
5.1.1.2 Result and discussion	96-97
5.1.1.3 Conclusion	97
5.1.2 The combined effect of RP-HChG laser beam and ion channel on electron acceleration	
5.1.2.1 Governing equations	98-100
5.1.2.2 Numerical calculation and discussions	100-106
5.1.2.3 Conclusion	107

CHAPTER 6: SUMMARY AND FUTURE SCOPE	108-112
--	---------

REFERENCES	113-119
PUBLICATIONS	120
COMMUNICATIONS	121
LIST OF PUBLISHED WORK	122-126
CONFERENCE CERTIFICATES	127-128
BIO-DATA	129-130

LIST OF FIGURES

Figure 1: A schematic diagram showing electron acceleration by a Polarized chirped laser pulse in the presence of axial magnetic field in vacuum.

Figure 2: EM Wave

Figure 3: E M Spectrum

Figure 4: Showing action of laser

Figure 5: Diagrammatic representation of beam waist parameter

Figure 6: Ponderomotive Force

Figure 7: Polarization diagram

Figure 8: CPA Concept

Figure 9: Up and Down frequency chirp

Figure 10: Plasma

Figure 11: Excitation of plasma oscillations by intense laser pulse and laser wakefield acceleration.

Figure 12: PBWA

Figure 13: SM-LWFA

Figure 14: A schematic diagram of laser wakefield acceleration in bubble regime.

Figure 15: Schematic diagram of electron acceleration in plasma ion channel

Figure 3.1. Electron's energy gain with the normalized time for different values of $r'_0 = 50, 75, 100,$ and 125 at $a_0 = 10, b = 2.0$ and $s = 1$.

Figure 3.2. Electron's energy gain with normalized time for $b = 0.5, 1.0, 1.5,$ and 2.0 for $a_0 = 20, r'_0 = 100$ and $s = 1$.

Figure 3.3. Electron's energy gain with normalized time for $a_0 = 10, 15, 20,$ and 25 for $r'_0 = 68, 80, 103, 118, b = 1$ and $s = 1$.

Figure 3.4. Electron's energy gain with normalized time for specific values of the laser intensity parameter $a_0 = 10, 15, 20, 25$ for $r'_0 = 10, b = 1$ and $s = 3$.

Figure 3.5. Electron's energy gain with laser beam waist width for $a_0 = 10, 15, 20, 25, b = 1$ and $s = 1$ & 3 .

Figure 3.6 represents the changing of maximum energy gain (γ_m) with intensity parameter (a_0) for $b=1, s=1, r_0 = 50$ for CP and LP HChG laser pulse. $v_z = 0$ for fig. 3.6 (a) and $v_z = 0.4$ for fig.3.6 (b).

Figure 3.7 displays the changing of energy gain (γ_m) with normalized time (t') for $a_0 = 5, 10, 15$ for figure 3.7 (a), 3.7 (b) and 3.7 (c) respectively and $b = 1, s = 1, r_0 = 50$ for CP and LP HChG laser pulse. $v_z = 0, 0.5$.

Figure 3.8. The variation of maximum energy gain (γ_m) with decentered parameter (b) for $a_0 = 15, s = 1, r_0 = 100$ for CP and LP HChG laser pulse. $v_z = 0$ for fig. 3.8 (a) and $v_z = 0.4$ for fig. 3.8 (b).

Fig. 3.9. displays the variation between maximum energy gain (γ_m) with different values of decentered parameter (b) at fixed $a_0 = 15, r_0 = 50, s = 1$ and $v_z = 0.5$ for LP HChG laser pulse.

Fig. 3.10 depicts the variation between maximum energy gain (γ_m) with different values of decentered parameter (b) at fixed $a_0 = 15, r_0 = 50, s = 1$ and $v_z = 0.5$ for CP HChG laser pulse.

Figure 3.11 (a) shows the variation of electron's energy gain (γ) with normalized time (t') at $a_0 = 10, r'_0 = 100, b = 1.5$ and $s = 1$ for without chirp, with chirp and chirp with axial magnetic field.

Figure 3.11 (b) shows the variation of electron's energy gain (γ) with normalized time (t') at $a_0 = 15, r'_0 = 75, b = 2$ and $s = 1$ for without chirp, with chirp and chirp with axial magnetic field.

Figure 3.12 (a) shows the variation of maximum energy gain (γ_m) with different values of decentered parameter (b) at $a_0 = 10, r'_0 = 50$ and $s = 1$ for without chirp, with chirp and chirp with axial magnetic field.

Figure 3.12 (b) shows the variation of maximum energy gain (γ_m) with different values of decentered parameter (b) at $a_0 = 15, r'_0 = 100$ and $s = 1$ for without chirp, with chirp and chirp with axial magnetic field.

Figure 3.12 (c) shows the variation of maximum energy gain (γ_m) with different values of decentered parameter (b) at $a_0 = 20, r'_0 = 75$ and $s = 1$ for without chirp, with chirp and chirp with axial magnetic field.

Figure 3.13 shows the variation of maximum energy gain (γ_m) with decentered parameter (b) and linear chirp parameter (α) with decentered parameter (b) at fixed $a_0 = 15, r'_0 = 75$ and $s = 1$.

Figure 3.14 shows the variation of maximum energy gain (γ_m) with decentered parameter (b) and normalized axial magnetic field (b_0) with decentered parameter (b) at $a_0 = 10, r'_0 = 75$ and $s = 1$.

Figure 3.15 shows the variation of linear chirp parameter (α) with decentered parameter (b) and normalized axial magnetic field (b_0) with decentered parameter (b) at fixed maximum energy gain $\gamma_m = 3\text{GeV}$, $a_0 = 10, r'_0 = 100$ and $s = 1$.

Figure 4.1. Maximum energy gain with different phase for without chirp and with chirp at intensity parameter $a_0 = 3$, for trapezoidal laser pulse envelope.

Figure 4.2. Maximum energy gain with different chirp parameter (b) at intensity parameter ($a_0 = 3$), for trapezoidal laser pulse envelope.

Figure 4.3. Maximum energy gain with different chirp parameter (b) at intensity parameter $a_0 = 3$, for Sin^4 laser pulse envelope.

Figure 4.4. Maximum energy gain with different phases for without chirp at intensity parameter $a_0 = 3$ for Sin^4 laser pulse envelope.

Figure 4.5. Maximum energy gain with different phases with chirp at intensity parameter $a_0 = 3$ for Sin^4 laser pulse envelope.

Figure 4.6 (a). Maximum energy gain with different chirp parameter (b) at intensity parameter $a_0 = 3$ for trapezoidal laser pulse envelope.

Figure 4.6 (b). Maximum energy gain with normalized time at intensity parameter $a_0 = 3$, chirp parameter $\alpha = -0.02$ for trapezoidal laser pulse envelope.

Figure 4.7. Maximum energy gain with different phases for with chirp and without chirp at intensity parameter $a_0 = 3$ for trapezoidal laser pulse envelope.

Fig. 4.8. Maximum energy gain with normalized magnetic field (b_0) at intensity parameter $a_0 = 3$ and chirp parameter ($\alpha = -0.02$) for trapezoidal laser pulse envelope.

Figure 4.9. Maximum energy gain with normalized time at intensity parameter $a_0 = 3$, chirp parameter $\alpha = -0.02$, normalized magnetic field $b_0 = 0.0008$ for trapezoidal laser pulse envelope.

Figure 4.10. Maximum energy gain with different phases 4.10 (a) with chirp ($\alpha = -0.02$), 4.10 (b) without chirp at intensity parameter $a_0 = 3, 5, \text{ and } 7$ for cos^2 laser pulse envelope.

Figure 4.11. Maximum energy gain with normalized time at intensity parameter $a_0 = 3, 5, \text{ and } 7$ with chirp parameter $\alpha = -0.02$ for cos^2 laser pulse envelope.

Figure 4.12 Maximum energy gain with normalized magnetic field (b_0) at intensity parameter $a_0 = 3$ in 8.3(a) and $a_0 = 5, 7$ in 4.12 (b) with optimum chirp parameter ($\alpha = -0.02$) for cos^2 laser pulse envelope.

Figure 4.13 Energy gain with normalized time at intensity parameter $a_0 = 3, 5, \text{ and } 7$ chirp parameter $\alpha = -0.02$, normalized magnetic field $b_0 = 0.0008$ for trapezoidal laser

pulse envelope.

Figure 4.14 shows the variation of normalized magnetic field (b_0) and maximum energy gain (γ_m) with respect to intensity parameter (a_0).

Figure 5.1: Energy gain vs normalized time for $b = 1.0$ for $a_0 = 5, 7, \text{ and } 10$, $r'_0 = 20$, $s = 1$, ion density $n_i = 0.00001$.

Figure 5.2. Maximum energy gain with ion density at fixed value of laser spot size $r'_0 = 20$, intensity parameter $a_0 = 10$, decentered parameter $b = 1$, hermite order $s = 1$.

Figure 5.2 (a) is for $n_i = 0, 0.0001, 0.0003, 0.0006, 0.0008$ and **Figure 5.2 (b)** is for $n_i = 0, 0.00001, 0.00003, 0.00006, 0.00008$ respectively.

Figure 5.3. Maximum energy gain with ion density by varying laser spot size $r'_0 = 10, 20, 30, \text{ and } 40$ for decentered parameter $b = 1$, hermite order $s = 1$, and intensity parameter $a_0 = 10$.

Figure 5.4. Maximum energy gain with decentered parameter $b = 0.5, 1.0, 1.5, 2.0, 2.5, \text{ and } 3.0$ for $a_0 = 10$, $r'_0 = 20$, $s = 1$, and $n_i = 0.00001$.

Figure 5.5. Maximum energy gain with ion density by varying initial velocity of electron at $v_r[0] = 0.3c$, $v_z[0] = 0.8c$ (black line) and $v_r[0] = 0.5c$, $v_z[0] = 0.85c$ (red line) at fixed laser spot size $r'_0 = 30$, decentered parameter $b = 1$, hermite order $s = 1$, and intensity parameter $a_0 = 12$.

Figure 5.6. Electron's energy gain with normalized time for ion density $n_i = 0, 0.00001, 0.00003, 0.00006, \text{ and } 0.00009$ at specific values of $b = 1.0$, $a_0 = 5$, $r'_0 = 40$, $s = 1$, $v_r[0] = 0.5c$, and $v_z[0] = 0.8c$.

Figure 5.7 Electron's energy gain with normalized time for specific values of the decentered parameter $b = 1.0$ for $a_0 = 5, 7, \text{ and } 10$, $r'_0 = 20$, $s = 1$, ion density $n_i = 0.00001$.

LIST OF TABLES

Table 3.1. provides the value of maximum energy gain (γ_m) : fig. 7.2(a) is for $a_0 = 10, r'_0 = 50, s = 1$; fig. 7.2(b) is for $a_0 = 15, r'_0 = 100$ and $s = 1$; fig. 7.2(c) is for $a_0 = 20, r'_0 = 75$ and $s = 1$ for without chirp, with chirp and chirp with axial magnetic field respectively.

Table 3.2. is showing the result of optimum axial magnetic field (b_0), maximum energy gain (γ_m) correspond to decentered parameter $b = 0.5, 1, 1.5$ and 2 respectively.

LIST OF ABBREVIATIONS

- ❖ CAS- CAPTURE AND ACCELERATION SCENARIO
- ❖ LP- LINEARLY POLARISED
- ❖ CP- CIRCULARLY POLARISED
- ❖ RP- RADIALLY POLARISED
- ❖ DLA- DIRECT LASER ACCELERATION
- ❖ LWFA- LASER WAKEFIELD ACCELERATION
- ❖ PBWA- PLASMA BEAT WAVE ACCELERATION
- ❖ SM-LWFA- SELF MODULATED LASER WAKEFIELD ACCELERATION
- ❖ CPA- CHIRPED PULSE AMPLIFICATION
- ❖ EM WAVE- ELECTROMAGNETIC WAVE
- ❖ GeV- GIGA ELECTRON VOLT
- ❖ MeV- MEGA ELECTRON VOLT
- ❖ fs- FEMTO SECOND
- ❖ ps- PICO SECOND
- ❖ PW- PETA WATT
- ❖ TW- TERA WATT
- ❖ FRS- FORWARD RAMAN SCATTERING
- ❖ HG-HERMITE GAUSSIAN
- ❖ TPS-TRAPEZOIDAL PULSE SHAPE
- ❖ GPS-GAUSSIAN PULSE SHAPE
- ❖ HSPS-HALF SINEWAVE PULSE SHAPE
- ❖ HChG- HERMITE-COSH-GAUSSIAN
- ❖ KG-KILLOGAUGE
- ❖ MG-MEGAGAUGE

LIST OF SYMBOLS

- E- ELECTRIC FIELD
- B- MAGNETIC FIELD
- V- VELOCITY
- P- MOMENTUM
- F- FORCE
- e- ELECTRONIC CHARGE
- m – MASS OF ELECTRON
- c- SPEED OF LIGHT IN VACUUM
- t- TIME
- I- INTENSITY OF LASER
- λ - WAVELENGTH OF LASER LIGHT
- ω - ANGULAR FREQUENCY OF LASER
- k- WAVE VECTOR
- ϕ - PHASE
- μ_0 -PERMEABILITY OF FREE SPACE
- ϵ_0 -PERMITTIVITY OF FREE SPACE
- $\vec{\nabla}$ -DELTA OPERATOR
- q- CHARGE
- W- WATT
- w_0 -BEAM WAIST PARAMETER
- Z_R -RAYLEIGH LENGTH
- F_p -PONDEROMOTIVE FORCE
- λ_D -DEBYE LENGTH
- K_B -BOLTZMAN CONSTANT
- T-ABSOLUTE TEMPERATURE
- n_0 -PLASMA ELECTRON DENSITY
- ω_0 -FREQUENCY OF EM WAVE
- ω_p -PLASMA FREQUENCY

- P_C - CRITICAL POWER OF PLASMA
- λ_p -PLASMA WAVELENGTH
- C-COULOMB
- n C-NANOCOULOMB
- α -LINEAR CHIRP PARAMETER
- a_0 -NORMALIZED INTENSITY PARAMETER
- b_0 -NORMALIZED MAGNETIC FIELD PARAMETER
- b-DECENTERED PARAMETER
- s-HERMITE ORDER
- r_0 -LASER SPOT SIZE

CHAPTER 1

Introduction

Background

The demand for accelerators in medical science and industry [1-3], fundamental forces research, and tumor therapy [4-5] is rapidly expanding. A large number of researchers and scientists are being drawn to this sector in order to meet the need for accelerators. Because the electron is the lightest subatomic particle, researchers find electron acceleration incredibly appealing and exciting for acceleration up to higher energies. It is also highly beneficial to study the evolution of the world, modern cancer therapy, modern X-ray, and security systems, among other things. There are mainly two types of particle accelerator namely:

- [1] Electrostatic Accelerator
- [2] Electromagnetic Accelerator

Former class uses static electric field to accelerate particles. The most common type of such accelerators is the Van de Graff generator and Cockcroft generator. Later class of accelerators use oscillating electromagnetic field to accelerate particles. All modern accelerators such as Cyclotron (for the acceleration of charge particle and ions like protons, deuterons or α - particles) and Betatron (for the acceleration of electrons) will come in this group. The electromagnetic particle accelerator are of two types, depending upon the trajectory of the charged particles. They are:

- [1] Linear accelerator
- [2] Circular accelerator

Linear particle accelerator, commonly known as “LINAC”, accelerate particles along the straight line. Microwave technology is used in linear accelerator to accelerate electrons. After that it allows these electrons to stumble a metal target to produce high energy X-ray. In that case, charged particles follow straight beam line. Such types are used

for fixed target experiments. In circular accelerator, electromagnetic waves and, or electric field are used to accelerate charged particles. It can be used for both colliding beam and fixed target experiments.

According to the International Atomic Energy Agency (IAEA), there are near about 30000 particle accelerators in the world till date. At “CERN”, the largest particle accelerator is situated, which is the Large Electron-Positron (LEP) collider. It was a circular collider of 27 Kilometer circumference built in a tunnel roughly 100 meter underground passing through Switzerland and France in 1989 [www.epa.gov]. LEP hits electron with positron and touched the energy up to 209 GeV. Knowledge of elementary particle takes part to describe different branches of Physics. After 10 years from inauguration, CERN reached much higher energies, colliding protons with antiprotons up to 450 GeV which is called Super Proton Cyclotron. In 2009, LHC generated to 1.18 TeV Proton beams. By achieving this landmark, it got the title of “World's highest energy particle accelerator” [https://home.cern]. For the betterment of Particle Physics, the demand of high energy particle beam is required. To grow beam energy proportionally, the size of the accelerator kept increasing which increases the cost of the accelerator too. Though the circular accelerator decreases the size as well as cost but, it had some limitations concerning Synchrotron radiation loses. The radio frequency cavity accelerator has some limitation with working on accelerating field. The accelerating field is confined up to 100 MeV/m. Though the quality of the beam generating from conventional accelerator is merciful, but the size and manufacturing cost of the conventional accelerator are a big problem. Also they are unable to register high accelerating gradients. These are the major challenges to the scientist to conventional accelerators. These limitations would be removed when laser play a key role on accelerator.

There are two fundamental mechanisms of subatomic particle acceleration:

- [1] Via the excitation of a plasma wave (Wakefield) [6,7,8]
- [2] Direct laser acceleration (DLA) [9,10]

Among the sub atomic particles, electron has the mass comparatively less than others. That's why electron acceleration is very much attractive and fascinating than others. Throughout this thesis, I will discuss on “Efficient electron acceleration by short pulse laser” which is my thesis’ topic. In this mechanism, the core of the laser propagation path captures and accelerates electron to relativistic energy in the order of GeV with acceleration gradient GeV/m [11]. Such process of electron acceleration technique is regarded as “Capture and Acceleration Scenario” (CAS). Capture and acceleration scenario technique mainly depends on laser profiles like:

- Laser intensity
- Laser spot size
- Laser pulse duration
- Impact Parameter
- Injection angle [12]
- Beam Waist parameter.
- Rayleigh length etc.

There is lot of research in this field after the discovery of the Noble Technique Chirped Pulse Amplification (CPA) in 1985 [13]. CPA technique can produce peak focused intensity in the order of ($10^{21} - 10^{22} \text{ W.cm}^{-2}$) corresponding to the electric field $10^{12} \text{ V.cm}^{-1}$. So, such high power intensity and large accelerating gradients resolve all the limitations of traditional acceleration such as: size, cost, and standby of traditional accelerator which can accelerate particles to relativistic energy. In 1961, Simoda [14] was the pioneer to propose the use of laser for accelerating particle. After that, laser has been used to study charged particle acceleration in plasma, gases and vacuum [10, 15-21].

About 44 years ago Tajima & Dawson were the first acceleration scientist who introduced plasma as a medium for laser driven and electron acceleration in 1979 [10]. They proposed that a nonlinear force termed as ponderomotive force associated with laser pulse ($\tau \approx \lambda_p$) excites a plasma wave (Wakefield) that propagates with \approx velocity of light in free space (c). After that electron acceleration scenario has been investigated

theoretically [22-26] in vacuum medium for a long time and then experimentally [18, 27-29]. Vacuum medium, has some superiority over plasma [18, 27, 30-39] like: the problem inherent (instabilities) [40] in the time of laser-plasma interaction are vanished in vacuum, the peak energy attained by electron is a function of initial energy of electron in case of vacuum medium and it follows directly proportional relationship and also pre-accelerated electron injection technique is easy, though dephasing problem arises in vacuum which negatively impacts on energy gain. In 1988 Hora [32] was the pioneer of vacuum acceleration by nonlinear mechanism. The first experimental verification of vacuum acceleration has been performed by Malka et al., in 1997 [18]. For their setup, they employed 10^{19} Wcm^{-2} , 300fs, linearly polarized intense laser pulse. They noted MeV energies.

Some keywords of my thesis are discussed below.

1.1 Electromagnetic waves:

When both electric and magnetic field comes into contact, an electromagnetic waves which are the solution of Maxwell's equations, are produced. Maxwell's equations are also the fundamental equations of Electrodynamics like as Newton's laws of motion in Classical Physics. A subject which deals with electrostatics and magnetostatics is called electromagnetic theory. This theory has been developed by Maxwell.

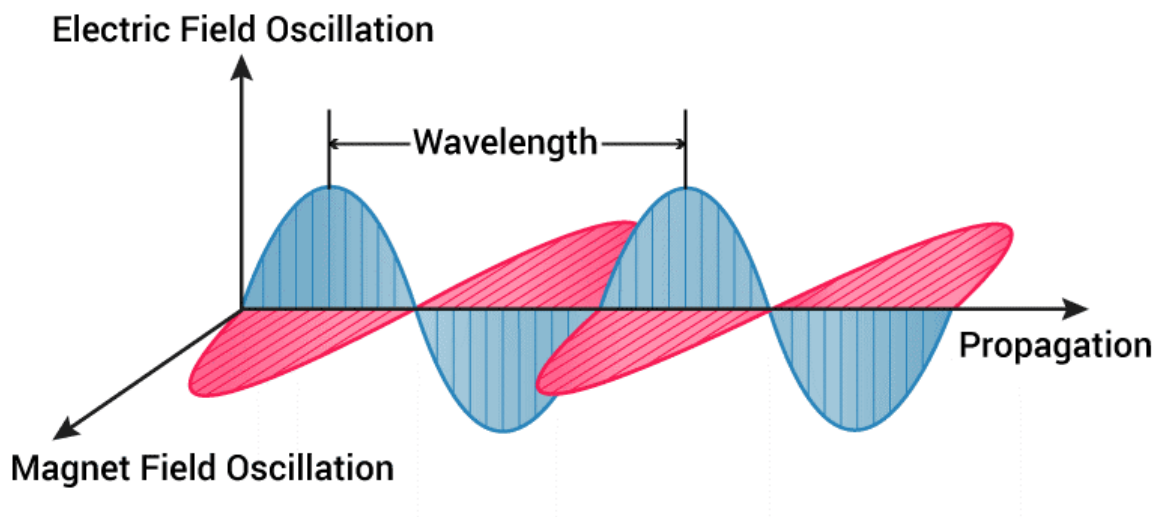


Figure 2: EM Wave

1.1.1 Characteristics:

1.1.1.1 A charged particle can produce an electric field.

1.1.1.2 A moving charged particle can produce a magnetic field.

1.1.1.3 Electromagnetic waves travel with $c = 3 \times 10^8 \text{ms}^{-1}$. If angular frequency of charged particle is ω , the wavelength λ of this wave is given by: $\lambda = \frac{c}{\omega}$

1.1.2 Mathematical representation

A plane electromagnetic (EM) wave in the “z-direction” is represented as

$$\vec{E}(z, t) = E_0 \sin(\omega t - kz + \phi) \hat{x}$$

$$\vec{B}(z, t) = \frac{\vec{k} \times \vec{E}}{\omega}$$

Where, the wave number $k = \frac{\omega}{c}$, ϕ represents the absolute phase.

The EM wave propagates along $\vec{E} \times \vec{B}$ direction.

The energy per unit time transfer by the electromagnetic wave can be described by the Poynting vector ($\vec{E} \times \vec{H}$) its dimension is $[MT^{-3}]$. Intensity of electromagnetic wave $I = \frac{1}{2} c \epsilon_0 E_0^2 = \frac{1}{2} \frac{c}{\mu_0} B_0^2$.

1.1.3 Electromagnetic spectrum

In the order of increasing wavelength

γ ray > x – ray > UV ray > Visible ray > Microwave > FM, AM Radiowave
> Long Radiowave

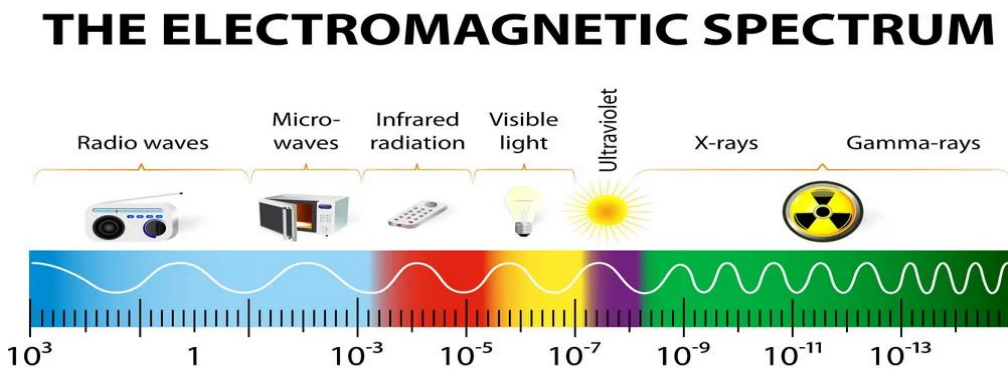


Figure 3. EM Spectrum

1.2 Maxwell's equations:

To describe electromagnetic waves, Maxwell formulated four equations known as Maxwell's equations. These are not new, but mathematical observation of existing laws and observations of electromagnetics and magnetostatics.

$$1^{\text{st}} \text{ equation: } \vec{\nabla} \cdot \vec{E} = \frac{\rho}{\epsilon_0}$$

It is nothing but differential form of Gauss' theorem in electrostatic.

$$2^{\text{nd}} \text{ equation: } \vec{\nabla} \cdot \vec{B} = 0$$

It is nothing but different differential form of Gauss' theorem in magnetostatics.

$$3^{\text{rd}} \text{ equation } \vec{\nabla} \times \vec{E} = -\frac{\partial \vec{B}}{\partial t}$$

It is nothing but differential form of Faraday's law in electromagnetic induction.

$$4^{\text{th}} \text{ equation } \vec{\nabla} \times \vec{B} = \mu_0 \vec{J} + \frac{1}{c^2} \frac{\partial \vec{E}}{\partial t}$$

It is the modified form of Ampere's law. Maxwell equation for electromagnetism have been called second grade unification in Physics where the first one has been realized by Sir Isaac Newton.

1.3 Constitutive relation:

The following sets of equations are known as constitutive relation.

- | | | |
|-----|------------------------------|---|
| [1] | $\vec{J} = \sigma \vec{E}$ | It is vector form of Ohm's Law.
σ is the conductivity of the medium |
| [2] | $\vec{D} = \epsilon \vec{E}$ | $\epsilon (= \epsilon_0 \epsilon_r)$ is the permittivity of the medium |
| [3] | $\vec{B} = \mu \vec{H}$ | $\mu (= \mu_0 \mu_r)$ is the permeability of the medium |

1.4 Lorentz force:

Electromagnetic force is known as Lorentz force due the name of the discoverer Scientist Hendrik Lorentz. In Physics, the electric Lorentz force and magnetic Lorentz force together headed by Lorentz force. A charged particle experiences a force in an EM field which is termed as Lorentz force or electromagnetic force. The expression of Lorentz force is written as:

$$\vec{F} = q\vec{E} + q(\vec{v} \times \vec{B}) . \text{ [In S.I unit]}$$

B is measured in tesla (T), E is measured in V/m.

1.5. LASER

1.5.1 Properties

Monochromatic - Laser emits radiation of single wavelength. That means laser is highly monochromatic source of light.

Directionality - The light emitted by ordinary sources like: torch, bulb, lamp etc. scatter light in any direction. But laser radiation focuses in a particular direction.

Intensity – Laser is a source of strong intense radiation.

Coherence -The phase difference between two radiations emitted by laser is either constant or zero. Laser radiation is perfectly coherent.

1.5.2 Working principle:

Let, us consider two energy levels E_1 and E_2 ($E_2 > E_1$). There happens three distinct principles which are followed by laser.

Stimulated absorption - An atom in the lower energy level E_1 absorbs a photon of energy difference $E_2 - E_1$ and after that excited to higher energy level E_2 . This is called stimulated absorption. The radiation frequency $\nu = \frac{E_2 - E_1}{h}$.

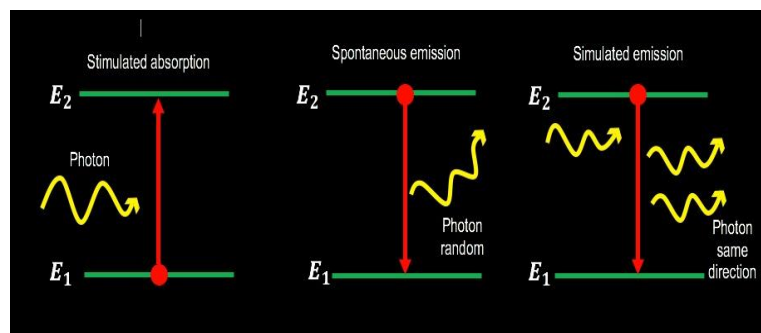


Figure 4. Showing action of laser

Stimulated emission - In this process absorbed photon stimulates atom to fall in the lower energy level. By using this process we can get coherent laser beam.

Spontaneous emission - The lifetime of atom in the higher energy level is of the order of 10^{-8} s. After spending lifetime it jumps to the lowered energy level by emitting of photon at random. We cannot control this process. This transition is known as spontaneous emission.

1.5.3 Types of lasers:

[a] Solid state laser - In this case lasing material is solid matrix. Its wavelength is 1064 nm. It works effectively up to 400 W power. Example: Nd:YAG laser.

[b] Gas laser - Here lasing material is gas or mixture of gases. In that case the wavelength of 632.8 nm and power is (5-50) MW. Example He-Ne laser, Carbon dioxide gas laser.

[c] Dye laser – In this case lasing material is a complex organic dye in liquid solution. It works more efficiently with a maximum power of 1 W at 600 nm. Example- Rhodamine 6G dye laser.

[d] Semiconductor laser - Here lasing material is 2 layers of semiconductor sandwich together. Example - Gallium-Arsenide laser.

1.5.4 Uses of laser:

[1] Laser is highly used in technical and industrial field to cut steel sheet, drill fine holes, melt and join metallic rods.

[2] In medical field Laser is used in eye surgery (Cornea grafting) and in treatment of kidney stone, cancer (Radiotherapy) and tumor.

[3] Since laser beam is very much parallel, so they are used for communication and measuring long distance.

[4] Laser is the key equipment of 'laser driven electron/proton/neutron/ion acceleration scenario'. Also there are many application of laser in different fields so laser is very much effective in our civilization.

1.6 Beam Waist parameter and Rayleigh length: The beam waist parameter [41] is the measurement of a beam size where the width of the beam is the smallest along the propagation of beam. It is denoted by w_0 . If beam width is smaller, laser field is stronger which is good for acceleration scenario.

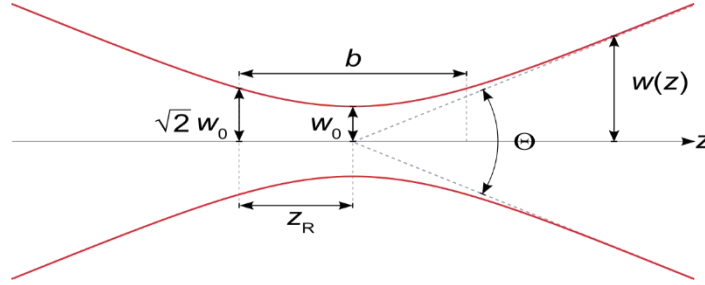


Figure 5: Diagrammatic representation of beam waist parameter

Confocal Parameter (b) = $2 \times Z_R$

$$w(z) = w_0 \sqrt{1 + \left(\frac{z}{Z_R}\right)^2} \quad \text{Where } Z_R = \text{Rayleigh Length}$$

The Rayleigh length (4) is the particular length along beam direction from the waist parameter to cross sectional area is doubled. For Gaussian beams, the Rayleigh length depends up on beam waist parameter. The expression of Rayleigh length is given below:

$$Z_R = \frac{\pi w_0^2}{\lambda}$$

where λ is the wavelength divided by the refractive index. w_0 is the beam waist parameter.

1.7 Ponderomotive force:

When a charged particle enters into a rapidly oscillating electromagnetic field, it experiences a non-linear force termed as ponderomotive force. It moves the particle towards the weaker field strength area.

FORMULA: $F_P = -\frac{e^2}{4m\omega^2} \nabla(E^2) \propto -\nabla I$

Here, e , m , ω , E , and I denote the Universal notation. The above equation signifies that a charged particle is accelerated by force F_P towards the weak field direction and oscillates with a frequency of ω .

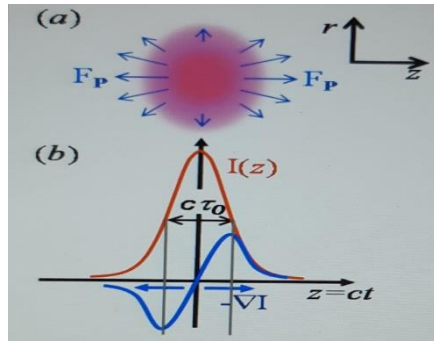


Figure 6: Ponderomotive Force

Figure: a) Laser pulse intensity distribution is shown in 2D and the associated ponderomotive force direction and magnitude is indicated with arrows, b) shows intensity profile of Gaussian function of the laser pulse (red) along the propagation axis and the associated ponderomotive force (blue). The peaks of the forward and backward ponderomotive force are separated by the pulse FWHM duration $c\tau_0$.

1.8 Polarization:

Polarization is the restriction of the vibration of light vector in a specified direction normal to the propagation of wave.

Types of Polarization:

- Linear polarization (LP)
- Circular polarization (CP)
- Elliptical polarization (EP)
- Radial polarization (RP)

In the context of electron acceleration laser field polarization plays a crucial role. Several authors have employed linearly polarized (LP) laser pulse [42-44]. In case of circular polarized (CP) laser pulse, electron can gain higher energy in comparison with other polarization pattern [45] due to axial symmetry. Radially polarized (RP) laser pulse is being utilized due to better trapping phenomena happen for such polarization [13, 46, 47].

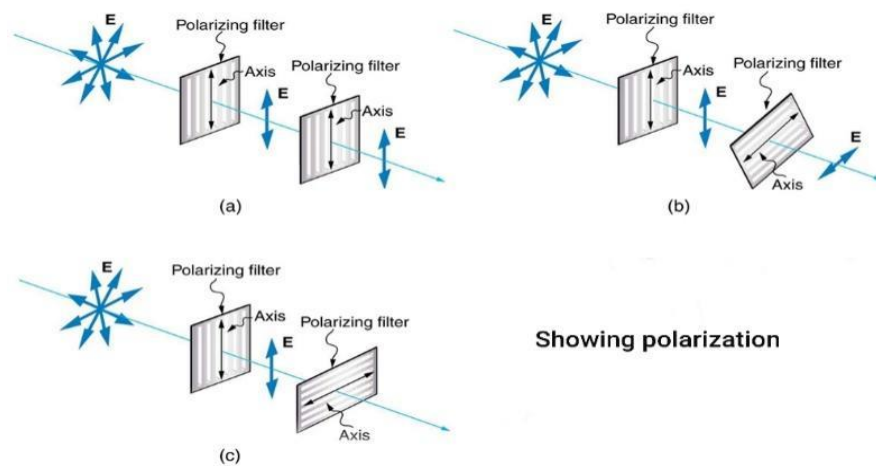


Figure 7: Polarization diagram.

1.9 Chirped pulse amplification (CPA):

Change of frequency in laser is known as chirp. There are different types of chirp: linear, nonlinear quadratic, periodic. Chirped pulse amplification is a technique [48-50] for amplifying laser pulse up to petawatt level. The pulse is first stretched by a factor of a 1000 or 100000. It is then amplified from nanojoules to kilojoules power level and is finally recompressed by the same stretching ratio. The peak output laser power is raised to multi terawatts and even petawatt (PW). CPA for lasers was introduced by Gérard Mourou and Donna Strickland at the University of Rochester in 1985. Due to the discovery CPA, they got Nobel Prize in Physics in 2018.

Since 20th century, electron acceleration with CPA technique has spread worldwide attention due to wide ranging applications such as: induced fusion, wakefield accelerator, Industries, Biology, Medical Sciences etc. Chirp destroys the symmetry of phase of laser pulse, as a result electron accelerates and enhances its energy. It was seen that the frequency chart gives us a successful interaction between chirp and electron [51-53]. In 2005, Singh showed that chirp pulse enhanced electron energy in vacuum [50]. In 2014, Salamin and Jisrawi observed twice energy gain for the linear chirp than a quadratic chirp [54]. In 2016, Ghotra and Kant [55] investigated that electron gains energy about twice in case of periodic frequency chirp as compared to linear frequency chirp.

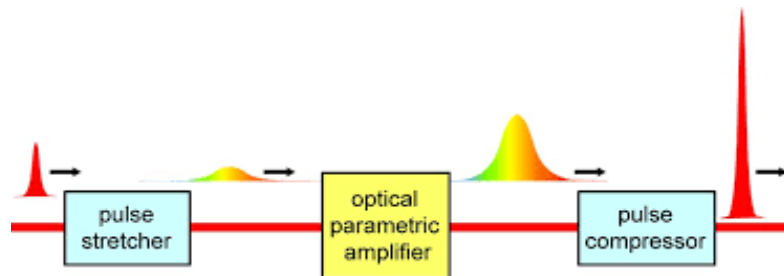


Figure 8: CPA Concept

General form of +vs / up chirp will be: $\omega(z, t) = \omega_0 \left[1 + \alpha \left(t - \frac{z}{c} \right) \right]$

General form of -vs / down chirp will be: $\omega(z, t) = \omega_0 \left[1 - \alpha \left(t - \frac{z}{c} \right) \right]$

General form of periodic chirp will be: $\omega(z, t) = \omega_0 \left[1 + \alpha \sin \left\{ \beta \left(t - \frac{z}{c} \right) \right\} \right]$

Where, α and β are the linear and periodic chirp parameter respectively. ω_0 & $\omega(z, t)$ represented the fundamental frequency and chirped frequency of laser pulse, t and z stands for time and propagation distance, respectively. Speed of light denoted by c in vacuum. Generally application of frequency chirp creates asymmetry due to which electron enhances more energy.

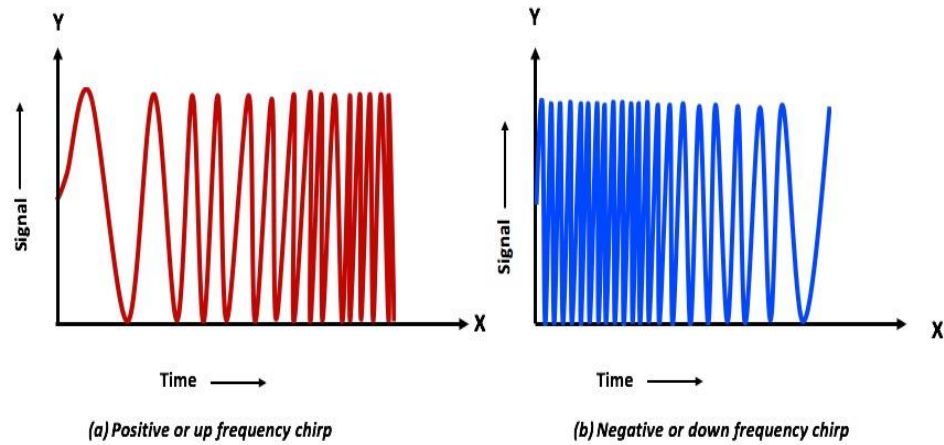


Figure 9: Up and Down frequency chirp

1.10 External Magnetic field:

Application of external Magnetic field plays a key role on electron acceleration. It not only increases the electrons energy but also retains the equal amount of energy for longer time. It increases the $\vec{v} \times \vec{B}$ force which ultimately increases the energy gain. We may use axial, azimuthal and wiggler magnetic field.

- (a) Axial magnetic field [56] boosts $(\vec{v} \times \vec{B})$ force which retains the betatron resonance for longer time. Hence much energy is enhanced.
- (b) Azimuthal magnetic field [11] enhances the electron energy and retained the high energy for longer distance. It has pinching effect, which forces electron to travel for longer distance.
- (c) Wiggler magnetic field [57] encloses the track of accelerated electron. It also boosts $(\vec{v} \times \vec{B})$ and retained the betatron resonance for longer corridor.

1.11 Plasma:

Plasma, the 4th state of matter was discovered by Noble Laureate Irving Langmuir in 1920s. He was the pioneer of the scientific study of ionize gases. It is a quasi-neutral gas of charged and neutral particle which manifests collective behavior. As plasma electrons possess very small mass, so their motion controls the plasma behavior in first process. In plasma only electrons are mobile, ions provide a neutralizing background of positive charges. The maximum matter of our universe is full of plasma. It may be laboratory and terrestrial plasma. Fluorescence bulb, exhaust from rocket and electric arc are the example of man-made plasma. Terrestrial plasma are found in the gas discharges as in lighting, star, auroras and interstellar space.

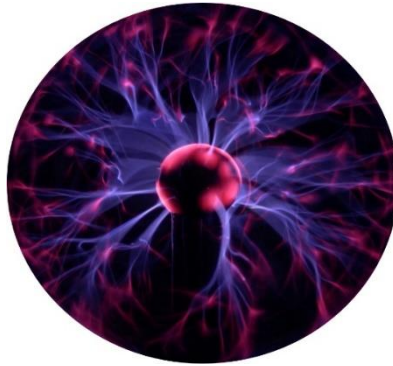


Figure 10: Plasma

1.11.1 Condition to be a plasma:

Any kind of ionized gas cannot be regarded as plasma. For an ionized gas to be categorized as plasma, the existence of the following conditions must be fulfilled:

- (1) The Debye length $\lambda_D = \frac{K_B T}{4\pi n_0 e^2}$ where K_B , T , n_0 , and e represent the Boltzmann constant, absolute temperature, plasma electron density and electronic charge respectively must be smaller than the plasma size.

- (2) The number of electrons within a sphere which has volume $\frac{4\pi\lambda_D^3}{3}$ must be greater than Unity ($\frac{4\pi\lambda_D^3}{3} \gg 1$).
- (3) Quasi-neutrality of Plasma implies that the ion density must be equal to the electron density.

1.11.2 Types of Plasma:

[a] When frequency of electromagnetic wave (ω_0) is greater than plasma frequency (ω_p), it is allowed to propagate in the plasma. Such type of plasma is known as under dense plasma.

[b] When frequency of electromagnetic wave is equal to plasma frequency then the plasma is said to be critically dense plasma.

[c] If plasma frequency is greater than frequency of electromagnetic wave, the electromagnetic wave cannot propagate through plasma. Such class of Plasma is known as over dense plasma.

If quasi-neutrality condition is not achieved, due to charge separation and electric field is generated. Then the plasma electrons oscillate about the heavy ion. The frequency of these oscillation is termed as plasma frequency. It is denoted by (ω_p). Its expression will be

$$\omega_p = \left(\frac{4\pi n_0 e^2}{m} \right)^{1/2}, \text{ where } m \text{ is the mass of electron.}$$

1.11.3 Propagation of electromagnetic waves through plasma:

Plasma also acted as a medium of electron acceleration as vacuum has some limitations. When an electromagnetic wave propagates through plasma medium, and is governed by the dispersion relation: $c^2 K_0^2 = \omega_0^2 - \omega_p^2$, where ω_0 and K_0 are free space radiation angular momentum frequency and wave number respectively.

1.11.4 How electron accelerates through plasma:

To propagate electron through plasma, high quality laser beam is needed. Even there are many challenges. Out of them, main two are: (1) Accelerating structure mechanism. (2) CAS mechanism. In that purpose, a focused ultra-laser pulse has been employed. Wakefield can fulfill the above dilemma. Wakefield is nothing but a plasma wave incited by laser ponderomotive force. When laser pulse length $c\tau$ ($c = 3 \times 10^8 \text{ ms}^{-1}$, $\tau =$ pulse duration) is comparable λ_p , the ponderomotive force effectively shoves plasma electrons which expelled from the ion. The accumulated electrons create a plasma wave.

1.11.5 Important phenomena when electron accelerates through plasma:

Distinct interesting phenomena are observed when electron accelerates through plasma medium. The interaction between laser pulses with plasma produces some nonlinear phenomena like self-focusing, pulse compression, wakefield generation, and harmonic generator. These nonlinear phenomena are the principle of wide application such as internal confinement fusion [58-60], high energy particle acceleration [10, 61, 62], X-ray sources [63, 64], terahertz radiation generation [65-68].

Several mechanisms which follow the wakefield route are Plasma Wakefield Acceleration, Laser Wakefield Acceleration, Plasma Beat Wave Acceleration, Self-Modulated Laser Wakefield Acceleration, Blow out etc. In LWFA, a single laser pulse of short duration, $\tau \approx 2\pi\omega_p^{-1}$ is employed that guides a plasma wave in the wake of the pulse, where $\omega_p = \sqrt{4\pi n e^2 / m}$ is the plasma frequency and n, e, m are the density, charge and mass of electron respectively. In the LWFA [6, 69] mechanism, a single, short ($\leq 1\text{ps}$), high-intensity ($\geq 10^{17} \text{ W. cm}^{-2}$) laser pulse can drive a high amplitude plasma wave. When an intense laser pulse passed via an under dense plasma ($\omega_p^2 / \omega^2 \ll 1$), the ponderomotive force linked with the laser pulse envelope, $F_p \sim \nabla a_0^2$ pushes electrons from the surrounding. The ions remain stationary due to their large mass and thus a charge separation region is created. The electrons tend to come back to their equilibrium position due to the Coulomb

force of the charge separation region. A plasma wave is thus generated behind the laser pulse. Under this condition $L_z \sim \lambda_p$, the ponderomotive force accelerates wakefield with phase velocities almost same to the group velocity. When an electron bunch gets properly injected into the wakefield region, it co-propagates with the laser wakefield and gets accelerated to relativistic energies [7]. Experimental evidence of electrons accelerated via Hamster et al. [70] illustrated first LWFA mechanism.

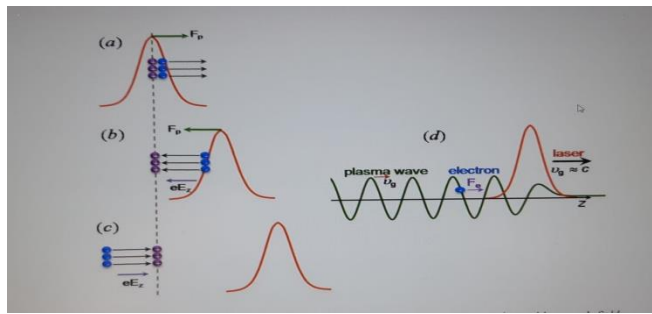


Figure 11: Excitation of plasma oscillations by intense laser pulse and laser wakefield acceleration.

In LBWA, two collinear lasers of frequencies ω_1 and ω_2 are propagated through an under dense plasma with plasma frequency $\omega_p \approx \omega_1 - \omega_2$. This idea was proposed for the first time by Rosenbluth et al. [71] and the concept was carried forward by Tajima and Dawson in place of LWFA since compact, ultra-short pulse, ultrahigh power technology [72, 73] was not available in 1979. Laser pulse of intensities $\sim 10^{14} - 10^{16} \text{W.cm}^{-2}$ and long pulse duration (~ 100 ps) should be used in order to resonantly excite large amplitude plasma waves [74]. Forslund et al., [53] showed the generation of plasma beat wave using two collinear laser beams for the first time in their 2D-PIC simulations. Clayton et al. [75] have experimentally observed the excitation of a relativistic plasma wave using two copropagating CO_2 lasers.

Clayton et al., [76] and Amiranoff et al., [77] have reported the result of an externally injected electron bunch in PBWA experiments.

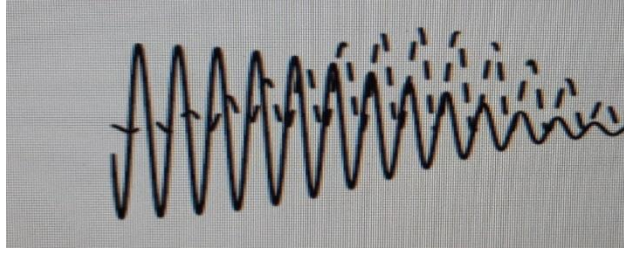


Figure 12: PBWA

In SM-LWFA [78-80], the laser pulse envelope gets modulated as it propagates through the under-dense plasma. The long laser pulse undergoes Forward Raman Scattering (FRS) and gets decayed into Stokes and anti-Stokes waves and a relativistic plasma wave. When intensity of Stokes and anti-Stokes waves are high enough, then they strike with the pump wave and modulate the envelope.

The plasma wave traps the electrons and accelerates them to relativistic energies. Enhanced electron acceleration is achieved in the SM-LWFA regime due to its several advantages. (i) The SMLWFA is achieved at comparatively higher densities, hence high amplitude Wakefield is generated. (ii) As $P > P_c$, the laser gets focused to higher intensity which guides to an increase in the wakefield amplitude. (iii) The wakefield gets vibrantly stimulated by a train of pulses and is thus stronger as compared to LWFA regime. (iv) Due to relativistic optical guiding, the laser pulse propagates up to several Rayleigh lengths which cause an increase in the accelerating length.

The drawbacks of the SM-LWFA regime are (i) at higher intensities, the group velocity laser pulse decreases which may cause the electrons to get dephased from the wakefield and hence reducing the accelerating length (ii) the energy spectrum gets broadened because of continuous trapping and short electron dephasing lengths as balanced to the laser propagation lengths and (iii) the modulated phase gets diffracted in time [81].

Krall et al. [82] in their fluid simulations have illustrated the properties of the electrons accelerated in the SM-LWFA mechanism. The role of Forward Raman Scattering in the acceleration of electrons was reported for the first time by Joshi et al. [78] in the

experiments done by using a 700 ps long CO₂ laser pulse at intensity 10^{15} Wcm⁻² interacting with a thin carbon foil producing 1.4 MeV electrons. Coverdale et al. [83] for the first time have experimentally observed the generation of plasma wave. Modena et al., [84] have experimentally reported the acceleration of electrons up to 44 MeV from the breaking of relativistic plasma waves due to FRS. An intermediate regime was demonstrated in the experiments and simulations reported by Malka et al., [18] by using a longer laser pulse.

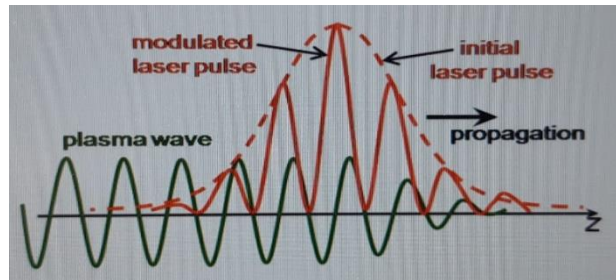


Figure 13: SM-LWFA

Another regime of acceleration is operated at high intensity limit ($a_0^2 \geq 1$), where a_0 the laser initial intensity and all the plasma electrons are completely expelled from the vicinity of the laser propagation axis. An ion cavity is formed which is surrounded by a thin layer of expelled electrons. It is referred to “blow-out”, “bubble” or “cavitation” regime.

A part of the plasma electrons are self-trapped in the ion cavity. They are accelerated to high energies [85-87]. Acceleration of electrons up to 40 GeV in the tail of the bunch has been observed in this regime [88].

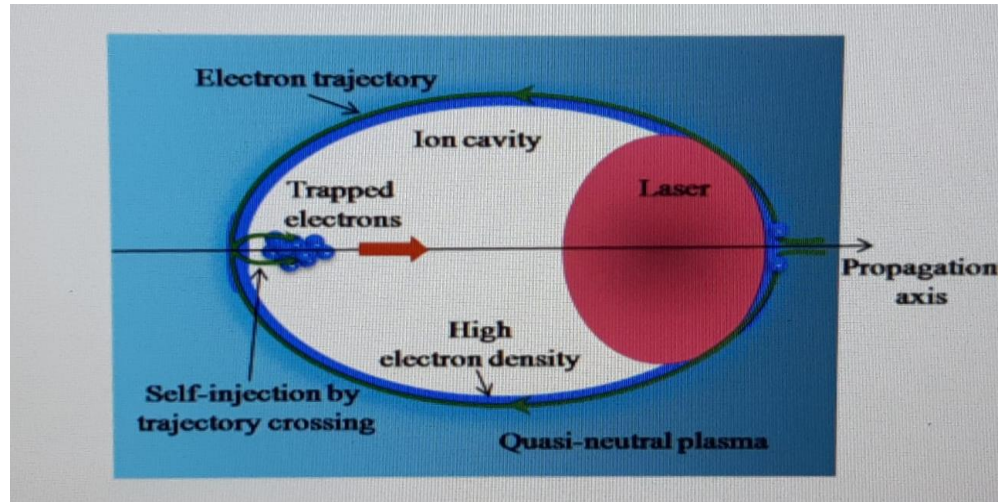
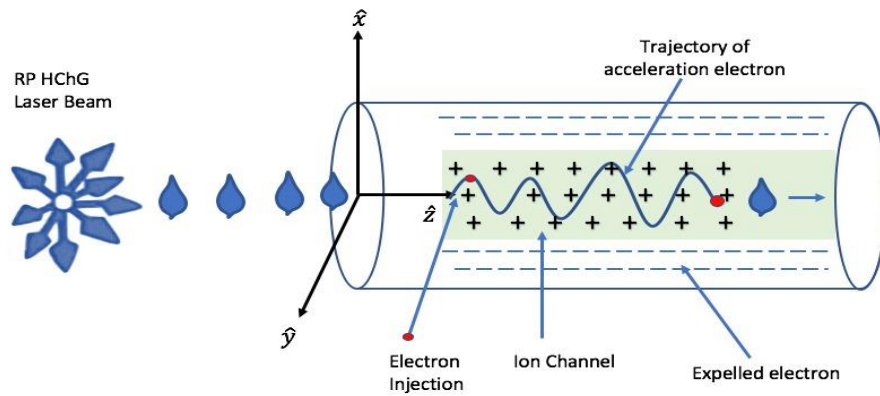


Figure 14: A schematic diagram of laser wakefield acceleration in bubble regime.

1.12 Electron acceleration through plasma channel:

It is very much needed to propagate laser pulses for several Rayleigh Length $Z_R \left(= k_0^2 r_0^2 / 4 \right)$, where r_0 is laser spot size. This is the key property of many application like: Laser fusion, Harmonic generation, and Laser Wakefield acceleration. For this purpose, plasma ion density channel [89-91] is suited properly. A plasma channel not only apply for guiding laser pulses over extended distance, but also prevents diffraction of laser beam. There are many methods to create plasma channel. The first one was created by Hydrodynamics Expansion of a plasma column [92]. In this method, 100 mille Joule and 100ps laser pulse was focused with 100 mille bar pressure. Such type of plasma channel is not fully ionized, it would be further ionized. Presently, high intensity femtoseconds laser pulse is used. Plasma ion channel is also used as an effective medium. Ion channel is used to focus and guide device for compressing and carrying relativistic electron beam and it is replaced in place of focusing magnet. Electron acceleration has been analyzed experimentally in ion channel [1, 93-96]. In such cases, energy gain is much greater in plasma ion channel than in vacuum by employing same laser intensity. Electric field of ion

density channel plays an important role in enhancing electron energy during the interaction between laser pulse and plasma. Also, we have received many explanations from several mechanism [97-100] for gaining electron energy. Channel depth is an important factor in plasma density profile. When channel depth and critical value of ion density Δn_c [101] are equal, the laser pulse propagates with constant spot size. Pulse length variation and presence of wakefield play a crucial role on the propagation characteristics of the laser pulse [102].



Schematic diagram of electron acceleration by RP HChG laser beam in a plasma ion channel

Figure 15: Schematic diagram of electron acceleration in plasma ion channel

The combined effect of radial polarization and ion density channel on electron acceleration has been theoretically analyzed by Kaur and Gupta [103]. By employing RP ChG laser pulse electron acceleration has been studied in ion channel [104]. Authors successfully analyzed various parameters on electron acceleration.

1.13 Direct Laser Acceleration (DLA):

Another applicable acceleration mechanisms in laser created channels in the long laser pulse regime i.e. in $L \gg \lambda_p$ (using hundreds of fs laser pulse duration) or even in $L > \lambda_p$ (using tens of fs laser pulse duration) regime is the DLA of electrons, where λ_p is the plasma wavelength. One way to observe DLA in plasma is by the ponderomotive acceleration [105]. At very high intensities, the $\mathbf{v} \times \mathbf{B}$ force of the laser field becomes strong enough to eject electrons radially as well as in the longitudinal directions. Typically, the energy gained by this process is due to the quivering of the electrons in the laser ponderomotive potential. So, typically with intensity parameter $a_0 = 1$, the electron energy results to be 200-300 keV and $\theta \sim 64^\circ$, suggesting generation of very low diffused energy electron beams. Electron acceleration through this scheme was experimentally demonstrated by G. Malka et al. where energy gain of ~ 2.7 MeV was achieved [18].

The second very dominant DLA mechanism in this regime is the betatron resonance acceleration was first investigated through 2D PIC simulation by Pukhov et al. [97]. In this scheme, the electrons oscillate at betatron frequency in the self-generated static fields in under-dense plasma. The static electric field is generated by the depletion of electrons from the laser channel axis by the radial ponderomotive force of the laser and the static magnetic field is generated from the stream of accelerated electrons. When this betatron frequency becomes equal to the Doppler shifted laser frequency, resonant transfer of energy from the laser field to the electrons occurs. This transverse energy gain of electrons is converted into longitudinal direction by the $\vec{\mathbf{v}} \times \vec{\mathbf{B}}$ and as a result effective energy gain of the accelerated electron beams in the longitudinal direction occurs. In contrast to wakefield, in case of DLA, the electrons perform larger transverse oscillations in the laser field and hence become a better candidate for generation of high energy betatron radiation compared to the wakefield [106, 93, 107-110].

There are very few reports on the experimental study of DLA, particularly using long laser pulse duration of hundreds of fs in He gas-jet target [95, 111, 112]. The first

experimental demonstration was by Gahn et al. [111]. They showed acceleration of electrons of maximum energy of ~ 12 MeV with quasi-thermal distribution on interaction of long laser pulses of duration of 200 fs. Experiments on DLA have shown generation of electron beam with continuous [112], or quasi-thermal [95, 111] energy spectrum. Applicability of DLA mechanism has also been reported in other gas-jet targets such as clustering Ar gas-jet where mostly broad continuous spectrum has been observed [106, 113, 114].

1.14 IMPORTANCE OF ELECTRON ACCELERATION

We have acquired most of the knowledge of the sub atomic world by the using particle accelerators. At first, especially for the nuclear and particle physics research, accelerators were developed and there was a demand for higher and higher particle energies. Now in the whole world, a number of particle accelerators are operational. They are also used for other many applications. They cover widely many fields such as understanding the structure and dynamics of material and their properties. Particle accelerators are also operational in the application of medicine such as treatment of tumors and cancer that also help in production of medical isotopes, sterilization, ion implantation etc. industrial applications such as cross-linking, polymerization of tires, rubbers, plastics can also be done by those. Particle accelerators play a vital role in semiconductor manufacturing, food irradiation, welding, cutting etc. They are also now employed in the applications of security such as scanning of materials, radiography etc. Scientists now use beams of accelerated particles to produce beam of secondary particles: Beams of electrons (light sources) generate photons (X- rays, gamma- rays, visible light and neutrons are generated from beams of protons (spallation neutron sources).

CHAPTER 2

LITERATURE REVIEW

A literature review is the recap of past work published on a particular topic. It helps us to find out the objectives of research scholars. It is very crucial for a research scholar. Here I have included the findings of some papers of my research field chronologically.

Tajima and Dawson, 1979 *Phys. Rev.* 43 267-270: The first accelerator researchers, Tajima and Dawson, established plasma as a medium for laser-assisted electron acceleration in 1979. They are the pioneer of generating wakefield of plasma oscillation by an intense electromagnetic pulse. Intensity gradient $10^{18} W cm^{-2}$ and plasma density $10^{18} cm^{-3}$ can generate GeV order of electron energy.

Strickland and Mourou, 1985 *Opt. Commun.* 56 219-221: Their work revolutionized in the acceleration process. They have showed that by stretching a chirped optical pulse first and then amplify and compress. On that time they produced 2 ps pulses with an energy of 1 mJ. This technique is known as CPA technique. Due to this technique, they got Nobel Prize in 2018.

Maine et al., 1988 *IEEE Journal of Quantum Electronics* 24 398 – 403: Authors have employed CPA technique to produce single picosecond pulse to the terawatt level. From this study 1 kJ energy can be extracted with 1 ns pulse. 1 GeV/m amplitude wakefields have been developed by propagating ultra-high power, short laser beams ($P \geq 10^{15} W$, $T_L \approx 2\pi\omega_p^{-1} \sim 1 ps$) in plasma.

Hora, 1988 *Nature* 333 337-338: Vacuum acceleration of by a non-linear mechanism was invented by Hora (1988). He solved plasmas encounter problems like instabilities, self-focusing etc. All these problems limit the energy to MeV. He proposed a laser acceleration system that does not require a plasma. With the help of very high laser power (100 TW) and 250 nm laser pulse wavelength electron accelerated as $600 GeV. cm^{-1}$.

Esarey, 1995 *Physical Rev. E* 52 5443-5453: Election acceleration in vacuum has been studied by using two laser beams of different frequencies. These beams are co-propagated. Such type of accelerator is known as Vacuum Beat Wave Acceleration (VBWA). VBWA depends (relies) on the nonlinear ponderomotive forces associated with the $\vec{v} \times \vec{B}$ force. it does not obey the assumptions of the LW theorem.

Malka, 1997 *Phys. Rev. Lett.* 78 3314: The first experimental verification of electron acceleration in vacuum had been done by Malka et al., in 1997. Experimental observation on the MeV & generation and acceleration in vacuum by the Lorentz force of an ultra-intense sub-Pico second LP laser pulse (10^{19}w/cm^2 , 300fs). This experimental results are in good agreement with the computation of the electron trajectories in the laser field.

Moore, 1997 *International Statistical Review* 65 123-137: Author observed SM-LWFA at 30 MeV electron's energy (up to) at low laser power (2.5 TW) in this paper. He estimated more than 47 GeV/m acceleration gradient. Both experiment and simulation showed that the SM-LWFA regime strongly depends on the wakefield amplitude. Because wakefield amplitude effects the trapping and the acceleration process of electrons.

Malka, 2000 *Rev. Sci. Instrum.* 71 2329: Experimentally reported the generation of electron (70 MeV) in the SMLWF regime for ultra-relativistic laser pulses $a_0 > 1$, where a_0 is the normalized vector potential of the laser.

$$\text{Max}^m \text{ Electron Energy} \propto \text{Laser Intensity}$$

$$\text{Max}^m \text{ Electron Energy} \propto \frac{1}{\text{electron density}}$$

Malka et al., 2002 *Science* 298 1596: This review paper is the generation of bright, energetic, collimated ultrashort electron beam by focusing a 30fs, 30TW laser beam onto a gas jet. This technique may be used in many applications in Physics, Chemistry, and Biology.

Wang, et al., 2002 *Journal of Appl. Phys.* 91 856-866: It is a review article. The interaction of free electrons with intense laser beams in vacuum is studied using a three-dimensional test particle simulation model that solves the relativistic Newton–Lorentz equations of motion in analytically specified laser fields. Recently, a group of solutions was found for very intense laser fields that show interesting and unusual characteristics. In particular, it was found that an electron can be captured within the high-intensity laser region, rather than expelled from it, and the captured electron can be accelerated to GeV energies with acceleration gradients on the order of tens of GeV/cm. This phenomenon is termed the capture and acceleration scenario ~CAS, and is studied in detail in this article. The dependence of the energy exchange in the CAS on various parameters, e.g., a_0 ~laser intensity, w_0 ~laser radius at focus, τ ~laser pulse duration, b_0 ~the impact parameter, and θ_i ~the injection angle with respect to the laser propagation direction, are explored in detail.

Singh, 2004 *Physical Review E* 69 056410: In this review paper energy gain occupied by electron depends on various parameter. An electron gains energy during the rising part of the laser pulse and loses it during the trailing part. The presence of a suitable static magnetic field during the trailing part of the pulse leads not only to an enhancement of the energy gain but also to the retention of most of the energy in the form of cyclotron oscillations after the passing of the laser pulse. If the value of magnetic field is low, the electron experiences some deceleration, interacting with the trailing part of the pulse, and if it is too high, the electron escapes from the pulse; hence, the energy gained by the electron peaks for an optimum magnetic field. Similarly, for a small spot size the electron escapes from the pulse and for a large spot size the electron experiences some deceleration, interacting with the trailing part; therefore, the energy gain peaks for a suitable spot size. The energy gain increases with initial electron energy because the duration of interaction between laser pulse increases with initial electron energy. The electron gains very high energy at high laser intensity and high initial energy; however, the required value of the spot size also increases. At low laser intensity and low initial electron energies, the optimum values of the magnetic field are very high; however, intense magnetic fields with duration several orders of magnitude longer than that of a short laser pulse are available [21]. If such a strong magnetic field is not available at a laboratory, then the experiment can be carried out at high initial electron energy and high laser intensity because the optimum value of the magnetic field decreases with laser intensity and initial electron energy.

Singh, 2005 *App. Phys. Lett.* 87 254102: Net energy gained of electron due to chirp short intense laser pulse in vacuum has been investigated successfully in this paper. Frequency chirp not only increases the transverse momentum of electron but also helps to electron to escapes from the laser pulse near the pulse peak. Another finding of this

paper is that longitudinal momentum also increases with increase in longitudinal force $\vec{v} \times \vec{B}$.

Singh, 2006 *J. Opt. Soc. Amer. B, Opt. Phys.* 23 1650-1654: Author concluded in this paper that frequency chirp plays a crucial role to enhance electron's energy. For this purpose he used a chirped short intense laser pulse in vacuum. Because freq. chirp creates asymmetry in the laser pulse, as a result quasi-static electric field is generated, which increases the drift velocity of electron and transverse momentum of electron.

Gupta et al., 2007 *Phys. Plasmas* 14 044701: They concentrated their study on electron acceleration in vacuum. They used CP Gaussian chirped laser pulse. They compared their result with previously worked on LP laser pulse. CP laser pulse gives better result due to axial symmetry.

Sohbatzadeh, 2009 *Phys. Plasmas* 16 023106: In this paper we have seen the comparison between elliptical, circular and linear polarization on electron acceleration using a chirped laser pulse. The linear polarization is more effective for a single electron acceleration and for electron bunch, circular & elliptical polarization are more effective.

Gupta et al., 2009 *Journal of Applied Physics* 105 106110: Jointly frequency chirp and tight focusing of a laser beam have been investigated in this paper for electron acceleration in vacuum. Electron achieved to GeV-level energy. The effect of waist of the laser beam with tight focusing has been studied in this paper. Also the role of frequency chirp on electron acceleration has been noticed successfully. It enhance the electron energy gain significantly.

Esarey et al., 2009 *Rev. Mod. Phys* 81 1229: Esarey et al. presented the developments of theoretical and experimental models for electron acceleration based on laser-plasma interactions. They reviewed the concepts leading to generation of high energy gradients of the order 100GV / m. They discussed the plasma-based techniques for electron acceleration such as LWFA, PBWA, self-modulated LWFA. They discussed the linear

and nonlinear properties of plasma waves with respect to the acceleration of electron in plasma waves. They also presented the related instabilities due to intense short-pulse laser-plasma interactions.

Li et al., 2010 *Bioresource Technology* 101 3430–3436: Authors studied the vacuum electron acceleration. For this purpose they induced tightly focused chirped laser pulse. With a tightly focused linearly polarized laser pulse it is possible to focus the laser beam to the order of wavelength with inclusion of third order in diffraction angle. Additionally, the chirp parameter contributes in electron energy enhancements. Further the phase slippage between the energetic electrons and laser pulse remains small and such electrons retain energy for longer duration.

Malka, 2012 *Phys. of Plasmas* 19 055501 : This review article shows the evolution of research on laser plasma accelerators which has led to the production of high quality electron beams at relativistic energy using compact laser system and investigated various injection pattern.

Jokar and Eslami, 2012 *Optik*. 123 1947-1951: In this paper authors studied the effect of pulse shape on the fs pulsed laser-plasma interaction. Wakefield generation strongly depends on the laser intensity, pulse duration, beam spot size and also temporal pulse shape. They measured the magnitude of wakefield for different laser profile like: TPS > GPS > HSPS at high intensity but for lower intensity it will be reversed [33]. So at higher intensity electron can accelerate more efficiently in case of trapezoidal laser pulse envelope.

Salamin, 2012 *Phys. Lett. A* 376 2442-2445: According to Lawson-Woodward theorem, an ideal plane wave cannot enhance electron's energy. He showed that if frequency chirp is employed to it, ten-fold increase in energy gain achieves by electron. In this paper he used a \cos^2 pulse-shape envelope.

Jha et al., 2013 *Laser and Particle Beams* 4 583-588: presented a 2D PIC simulation for acceleration of electron by an intense super-Gaussian laser pulse through wake field

generation in plasma. The electron trapping, dynamics and energy gain was analyzed for an injected electron accelerated by wake field. With a super-Gaussian pulse, the generated wake field appeared to be 23% higher than that with a Gaussian laser pulse. Author concluded that super Gaussian laser pulse is better than a Gaussian laser pulse in the contest of electron acceleration.

Salamin and Jisrawi, 2014 *J. Phys. B: At. Mol. Opt. Phys.* 47 025601: Salamin and Jisrawi employed trapezoidal terser pulse envelope to study electron acceleration and used studied the comparison between linear and quadratic chirp. They observed the absolute maximum energy gain of almost 2 folds for a linear chirp as compared to quadratic chirp.

Ghotra and Kant, 2015 *Appl. Phys. B* 120 141–147: In this paper, authors analyzed electron acceleration in vacuum. For this purpose, they employed CP Gaussian laser pulse. Also, they studied the combined effect of linear chirp with azimuthal magnetic field on it. Electron accelerates with high magnetic field and linear frequency chirp increases the interaction time between laser pulse and electron. They observed 2.66 GeV energy gain for laser intensity $2.74 \times 10^{20} W.cm^{-2}$ with chirp parameter 0.000875 and azimuthal magnetic field 94 KG.

Ghotra and Kant, 2016 *Optics Communications* 365 231-236: Authors studied polarization effect on electron acceleration in vacuum. They also noticed the effect of azimuthal magnetic field. In this case they compared LP and CP laser pulse. They observed higher energy gain with CP laser pulse than LP laser pulse. The energy gain of ~ 2 GeV is observed with a CP laser pulse of peak intensity $2.74 \times 10^{20} W cm^{-2}$ in the presence of azimuthal magnetic field of 534 kG.

Ghotra and Kant, 2016 *Phys. Plasmas* 23 013101: Electron acceleration under CAS system has been studied by an RP laser pulse under the influence of wiggler magnetic field. The authors showed that magnetic wiggler increases 4 times energy them without wiggler magnetic field. Also wiggler magnetic field retains the gained energy for longer corridor for longer time and maintain the betatron resonance for longer corridor. The

authors also observed that the side way injection of electron which gives 1.3 times higher energy that with axial injection.

Rajput et al., 2017 *AIP Conference Proceedings* 1860 020005: Electron acceleration in vacuum has been studied in this paper. Here authors employed chirped axicon RP Gaussian laser pulse. As focused axicon laser pulse produces a very strong longitudinal electric field and RP laser has unique property, authors observed 10.5 GeV energy gain in vacuum. They used intensity parameter $a_0 = 20$ ($I \sim 5.52 \times 10^{20} W cm^{-2}$) with optimum chirp and wiggler magnetic field at initial phase $\psi_0 = 0$.

Kaur, 2017 *IEEE Transactions on Plasma Science* 45 2841-2847: Authors analyzed electron acceleration in plasma ion channel by employing RP laser pulse. Due to unique property of RP laser pulse that improves the trapping and accelerating process so that electron can accelerate with higher energy in the longitudinal direction because radial field vanishes and axial field is the key factor to propagate electron to longitudinal direction. For efficient acceleration of this model pre-accelerated electrons with large initial velocity are preferred.

Ghotra et al., 2018 *Laser and Particle Beams* 36 154-161: In this paper, Ghotra et al. analyzed the effect of various TEM modes of Hermite function. They employed CP Hermite-Gaussian laser beam and axial magnetic field in Z-direction to study electron acceleration in DLA mechanism. Using laser intensity $a_0 = 25$ ($I \sim 8.5 \times 10^{20} W/cm^2$) and laser spot size $r_0 = 150$ ($\sim 25 \mu m$) for mode (0, 4), electron energy gain of above 1 GeV is observed due to externally applied axial magnetic field. The laser peak power for such case is calculated as 8.3PW. This study is helpful in development of better table-top accelerator.

Ghotra and Jaroszynski, 2018 *Laser Part. Beams* 36 154: Application of axial magnetic field in DLA scheme by Hermite-Gaussian (HG) TEM modes has been analyzed theoretically in this paper. A CP HG laser beam is considered for that purpose. Increase in mode indices increases the energy gain. Presence of external applied axial magnetic field

enhances 30% higher energy gain and less dephasing phenomena. The outcome of this research with various TEM modes is for better table-top accelerators.

Singh et al., 2019 *Atomic, Molecular, Condensate & Nano Phys.* 6 81-91: Enhancement of electron energy depends on laser intensity parameter a_0 , electron's injection angle ($<20^\circ$ gives better result) and initial momentum. Energy is proportional to a_0 and if initial momentum is small, higher energy gain occurs (also acceleration gradient increases). Chirp parameter and phase play important role for energy enhancement. On varying the chirp parameter with corresponding values of electric and magnetic field as well as phase the maximum energy gain can be achieved. We investigated electron acceleration by a chirped short intense laser pulse when an external magnetic field is applied along y-direction.

Kant, 2020 *Eur.Phys. J.D* 74 142: Combined effect of tightly focused and axial magnetic field on electron acceleration has been studied. Here, authors employed chirped tightly focused LP laser pulse. They observed 5.78 GeV energy gain of initial 0.75 MeV energy of electron at intensity $1.38 \times 10^{20} W.cm^{-2}$.

Singh et al., 2020 *J. Phys.* 1531 2027-2030: Vacuum electron acceleration has been investigated by appointing RP Cosh-Gaussian laser beam (CGLB). This laser beam in good for early focus. As a result electron captures high energy over small interval. It is known from the study that energy gain is strongly depends on the decentered parameter of laser profile. It is also observed that increase in decentered parameter decreases in intensity when authors fixed the amount of energy gain. Also, energy gain has been studied by varying laser spot size and laser intensity. It is also observed that small spot size occurs large scattering which diverse quickly. As a result electron cannot attain efficient energy gain.

Ghotra, 2022 *Laser Phys. Lett.* 19 096002: Author studied electron acceleration theoretically in an ion density ($\sim 10^{22} m^{-3}$) at intensity $\sim 10^{20} W.cm^{-2}$. He employed RP ChG laser pulse for this study. He studied the effect of ion density, decentered

parameter, initial velocity of electrons, initial phase, and laser intensity on electron acceleration. Author reached his expectation energy gain.

Rajput et al., 2023 *Iran J Sci.* 47 1397-1405: A tightly-focused short intense radially polarized Gaussian laser pulse has been used to investigate electron acceleration in vacuum. They also employed an external axial magnetic field. A combined effect make the profile more beauty. They studied the combined effect on electron acceleration and electron gains its energy GeV level.

Ghotra, 2023 *Optik* 286 170992: The role of higher order of Cosh-Gaussian (ChG) laser pulse has been employed by author in vacuum to study electron acceleration and energy gain. Author assumed pulse order $m = 0, 1, 2, \text{ and } 3$ classified as Gaussian, ChG, Ch-Square-G, Ch-Cube-G laser pulse. He noticed that increase in m effectively increases energy gain and make ready to electron for longer distances. Author noticed GeV order energy with intensity $\sim 10^{20} Wcm^{-2}$ and decentered parameter $b = 2$ in vacuum.

Ghotra, 2023, *Phys. Sci.* 98 125602: By exploring low order axisymmetric modes of HChG laser pulse author studied electron acceleration and energy gain in vacuum. He investigated the role of decentered parameter (b) and Hermite polynomial. He noticed that the intensity distribution of HChG laser is affected by b and Hermite polynomial. Increase in b changes from fundamental Gaussian to more complex Gaussian type ring shapes form. As a result electron quickly accelerates and possesses high energy over a short period of time with intensity $\sim 10^{21} Wcm^{-2}$.

Gupta et al., 2023 *Phys. of Plasmas*: Initially authors splitted a laser pulse into two different polarization: linear and circular polarization laser pulse. These splitted polarization radiation have been used to accelerate proton from near critical density targets. These different polarization combinedly generate a shock wave at the front surface of the target, hence proton at the front accelerate.

RESEARCH HYPOTHESIS

The laser assisted electron acceleration in vacuum and plasmas has been studied. In this work, we have examined the laser induced dynamics of electron in vacuum and plasmas. We have studied the electron trajectory under interaction with by varying laser parameters. Electron acceleration by laser is widely studied by researchers and scientists as the accelerated electron attains high energy during interaction by various conditions. We examine the role of polarization of laser pulse envelope, frequency chirp, external magnetic field, ion density, decentered parameter, hermite order etc. for electron acceleration. We have focused our attention on enhancing the electron energy gain by the proper selection of various parameters in vacuum and plasma.

- ❖ **The aim of all kinds of research should be enhancing our knowledge, saving our mankind and make our life more comfortable.**
- ❖ **We are not exceptional from them. Our first priority will be technology based upgradation of accelerator which is very essential to medical science, enhance our knowledge about universe.**
- ❖ **This research may significantly improve the acceleration scenario.**
- ❖ **The main hypothesis of my research is to enhance electrons energy by short pulse laser. This hypothesis is based on the previous theoretical, experimental as well as simulation result.**

RESEARCH OBJECTIVES

The aim of this proposed thesis is to significantly enhance our understanding of physics and laws of physics which will be achieved by the following objectives:

- 1. Electron acceleration of a radially polarized Hermite-Cosh-Gaussian laser beam by a periodic / linear chirp.**
- 2. Chirping effect of different laser pulse envelopes (Gaussian, Trapezoidal, Cos^2 , and Sin^4) on electron acceleration phenomena.**
- 3. Effect of external magnetic field on electron acceleration in a plasma micro channel.**

METHODOLOGY

- 1. Formulation of hypothesis:** The relativistic Newton-Lorentz equations of motion in analytically specified laser fields are used to study the electron acceleration in plasma and vacuum. The Newton-Lorentz equations of motion and relativistic energy equation are used to find the trajectory and energy gain by the charged particle under different conditions respectively. The equation of motion and energy equation of the charged particle are derived and solved the Newton-Lorentz force equation numerically and analyzed the outcome by using **MATHEMATICA SOFTWARE** (PROGRAMMING SOFTWARE) and **ORIGIN SOFTWARE** (GRAPHICAL SOFTWARE). **ORIGIN SOFTWARE** is very much helpful for discussing our result by plotting graphs.
- 2. Sources of data:** Theoretical results will be compared with experimental results collected through various research paper.
- 3. Research Design:** Numerical and analytical analysis.
- 4. Tools:** **MATHEMATICA** and **ORIGIN** software.

CHAPTER-3

EFFICIENT ELECTRON ACCELERATION BY USING HERMITE-COSH-GAUSSIAN LASER BEAM IN VACUUM

3.1 Introduction

The demand for accelerators in medical science and industry [1-3], fundamental forces research, and tumor therapy [4-5] is rapidly expanding. A large number of researchers and scientists are being drawn to this sector in order to meet the need for accelerators. Because the electron is the lightest subatomic particle, researchers find electron acceleration incredibly appealing and exciting for acceleration up to higher energies. It is also highly beneficial to study the evolution of the world, modern cancer therapy, modern X-ray, and security systems, among other things. Laser-driven electron acceleration can take place in two ways: in the plasma medium (through wakefield generation) [6] and in the vacuum medium (by the direct laser acceleration (DLA) mechanism) [8]. The basic mechanism of laser-driven electron acceleration is known as the "Capture and Acceleration Scenario" (CAS). In CAS scheme, the laser propagating path's core captures and accelerates electrons to GeV, with accelerating gradients of GeV/m [11]. Laser beam profiles, polarization, the external magnetic field [1, 120, 121], and other laser parameters have a significant impact on this mechanism. A number of theoretical [22, 23, 126, 26] and experimental [27, 18, 28, 29] studies have already been reported for effective acceleration. The first accelerator researchers, Tajima and Dawson, established plasma as a medium for laser-driven electron acceleration in 1979 [10]. Hora [32] created the nonlinear vacuum acceleration mechanism in 1988. In 1995, Amiranoff et al. [77] accomplished experimental electron acceleration in a wakefield process. The Hermite-Sinusoidal-Gaussian family of beams, such as Hermite-Gaussian (HG), Cosh-Gaussian (ChG), Sinh-Gaussian (ShG), Hermite-Cosh-Gaussian (HChG), etc., are possible solutions to the wave equation. Casperson and Tovar [129, 130] introduced the paraxial solution of

these beams. Many sophisticated laser beams have already been used to examine electron acceleration, including HG beams [131], LG beams [121, 132], and BG beams [133]. Cosh-Gaussian laser beams (CGLB) have been found to have comparatively higher power and earlier focus capacity than well-known Gaussian beams [134-137]. In addition, CGLB has the ability to extract energy more efficiently from traditional laser amplifiers [138]. These are the key characteristics that ensure electron acceleration and energy enhancement, as envisaged. Short pulse terawatt technology maintains an important consistency in laser technology [13, 73]. Many frontier research area has emerged from this technology. In this situation intensity distribution of laser beam plays a key role on acceleration scenario. A lot of theoretical as well as experimental work has been completed successfully by employing ultra-intense laser [141-143]. Hermite-Gaussian (HG) beam has a great impact on laser and plasma physics in various conditions. A decade ago, self-focusing phenomenon analyzed in plasma for dark hollow Gaussian laser beam [13,34,73]. Narrow, low divergence [57,144] beam is generated by Gaussian laser envelope. This is the main cause of attraction of researchers to Gaussian laser. Carbajo et al., [145] experimentally noticed GeV/m order accelerating gradient along longitudinal direction by employing RP laser. For that same context the tightly focused Hermite Gaussian laser beam with greater correction has made several times in vacuum [146]. In comparison with standing waves, Fabry-Perot cavities led different scenario for laser parameters under compactness condition [147]. The strength of self-focusing for HG beam increases as we increase propagation distance [148]. Better result has been noticed replacing HG by HChG beam inside a nonlinear medium due to the compress of spot size [149]. Experimentally the polarized structure of HG beam was studied [150]. HG beams are also applied for air vehicles communication systems [151]. Time to time researchers met with these challenges, and solved the problems successfully [152, 153]. Lawson-Woodward theorem [36, 154] says that electron can't enhance its energy by a plane electromagnetic wave. It is fine for the rising portion of the laser pulse, but when the falling portion of the laser pulse interacts with the electron, the electron loses energy. To overcome this problem different mechanism were introduced time to time in CAS system. An investigation showed that

electron accelerates effectively by employing tightly focused chirped-pulse inverse free electron laser (CIFEL) scheme [155]. Another way to enhance electron's energy is to employ an external magnetic field which is more effective for the falling portion. It prevents the electron's energy from decreasing. In 2015, Ghotra and Kant noticed GeV energy gain. They employed LP Gaussian laser pulse. They studied the effect of linear chirp and azimuthal magnetic field [156]. It has been noticed that when frequency chirp with wiggler magnetic field are employed, energy enhances up to 10.5 GeV in vacuum [122]. Kant et al., have shown that tightly focused LP laser with frequency chirp and 8.5 MG optimum axial magnetic field electron can gain energy up to 5.78 GeV at intensity at $1.38 \times 10^{20} \text{ W/cm}^2$ [127]. When a radially polarized (RP) Gaussian Laser pulse with intense pulsed magnetic field introduced then electron attains 2.25 GeV energy in vacuum at optimized field parameters [157]. Hashemian et al. [158] produced high energy, low spread good quality electron beam. Better trapping has been investigated in case of RP laser [46].

In this chapter, I have used a RP HChG laser beam to study electron scenario in vacuum. We can easily make HChG profile by using Hermite-Gaussian and Cosh-Gaussian beams. The HChG profile is very efficient for electron acceleration due to better trapping and early self-focusing criteria [139]. As a result, the electron energy gain is influenced significantly by various modes of the generic beams family. Ghotra et al. observed GeV order energy gain of HG beam TEM mode under the influence of higher mode indices with axial magnetic field [24]. The RP laser pulse's cylindrical symmetry is critical for better electron entrapment [45]. In comparison to LP and CP laser pulses, RP laser pulses have narrow divergence and low spread power. Furthermore, RP radiation is easier to focus than LP light, and it has a lower irradiance threshold, allowing for deeper penetration into the skin with reduced danger of casualty, resulting in increased treatment safety and efficacy [140]. Our team is the pioneer of electron acceleration by employing HChG laser beam in vacuum. I have investigated a detailed study on HChG laser beam. I have also studied electron acceleration by using HChG laser beam with chirp, without chirp, chirp with external magnetic field in vacuum and plasma medium. I have also compared LP and CP

polarization on HChG laser beam. As literature survey shows CP polarization (45) is better performer than LP in Gaussian laser pulse. Here I have noticed the same result. I am really proud of my work.

3.1.1 Study of electron acceleration phenomena by Hermite-Cosh-Gaussian laser beam

3.1.1.1 Electron Dynamics

Let us consider a RP HChG laser beam which propagates to z direction in vacuum. The field equation is given by

$$\vec{E} = \hat{r}E_r + \hat{z}E_z \quad \dots\dots\dots (3.1)$$

The transverse component of the above field is expressed as

$$\vec{E}_r = \hat{r}E_0 H_s \left(\frac{\sqrt{2}r}{r_0} \right) \cosh \left(\frac{br}{r_0} \right) e^{-\left(r^2 / r_0^2 \right)} e^{i(kz - \omega t)} \quad (3.2)$$

The longitudinal component is represented as

$$\vec{E}_z = -\hat{z} \frac{i}{kr} E_r \left[1 + 2S\sqrt{2} \frac{r}{r_0} \frac{H_{s-1} \left(\frac{\sqrt{2}r}{r_0} \right)}{H_s \left(\frac{\sqrt{2}r}{r_0} \right)} + b \frac{r}{r_0} \tanh \left(b \frac{r}{r_0} \right) - 2 \frac{r^2}{r_0^2} \right] \quad (3.3)$$

Where, E_0 is the amplitude, r_0 is the beam width (waist width), r is the radial distance, s is the Hermite order and b signifies the decentered parameter of Hermite-Cosh function.

To investigate the momentum and energy of electron, we have to use the following equation which is also known as Newton-Lorentz force equation

$$\vec{F} = \frac{\partial \vec{p}}{\partial t} = -e [\vec{E} + (\vec{v} \times \vec{B})] \quad (3.4)$$

From the above eq. (4), the electron's momentum, energy and velocity equations are written as

$$\frac{dp'_r}{dt'} = a_0 H_S \left(\frac{\sqrt{2}r'}{r'_0} \right) \cosh \left(\frac{br'}{r'_0} \right) e^{-\left(r'^2 / r_0'^2 \right)} e^{i(k'z' - t')} (v'_z - 1) \quad (3.5)$$

$$\frac{dp'_z}{dt'} = a_0 H_S \left(\frac{\sqrt{2}r'}{r'_0} \right) \cosh \left(\frac{br'}{r'_0} \right) e^{-\left(r'^2 / r_0'^2 \right)} e^{i(k'z' - t')} \left[\frac{i}{k'r'} \left[1 + 2S\sqrt{2} \frac{r'}{r'_0} \frac{H_{S-1} \left(\frac{\sqrt{2}r'}{r'_0} \right)}{H_S \left(\frac{\sqrt{2}r'}{r'_0} \right)} + \right. \right. \\ \left. \left. b \frac{r'}{r'_0} \tanh \left(b \frac{r'}{r'_0} \right) - 2 \frac{r'^2}{r_0'^2} \right] - v'_r \right] \quad (3.6)$$

$$\frac{d\gamma'}{dt'} = a_0 H_S \left(\frac{\sqrt{2}r'}{r'_0} \right) \cosh \left(\frac{br'}{r'_0} \right) e^{-\left(r'^2 / r_0'^2 \right)} e^{i(k'z' - t')} \left[v'_z \frac{i}{k'r'} \left[1 + 2S\sqrt{2} \frac{r'}{r'_0} \frac{H_{S-1} \left(\frac{\sqrt{2}r'}{r'_0} \right)}{H_S \left(\frac{\sqrt{2}r'}{r'_0} \right)} + \right. \right. \\ \left. \left. b \frac{r'}{r'_0} \tanh \left(b \frac{r'}{r'_0} \right) - 2 \frac{r'^2}{r_0'^2} \right] - v'_r \right] \quad (3.7)$$

$$\frac{dv'_r}{dt'} = \frac{a_0}{c_1} H_S \left(\frac{\sqrt{2}r'}{r'_0} \right) \cosh \left(\frac{br'}{r'_0} \right) e^{-\left(r'^2 / r_0'^2 \right)} e^{i(k'z' - t')} (v'_z - 1) \quad (3.8)$$

$$\frac{dv'_z}{dt'} = \frac{a_0}{c_2} H_S \left(\frac{\sqrt{2}r'}{r'_0} \right) \cosh \left(\frac{br'}{r'_0} \right) e^{-\left(r'^2 / r_0'^2 \right)} e^{i(k'z' - t')} \left[\frac{i}{k'r'} \left[1 + 2S\sqrt{2} \frac{r'}{r'_0} \frac{H_{S-1} \left(\frac{\sqrt{2}r'}{r'_0} \right)}{H_S \left(\frac{\sqrt{2}r'}{r'_0} \right)} + \right. \right. \\ \left. \left. b \frac{r'}{r'_0} \tanh \left(b \frac{r'}{r'_0} \right) - 2 \frac{r'^2}{r_0'^2} \right] - v'_r \right] \quad (3.9)$$

Here, $P_r = \gamma m_0 v_r$ and $P_z = \gamma m_0 v_z$, (v_r, v_z) are the (r, z) components of velocity, $\gamma^2 = 1 + (p_r^2 + p_z^2)/m^2 c^2$. The normalized parameters are as follows: $a_0 = \frac{eE_0}{m\omega_0 c}$, $t' = \omega_0 t$, $r'_0 = \frac{\omega_0 r_0}{c}$, $r' = \frac{\omega_0 r}{c}$, $z' = \frac{\omega_0 z}{c}$, $v'_r = \frac{v_r}{c}$, $v'_z = \frac{v_z}{c}$, $p'_r = \frac{p_r}{mc}$, $p'_z = \frac{p_z}{mc}$, $\gamma' = \frac{\gamma}{mc^2}$ and, $k' = \frac{kc}{\omega_0}$.

3.1.1.2 Result and Discussion

In this manuscript, the analytical and numerical calculations have set up the different parameters in the following ways: normalized intensity parameter $a_0 = 10$ (corresponding intensity $\sim 1.36 \times 10^{20} \text{ Wcm}^{-2}$), $a_0 = 15$ (corresponding intensity $\sim 3.07 \times 10^{20} \text{ Wcm}^{-2}$), $a_0 = 20$ (corresponding intensity $\sim 5.47 \times 10^{20} \text{ Wcm}^{-2}$), $a_0 = 25$ (corresponding intensity $\sim 8.55 \times 10^{20} \text{ Wcm}^{-2}$) and the laser wavelength λ is $1\mu\text{m}$. The angular frequency of laser beam is $\omega_0 = 1.88 \times 10^{15} \text{ rad/s}$. The initial energy of electron has been taken 1.42 MeV . If we use pre-accelerated electron at $t = 0$, then it is easy to transfer energy from laser to electron and as a result electron enhances its energy to GeV order as reflected in the study.

Figure 3.1 is a graph between normalized time with laser beam waist width $r'_0 = 50, 75, 100,$ and 125 , a fixed value of $b = 2$ and $s = 1$. From this graph we may conclude that laser spot size and beam waist affects the enhanced energy gain of electron. It is known to us that if beam waist is small, then the laser beam is relatively aligned in the short distance. We have observed an energy gain of 1920 MeV at $r'_0 = 50$ which increases to 8430 MeV for $r'_0 = 125$. As beam waist is inversely proportional to divergence of the laser beam that's why we have noticed more energy gain by electron and travels several Rayleigh lengths.

Figure 3.2 indicates the change of energy gain with $b = 0.5, 1.0, 1.5$ and 2.0 for $a_0 = 20$, laser beam waist width $r'_0 = 100$ and Hermite order $s = 1$. We have noticed that the 'b' value affects the energy gain. When we have employed $b = 0.5, 1.0, 1.5,$ and 2.0 , then we have observed an energy gain of $1723 \text{ MeV}, 2417 \text{ MeV}, 4017 \text{ MeV}$ and 7608 MeV respectively due to increase in axial direction.

Figure 3.3. shows the variation of electron energy gain with normalized time at $a_0 = 10, 15, 20$ and 25 , $r'_0 = 68, 80, 103$ and 118 , $b = 1$ and $s = 1$. It is cleared from the study that increase in the intensity increases energy gain along propagation of laser beam. For $a_0 = 10, 15, 20$ and 25 an energy gain of about $1126 \text{ MeV}, 1583 \text{ MeV}, 2588 \text{ MeV}$

and 3256 MeV respectively have been noticed. It is at lowest order of Hermite function. The ponderomotive force generally includes the Lorentz force that a charged particle (electron) experiences in an inhomogeneous oscillating electro-magnetic field. In the leading edge portion electrons are accelerated with high energies. In the falling edge their energy gain almost saturated [33]. Also, with increase in r'_0 , the divergence is minimized. As a whole in case of increase in a_0 and r'_0 a remarkable energy gain has been noticed. The value of r'_0 are not in regular way in this case which has been discussed in next paragraph.

To get near about same amount of energy gain by electron another graph has been drawn. The above fact has been depicted in figure 3.4. To draw this figure, we have selected the various parameters as $a_0 = 10, 15, 20, 25$; $r'_0 = 10$; $b = 1$ and $s = 3$. Though the beam waist $r'_0 = 10$ is very low, yet we have observed the same (\approx) amount of energy gain as in figure 5.3 where r'_0 has been selected in such a way that both the energy gain at $s=1$ and $s=3$ will be near equal to same. In this case a noticeable parameter is $s = 3$ which manage the divergence of laser beam. Higher order of Hermite function imposes a better trapping of electron. As a result we observe a larger acceleration process for smaller distance. So here we can conclude that Hermite order (s) also plays an important role on electron acceleration.

Figure 3.5. shows the role of Hermite order on electron acceleration. As discussed in figure 5.4. To get same amount of energy we have to use larger beam waist width (r'_0) for lower Hermite order (s) and smaller beam waist width (r'_0) for higher Hermite order (s).

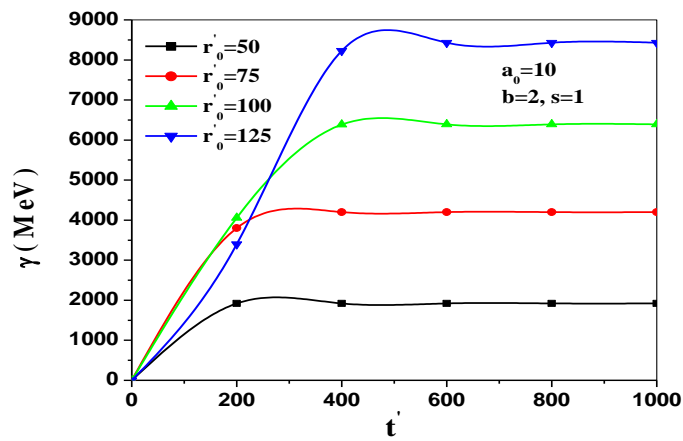


Figure 3.1. Electron's energy gain with the normalized time for different values of $r'_0 = 50, 75, 100,$ and 125 at $a_0 = 10, b = 2.0$ and $s = 1$.

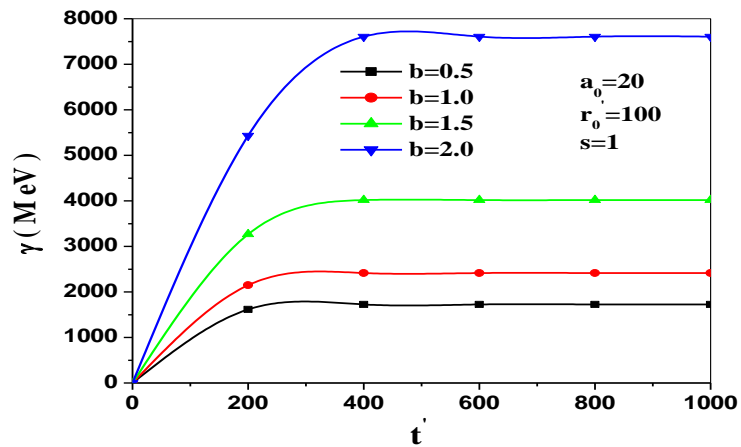


Figure 3.2. Electron's energy gain with normalized time for $b = 0.5, 1.0, 1.5,$ and 2.0 for $a_0 = 20, r'_0 = 100$ and $s = 1$.

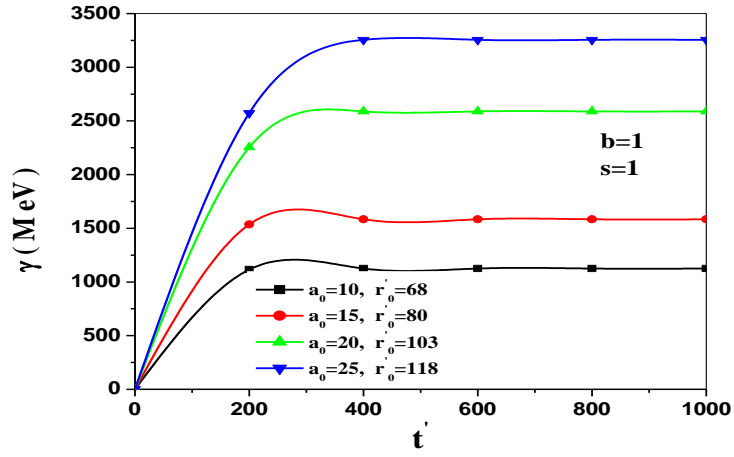


Figure 3.3. Electron's energy gain with normalized time for $a_0 = 10, 15, 20,$ and 25 for $r'_0 = 68, 80, 103, 118, b = 1$ and $s = 1$.

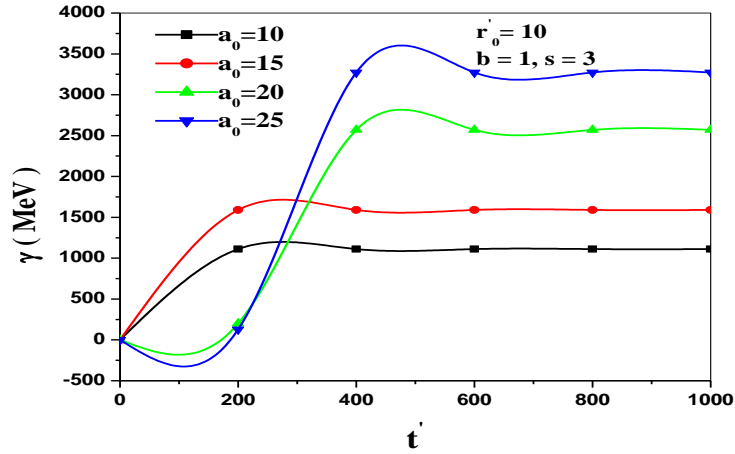


Figure 3.4. Electron's energy gain with normalized time for specific values of the laser intensity parameter $a_0 = 10, 15, 20, 25$ for $r'_0 = 10, b = 1$ and $s = 3$.

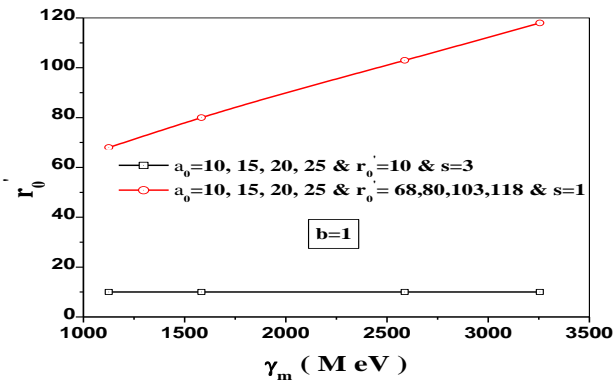


Figure 3.5. Electron's energy gain with laser beam waist width for $a_0 = 10, 15, 20, 25$, $b = 1$ and $s = 1$ & 3.

3.1.1.3 Conclusion:

This study is the first to demonstrate analytically the use of an RP HChG laser beam in vacuum. Increases in the decentered parameter (b) have resulted in a significant change in electron energy gain. The same foundation has been used to the order of the Hermite function (s), which is likewise important in electron acceleration in vacuum. The study looked at the relationship between beam waist width and laser beam divergence. The properties associated with this "golden profile" allow electrons to be easily captured and accelerate up to the order of GeV, which is ideal for future research. By choosing the right laser intensity parameter, beam waist width, decentered parameter, and Hermite order, electrons can increase their energy up to 8.43 GeV without using frequency chirp or an external magnetic field. As a result, the phrase "golden profile" has been used.

3.1.2 Effect of polarization on Hermite-Cosh-Gaussian laser beam

3.1.2.1 Electron dynamics

Consider the propagation of a HChG laser with electric and magnetic field as given below:

$$\mathbf{E} = \hat{x}E_x + \hat{y}E_y \quad (3.10)$$

$$E_x = E_0 H_s \left(\frac{r}{r_0} \right) \cosh\left(\frac{br}{r_0}\right) e^{-\left(\frac{r^2}{r_0}\right)} \cos\phi \quad (3.11)$$

$$E_y = \alpha E_0 H_s \left(\frac{r}{r_0} \right) \cosh\left(\frac{br}{r_0}\right) e^{-\left(\frac{r^2}{r_0}\right)} \sin\phi \quad (3.12)$$

$$\mathbf{B} = \frac{\mathbf{k} \times \mathbf{E}}{\omega} \quad (3.13)$$

Here, $\phi = \omega t - kz$ is the initial phase of laser, s is the mode index Hermite polynomial H_s , E_0 is the amplitude of HChG laser beam for central position at $r = z = 0$, r_0 is the initial spot size of the laser; b is the laser's decentered parameter and $r^2 = x^2 + y^2$. Here, $\alpha = 0$ for LP laser and $\alpha = 1$ for the CP laser. The related magnetic field has been calculated by using Maxwell's equation, $\nabla \times \mathbf{E} = -\partial \mathbf{B} / \partial t$.

The momentum and energy can be calculated from the equation $\frac{d\mathbf{P}}{dt} = -e(\mathbf{E} + \mathbf{v} \times \mathbf{B})$ and $\gamma^2 = 1 + (P_x^2 + P_y^2 + P_z^2)/m_0^2 c_0^2$ using the relativistic Newton-Lorentz equations of motion. The electron momentum and energy can be deduced from the following equations:

$$\frac{dP_x}{dt} = e[E_x - v_z B_y]. \quad (3.14)$$

$$\frac{dP_y}{dt} = e[E_y + v_z B_x] \quad (3.15)$$

$$\frac{dP_z}{dt} = e[v_x B_y - v_y B_x]. \quad (3.16)$$

$$\gamma = \left(1 + \frac{(P_x^2 + P_y^2 + P_z^2)}{m_0^2 c_0^2} \right)^{1/2} \quad (3.17)$$

Here, γ is the Lorentz factor, $P_x = \gamma m_0 v_x$, $P_y = \gamma m_0 v_y$ and $P_z = \gamma m_0 v_z$. Throughout this chapter, we normalized time by $1/\omega$, length by $1/k$ and velocity by $1/c$. We have used the following normalized parameters, $a_0 = \frac{eE_0}{m_0\omega c}$, where e is the charge and m_0 is the rest mass of electron.

3.1.2.2 Observation and Discussion:

The plot 3.6 (a) represents the disparity of maximum energy gain at a fixed value of initial velocity $v_z = 0$ for different intensity parameter. Where 3.6 (b) has been plotted for $v_z = 0.4$ and all other parameters are same. Both the plots have been plotted for LP and CP laser to compare the study. It is clear from the plot that electron gains more energy for CP laser. In this case ponderomotive force and initial velocity of electron play a crucial role on energy enhancement. For CP laser pulse, effective transfer of energy from laser to electron has been noticed. Which is reflected in the energy gain. As axial symmetry is in CP laser, we get the laser as an energy gain. When $v_z = 0.4$ we have noticed $\approx 84\%$ energy gain in case of CP than LP laser.

Figure 3.7 represents the change in energy with respect to normalized time for CP and LP laser. here we have plotted three pairs for $a_0 = 5, 10, 15$ and the other parameters are shown on the plots. Increase in intensity parameter increases the energy gain along propagation of laser beam. When electron interacts with leading edge of the laser wave, electron are captured by laser and electron accelerates with higher and higher energies buy in case of trailing edge, electron's energy remains constant.

In figure 3.8 we have selected we have selected $b = 0.5, 1.0, 1.5, 2.0$ and 2.5 . As we the value of b along the axial direction, intensity distributed properly. This signifies that a rise in focal depth compresses the focal spot size and enhances the energy gain. We have recorded 1.254 GeV energy gain for $b = 0.5$ which increases up to 7.948 GeV for $b = 2.5$ at $v_z = 0$. But when initial velocity of electron increases from 0 to 0.4 , then maximum energy gain has been noticed 1.678 GeV to 12.791 GeV for $b = 0.5$ and $b = 2.5$

respectively. This energy difference occurs due to decentered parameter which controls self focusing and trapping phenomenon. So decentered parameter plays a vital role on electron acceleration scenario.

Figure 3.9 and 3.10 represents the plot between maximum energy gain and initial velocity of electron (v_z) and the other parameters are depicted on the plot. Dependence of (v_z) on maximum energy gain has been noticed properly. It is also very much prominent the maximum energy difference in case of CP than LP laser. it is due to the symmetrical distribution of intensity for CP laser pulse.

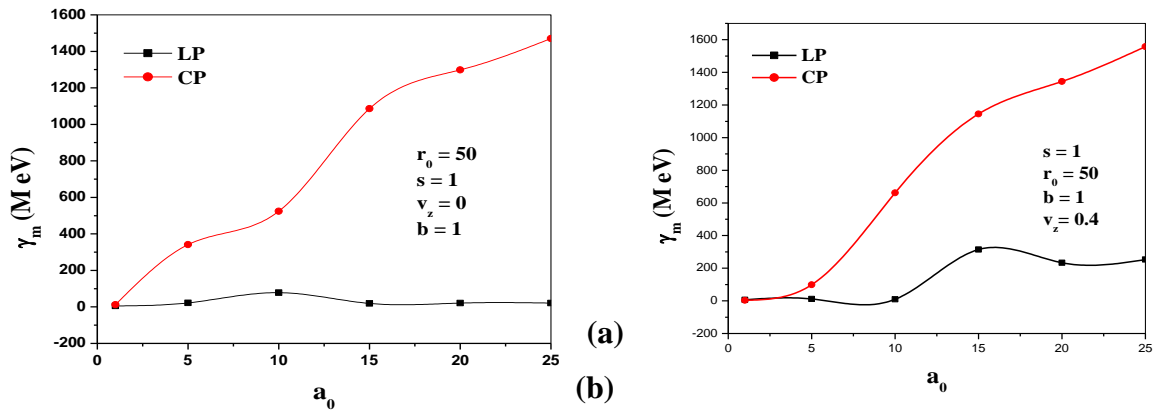


Figure 3.6 represents the changing of maximum energy gain (γ_m) with intensity parameter (a_0) for $b=1$, $s=1$, $r_0 = 50$ for CP and LP HChG laser pulse. $v_z = 0$ for fig. 3.6 (a) and $v_z = 0.4$ for fig.3.6 (b).

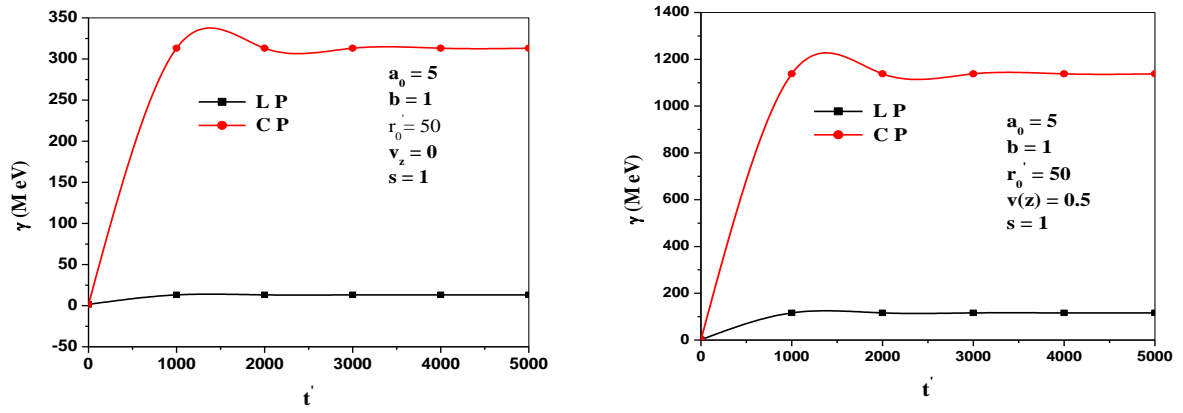


Fig. 3.7 (a)

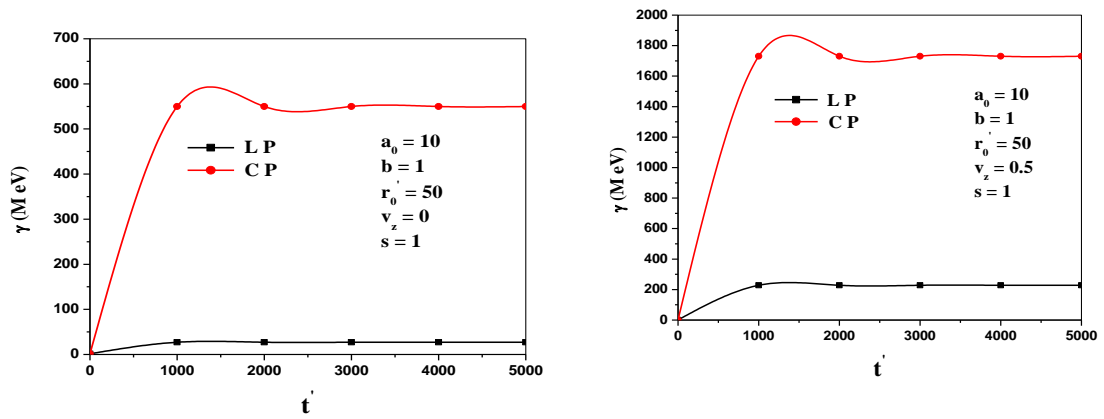


Fig. 3.7(b)

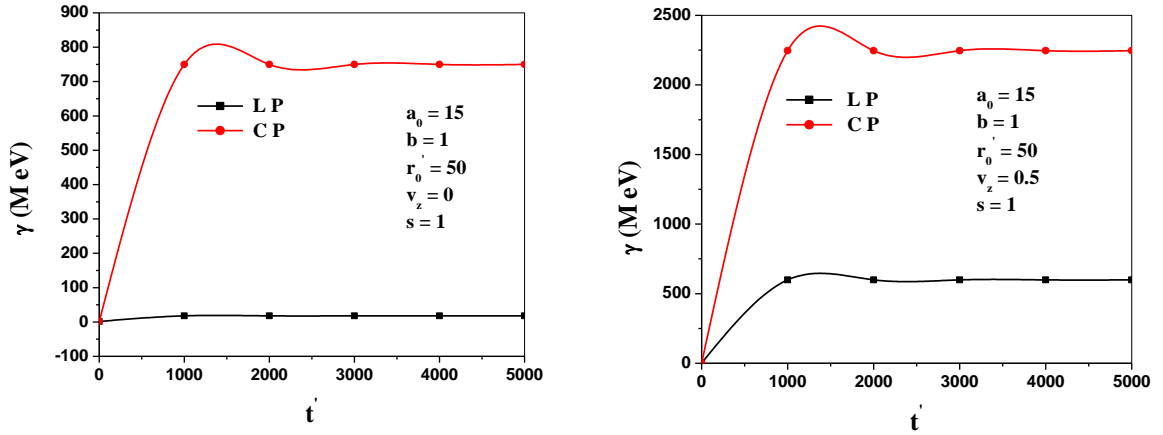


Fig. 3.7(c)

Figure 3.7 displays the changing of γ_m with t' for $a_0 = 5, 10, 15$ for fig 3.7 (a), 3.7 (b) and 3.7 (c) respectively and $b = 1, s = 1, r_0 = 50$ for CP and LP HChG laser pulse. $v_z = 0, 0.5$.

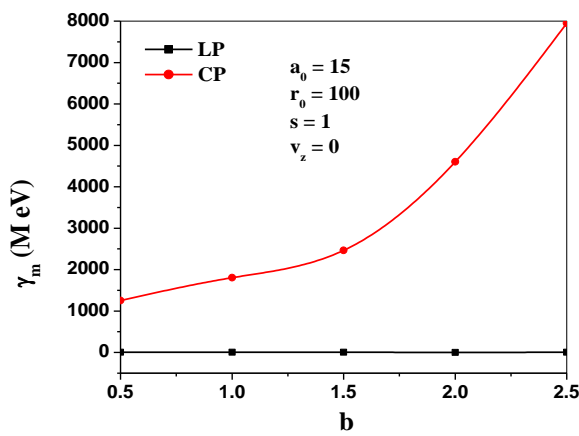


Fig. 3.8 (a)

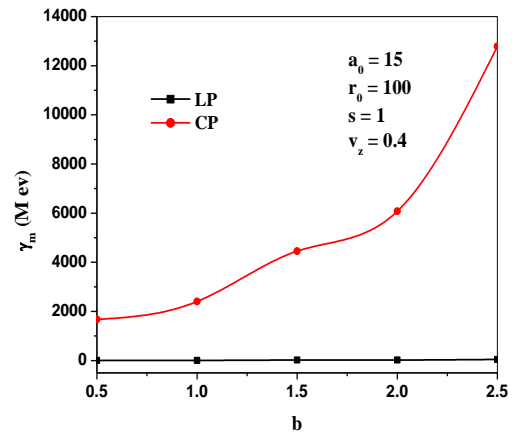


Fig. 3.8 (b)

Figure 3.8. The variation of γ_m with b for $a_0 = 15, s = 1, r_0 = 100$ for CP and LP HChG laser pulse. $v_z = 0$ for fig. 3.8 (a) and $v_z = 0.4$ for fig. 3.8 (b).

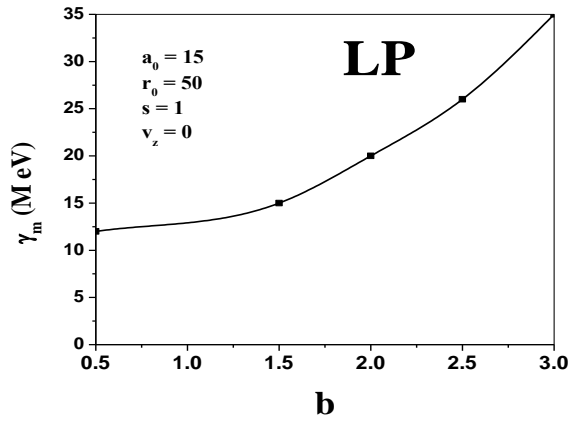


Fig. 3.9 (a)

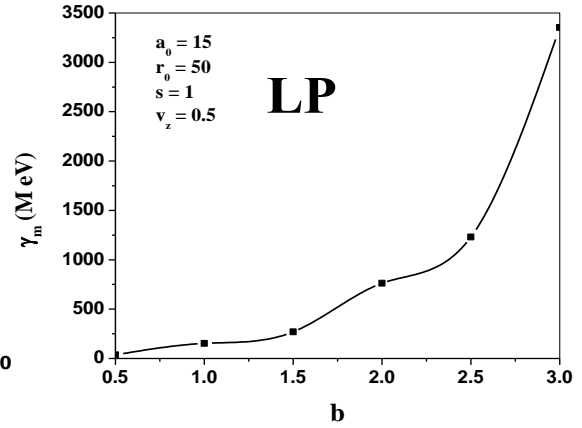


Fig. 3.9(b)

Fig. 3.9 displays the variation between γ_m with different values of b at fixed $a_0 = 15$, $r_0 = 50$, $s = 1$ and $v_z = 0.5$ for LP HChG laser pulse.

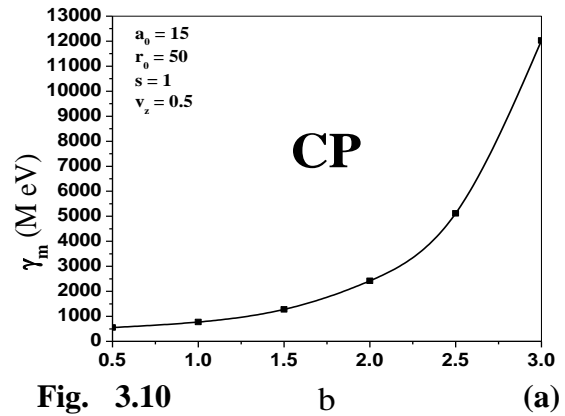
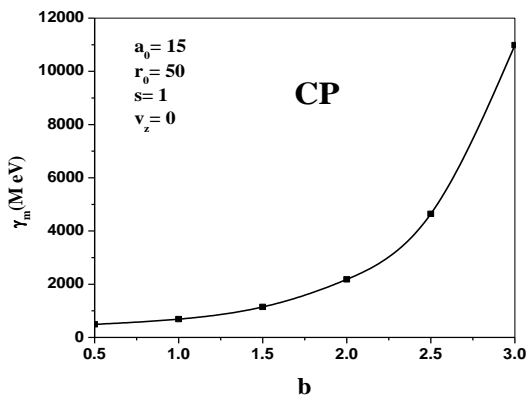


Fig. 3.10 (a)

Fig. 3.10 (b)

Fig. 3.10 depicts the variation between γ_m with different values of b at fixed $a_0 = 15$, $r_0 = 50$, $s = 1$ and $v_z = 0.5$ for CP HChG laser pulse.

3.1.2.3 Conclusion

This research work is the outcome of comparison between LP and CP HChG laser beam in vacuum. The main research is electron acceleration scenario that means energy gain. As we know polarization plays a vital role on acceleration process, which is also reflected in this study. We have successfully noticed more energy gain surely in the order of GeV in case of CP laser than LP laser. We have also observed that the increase in decentered parameter, enhances the energy. Energy gain is also increased as we increase v_z . This research work might be helpful for the study of remote sensing, beam splitting and air vehicle communication system.

3.1.3 Combined influence of linear chirp and axial magnetic field along with radially polarized (RP) Hermite-Cosh-Gaussian (HChG) laser beam

3.1.3.1 Electron dynamics

Consider a z direction RP HChG laser beam in vacuum. The field of this laser profile is given by

$$\vec{E} = \hat{r}E_r + \hat{z}E_z \quad (3.18)$$

Where, the transverse component of electric field is expressed as

$$\vec{E}_r = \hat{r}E_0 H_s \left(\frac{\sqrt{2}r}{r_0} \right) \cosh \left(\frac{br}{r_0} \right) e^{-\left(r^2/r_0^2 \right)} e^{i(kz - \omega t)} \quad (3.19)$$

here, E_0 , r_0 , r , s and b signify the amplitude, beam width, radial distance, hermite order, decentered parameter respectively of Cosh function. With the help of Maxwell's equations in vacuum, $\vec{\nabla} \cdot \vec{E} = 0$ we can find out the longitudinal component and represented as:

$$\vec{E}_z = -\hat{z} \frac{i}{kr} E_r \left[1 + 2S\sqrt{2} \frac{r}{r_0} \frac{H_{s-1} \left(\frac{\sqrt{2}r}{r_0} \right)}{H_s \left(\frac{\sqrt{2}r}{r_0} \right)} + b \frac{r}{r_0} \tanh \left(b \frac{r}{r_0} \right) - 2 \frac{r^2}{r_0^2} \right] \quad (3.20)$$

To investigate the momentum and energy of electron, we have to use the following equation

$$\vec{F} = \frac{\partial \vec{p}}{\partial t} = -e [\vec{E} + (\vec{v} \times \vec{B})] \quad (3.21)$$

The external axial magnetic is expressed as: $\vec{B}_s = \hat{z}B_0$

Where, B_0 is the peak value.

From the above eq. (7.4), momentum, energy and velocity equations are written as

$$\frac{dp'_r}{dt'} = a_0 H_S \left(\frac{\sqrt{2}r'}{r'_0} \right) \cosh \left(\frac{br'}{r'_0} \right) e^{-\left(r'^2/r_0'^2\right)} e^{i(k'z' - t')} (v'_z - 1) - v'_\theta b_0 \quad (3.22)$$

$$\frac{dp'_\theta}{dt'} = v'_r b_0 \quad (3.23)$$

$$\begin{aligned} \frac{dp'_z}{dt'} = a_0 H_S \left(\frac{\sqrt{2}r'}{r'_0} \right) \cosh \left(\frac{br'}{r'_0} \right) e^{-\left(r'^2/r_0'^2\right)} & \left[\sin(k'z' - t') \left[1 + 2S\sqrt{2} \frac{r'}{r'_0} \frac{H_{S-1} \left(\frac{\sqrt{2}r'}{r'_0} \right)}{H_S \left(\frac{\sqrt{2}r'}{r'_0} \right)} + \right. \right. \\ & \left. \left. b \frac{r'}{r'_0} \tanh \left(b \frac{r'}{r'_0} \right) - 2 \frac{r'^2}{r_0'^2} \right] + v'_r \cos(k'z' - t') \right] \quad (3.24) \end{aligned}$$

$$\begin{aligned} \frac{dv'_r}{dt'} = -v'_r a_0 H_S \left(\frac{\sqrt{2}r'}{r'_0} \right) \cosh \left(\frac{br'}{r'_0} \right) e^{-\left(r'^2/r_0'^2\right)} & \cos(k'z' - t') - v'_\theta b_0 + v'_r v'_\theta b_0 - \\ \frac{v'_z}{k'r'} a_0 H_S \left(\frac{\sqrt{2}r'}{r'_0} \right) \cosh \left(\frac{br'}{r'_0} \right) e^{-\left(r'^2/r_0'^2\right)} & \sin(k'z' - t') \left[1 + 2S\sqrt{2} \frac{r'}{r'_0} \frac{H_{S-1} \left(\frac{\sqrt{2}r'}{r'_0} \right)}{H_S \left(\frac{\sqrt{2}r'}{r'_0} \right)} + \right. \\ & \left. b \frac{r'}{r'_0} \tanh \left(b \frac{r'}{r'_0} \right) - 2 \frac{r'^2}{r_0'^2} \right] \quad (3.25) \end{aligned}$$

$$\frac{dv'_z}{dt'} = \frac{a_0}{c_1} H_S \left(\frac{\sqrt{2}r'}{r'_0} \right) \cosh \left(\frac{br'}{r'_0} \right) e^{-\left(r'^2/r_0'^2\right)} \cos(k'z' - t') (v'_z - 1) - \frac{b_0}{c_1} v'_\theta \quad (3.26)$$

$$\frac{dv'_\theta}{dt'} = \frac{b_0}{c_2} v'_r \quad (3.27)$$

$$\begin{aligned} \frac{dv'_z}{dt'} = -\frac{1}{k'r'} \frac{a_0}{c_3} H_S \left(\frac{\sqrt{2}r'}{r'_0} \right) \cosh \left(\frac{br'}{r'_0} \right) e^{-\left(r'^2/r_0'^2\right)} & \sin(k'z' - t') \left[\left[1 + 2S\sqrt{2} \frac{r'}{r'_0} \frac{H_{S-1} \left(\frac{\sqrt{2}r'}{r'_0} \right)}{H_S \left(\frac{\sqrt{2}r'}{r'_0} \right)} + \right. \right. \\ & \left. \left. b \frac{r'}{r'_0} \tanh \left(b \frac{r'}{r'_0} \right) - 2 \frac{r'^2}{r_0'^2} \right] - v'_r \frac{a_0}{c_3} H_S \left(\frac{\sqrt{2}r'}{r'_0} \right) \cosh \left(\frac{br'}{r'_0} \right) e^{-\left(r'^2/r_0'^2\right)} \cos(k'z' - t') \right] \quad (3.28) \end{aligned}$$

Here, $P_r = \gamma m_0 v_r$, $P_\theta = \gamma m_0 v_\theta$ and $P_z = \gamma m_0 v_z$. $\gamma^2 = 1 + (p_r^2 + p_\theta^2 + p_z^2)/m^2 c^2$. The normalized parameters are as follows: $a_0 = \frac{eE_0}{m\omega_0 c}$, $t' = \omega_0 t$, $r'_0 = \frac{\omega_0 r_0}{c}$, $r' = \frac{\omega_0 r}{c}$, $z' =$

$$\frac{\omega_0 z}{c}, v'_r = \frac{v_r}{c}, v'_\theta = \frac{v_\theta}{c}, v'_z = \frac{v_z}{c}, p'_r = \frac{p_r}{mc}, p'_\theta = \frac{p_\theta}{mc}, p'_z = \frac{p_z}{mc}, \gamma' = \frac{\gamma}{mc^2}, k' = \frac{kc}{\omega_0} \text{ and } b_0 = \frac{eB_0}{m\omega_0 c}.$$

3.1.3.2 Result and Discussion:

In this chapter, the analytical and numerical calculations have set up the different parameters in the following ways: normalized intensity parameter $a_0 = 10$ (corresponding intensity $\sim 1.36 \times 10^{20} \text{ Wcm}^{-2}$), $a_0 = 15$ (corresponding intensity $\sim 3.07 \times 10^{20} \text{ Wcm}^{-2}$), $a_0 = 20$ (corresponding intensity $\sim 5.47 \times 10^{20} \text{ Wcm}^{-2}$), and the laser wavelength λ is $1\mu\text{m}$. The angular frequency of laser beam is $\omega_0 = 1.88 \times 10^{15} \text{ rad/s}$. The initial energy of electron has been taken 1.42 MeV . If we use pre-accelerated electron at $t = 0$, it is easy to transfer energy from laser to electron and as a result electron enhances its energy to GeV order as reflected in the study.

The variation of energy gain (γ) has been studied in Figure 3.11. with normalized time (t') for three categories: without chirp, with chirp and chirp with axial magnetic field. Due to two key parameters b and s connected with this beam, the beam focuses earlier which controls the self-focusing phenomenon. As a result, laser beam passes its energy to injected electron and electron accelerates with GeV energy for a particular parameters of laser profile. Same study has been depicted by employing linear frequency chirp. We have noticed higher energy gain up to the order of GeV. From fig 3.11 (a) we have noticed maximum energy gain (γ_m) 3356 MeV , 3624 MeV and 5185 MeV for without chirp, with chirp and chirp with axial magnetic field respectively with $a_0 = 10$. Similarly for fig 3.11 (b), γ_m are 4296 MeV , 6797 MeV and 8982 MeV for the similar considerations respectively with $a_0 = 15$. Because frequency chirp creates asymmetry into the laser pulse, as a result there will be several times of interaction between laser beam and electron and duration of interaction also increases. That's why we have noticed more energy gain. Again, if we employ external axial magnetic field energy gain will be noticed and we have noticed significant energy gain. For fig. 3.11(a) and 3.11 (b) the optimum magnetic field is 0.019 which corresponds to magnetic field 2.03 MG . Magnetic field not only creates

betatron resonance but also enhances $\vec{v} \times \vec{B}$ force. As a result electron spends more time in laser's field. Hence electron enhances its energy and retains the same energy for several Rayleigh length. We have drawn two graphs on the basis of this study. Figure 3.11 (a) is for $a_0 = 10, r'_0 = 100, b = 1.5$ and $s = 1$ and figure 3.11(b) is for $a_0 = 15, r'_0 = 75, b = 2$ and $s = 1$. In case of figure 3.11(b) we have noticed more energy gain in comparison with figure 3.11(a) as various parameters change.

In figure 3.12, we have shown the changes of maximum energy gain (γ_m) Vs decentered parameter (b) graph for without chirp (black line), with chirp (red line) and combined effect of chirp with magnetic field (green line). We have changed the intensity parameter (a_0) from 10 to 15 to 20 which means captured and accelerated electron travels a longer distance with longer time. In this case, electron enhances its energy significantly at the rising edge of laser pulse and at the trailing edge electron's energy saturates due to ponderomotive force of laser. Increase in beam waist parameter (r'_0), increases the energy gain because divergence of laser beam decreases. Hence it is easy to gain energy. Moreover, decentered parameter (b) controls the intensity distribution. Also increase in decentered parameter (b) increases the axial intensity distribution. As a whole electron enhances more and more energy by changing a_0, r'_0 and b for without chirp, with chirp and chirp with axial magnetic field. The result according to this study has been shown in table 3.1. Different parameters of graph 3.12 (a), 3.12 (b) and 3.12 (c) have been displayed in the graphs and as well as in table 3.1.

Figure 3.13. is a calibration curve. The figure exhibits the variation of γ_m and linear frequency chirp parameter (α) as a function of decentered parameter (b) with $a_0 = 15, r'_0 = 75$, and $s = 1$. The optimum value of frequency chirp parameter decreases as we increase decentered parameter, whereas, maximum energy gain (γ_m) gradually rises with increase in decentered parameter (b). In this scenario the maximum energy gain (γ_m) attains 6.797 GeV at $b = 2$ and $\alpha = -0.000039$. This means at the lowest value of 'b' frequency chirp optimizes at higher value. In this particular variation we have also noticed that electron enhances higher energy at higher value of 'b' and attains maximum energy (γ_m) at lowest

value of frequency chirp parameter (α) which is optimum for that particular case. This case is for without magnetic field, only frequency chirp have been employed in this phenomena. That means decentered parameter dominates on the other parameters on electron acceleration.

Figure 3.14 shows another calibration curve. The figure displays the variation of γ_m and normalized magnetic field (b_0) with b . As γ_m and b_0 varies with 'b'. To draw this graph, we have considered $a_0 = 10$, $r'_0 = 75$ and $s = 1$. From this graph, it is clear that γ_m increases as increase in b and b_0 decreases with increase in b . From this study we may say that at higher value of 'b', optimum axial magnetic field (b_0) is lesser in comparison with other set of b and b_0 which has been shown in table 3.2. At lower optimum axial magnetic field (b_0) we have noticed maximum energy gain (γ_m) because the intensity distribution is directly proportional to the decentered parameter. This signifies that the compression of the focal size enhances the energy. This is good for future accelerator. So, we can produce low-cost accelerator in such process and the treatment cost of radiation therapy will be feasible to the patient. Relevant table has been shown in the figure 3.12.

In figure 3.15., we have drawn the graph between normalized axial magnetic field (b_0) with the various values of b and optimum value of α with b . We have changed $b = 0.5, 1, 1.5$ and 2 for a fixed amount of maximum energy gain (γ_m) 3 GeV at $a_0 = 10$, $r'_0 = 100$ and $s = 1$. Here, it is clear that increase in decentered parameter (b), decreases the normalized optimum axial magnetic field (b_0) and optimum linear chirp parameter (α). This signifies that focal

depth increases and focal spot compresses as a result external magnetic field attains the optimum value at which electron strongly enhances the energy gain.

FIGURES AND TABLES

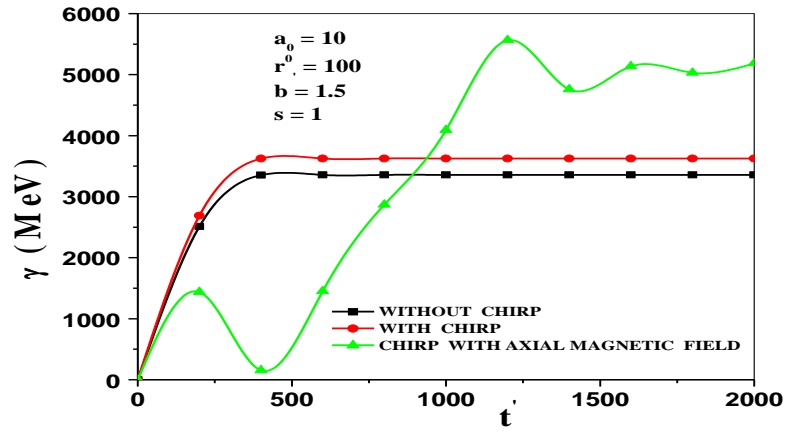


Figure 3.11 (a) shows the variation of electron's energy gain (γ) with normalized time (t') at $a_0 = 10$, $r'_0 = 100$, $b = 1.5$ and $s = 1$ for without chirp, with chirp and chirp with axial magnetic field.

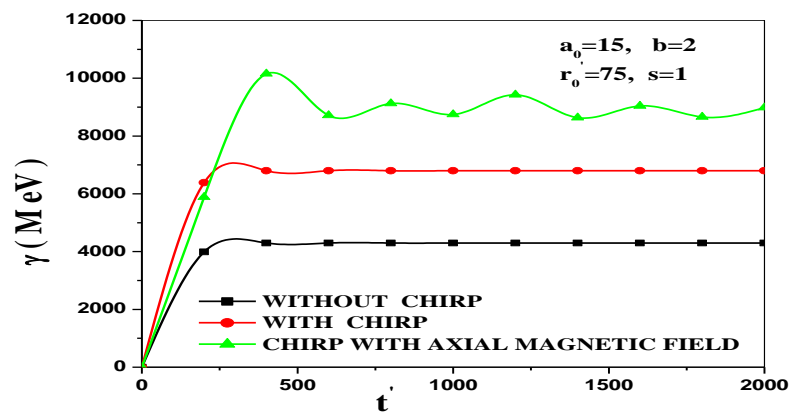


Figure 3.11 (b) shows the variation of γ with t' at $a_0 = 15$, $r'_0 = 75$, $b = 2$ and $s = 1$ for without chirp, with chirp and chirp with axial magnetic field.

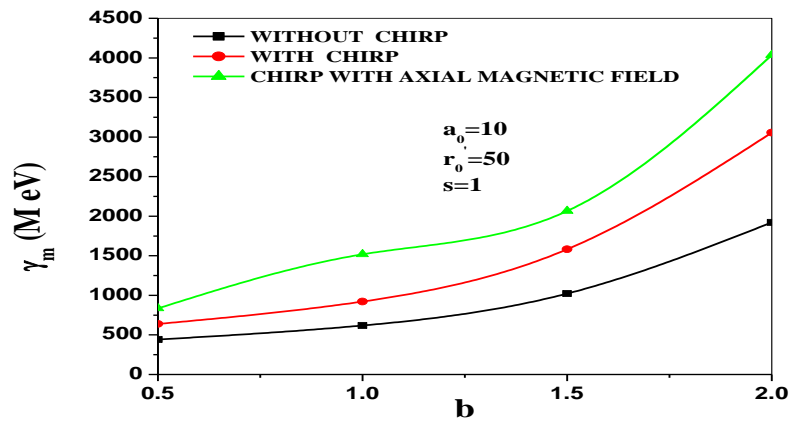


Figure 3.12 (a) shows the variation of γ_m with various b at $a_0 = 10$, $r'_0 = 50$ and $s = 1$ for without chirp, with chirp and chirp with axial magnetic field.

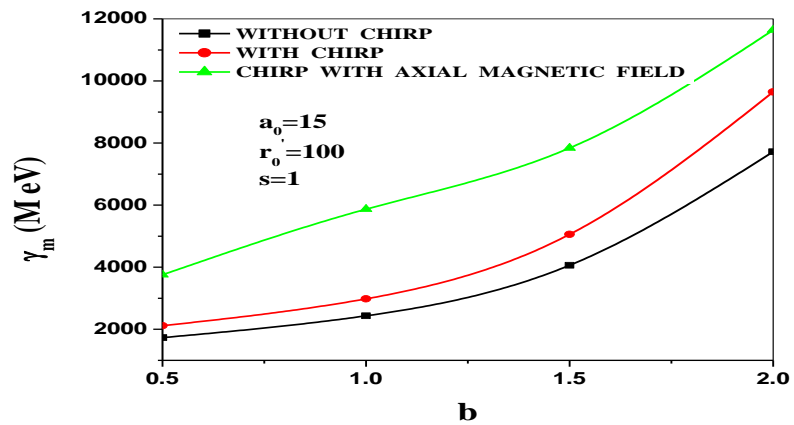


Figure 3.12 (b) shows the variation of γ_m with various b at $a_0 = 15$, $r'_0 = 100$ and $s = 1$ for without chirp, with chirp and chirp with axial magnetic field.

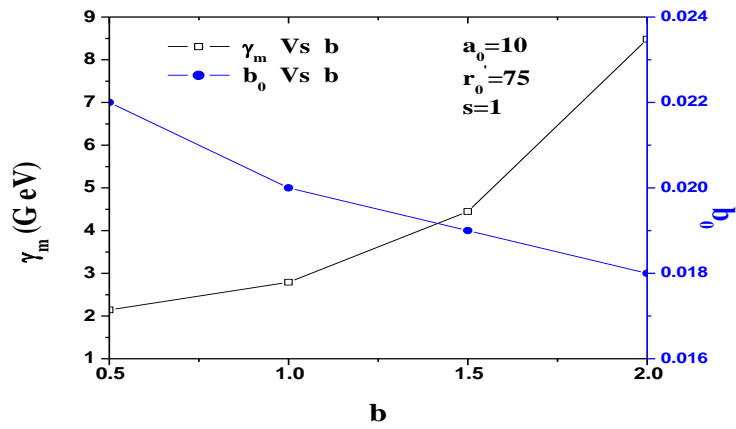


Figure 3.12 (c) shows the variation of γ_m with various b at $a_0 = 20$, $r'_0 = 75$ and $s = 1$ for without chirp, with chirp and chirp with axial magnetic field.

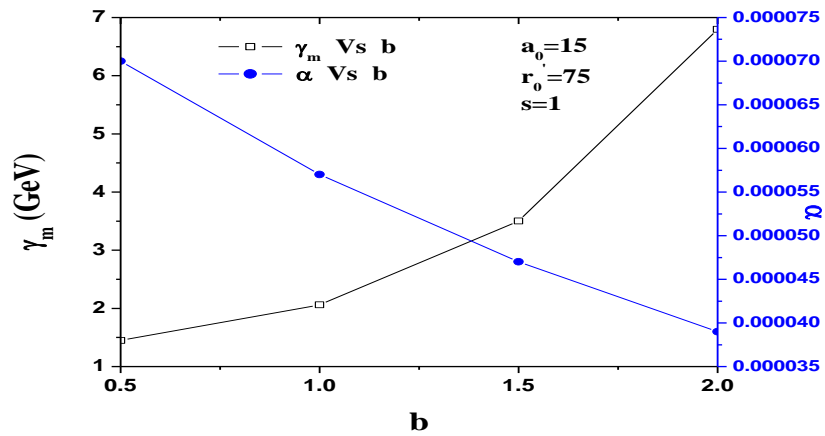


Figure 3.13 shows the variation of γ_m with b and α with b at fixed $a_0 = 15$, $r'_0 = 75$ and $s = 1$.

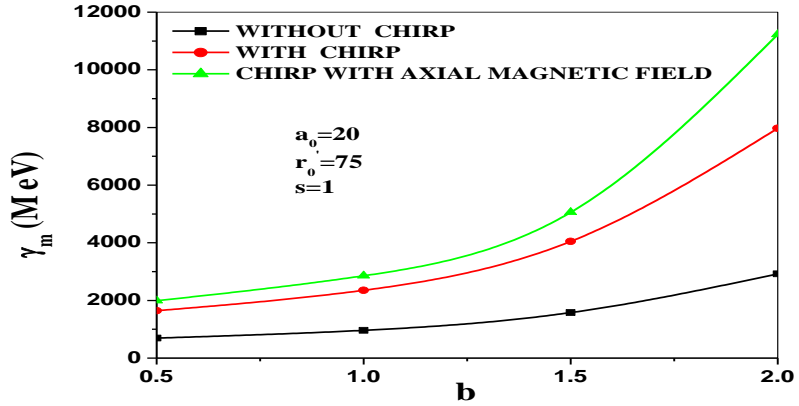


Figure 3.14 shows the variation of γ_m with b and b_0 with b at $a_0 = 10, r'_0 = 75$ and $s = 1$.

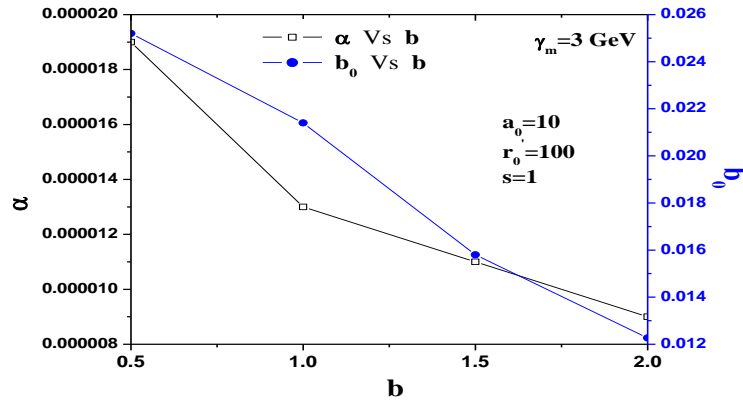


Figure 3.15 shows the variation of α with b and b_0 with b at fixed maximum energy gain $\gamma_m = 3\text{GeV}$, $a_0 = 10, r'_0 = 100$ and $s = 1$.

Maximum Energy Gain (γ_m) in MeV			
	Without Chirp	With Chirp	Chirp with Axial Magnetic Field
Fig. 2(a)	1920	3055	4032
Fig. 2(b)	7716	9648	11637
Fig. 2(c)	2923	7973	11226

Table 3.1. provides the value of maximum energy gain (γ_m) : fig. 3.12 (a) is for $a_0 = 10, r'_0 = 50, s = 1$; fig. 3.12 (b) is for $a_0 = 15, r'_0 = 100$ and $s = 1$; fig. 3.12 (c) is for $a_0 = 20, r'_0 = 75$ and $s = 1$ for without chirp, with chirp and chirp with axial magnetic field respectively.

		Decentered parameter (b)			
		0.5	1.0	1.5	2.0
Optimum Normalized Magnetic Field (b_0)	Fig. 4	0.022	0.020	0.019	0.018
Maximum Energy Gain (γ_m in GeV)	Fig. 4	2.144	2.791	4.447	8.481

Table 3.2. is showing the result of optimum axial magnetic field (b_0), maximum energy gain (γ_m) correspond to decentered parameter $b = 0.5, 1, 1.5$ and 2 respectively.

3.1.3.3 Conclusion:

In the theoretical and analytical study, we have used RP HChG laser beam for efficient electron acceleration in vacuum. Role of linear frequency chirp (negative chirp) and axial magnetic field have highlighted here to secure high electron energy gain. Energy gain (γ) and maximum energy gain (γ_m) have been studied by varying different parameters, such as: a_0 , r'_0 , b_0 , b and α . We have also observed the variation between linear chirp parameter (α) and optimum external axial magnetic field (b_0) with decentered parameter (b). In both the cases they (α and b_0) are inversely proportional to decentered parameter (b). A significant result has been noticed throughout this research. The properties associated with this "golden profile" allow electrons to be easily captured and accelerate up to the order of GeV, which is ideal for future research. Hopefully this study will minimize the cost of future accelerator and help to medical science for better radiation treatment & also reduce the expense of radiation treatment.

CHAPTER-4

Study of electron acceleration phenomena by employing different laser pulse envelope in vacuum

4.1 Introduction

Laser driven electron acceleration is one of the most spellbinding and promising area of scientific research. Also several frontier research area have flourished by this mechanism in vacuum and plasma. Laser techniques have marked the beginning of a new era for the generation of high energy protons, electrons, and ions [115]. The laser driven electron acceleration in vacuum medium is being analyzed for the last few decades theoretically [2, 22, 23, 25, 26] and as well as experimentally [18, 27-29]. Such acceleration mechanism is making quick development in scientific research because of its pivotal role in the field of industry & science [1-3], study of fundamental forces, tumor therapy [4,5] etc. In the laser electron acceleration scenario, the center of the propagation path traps and accelerates electron to high energies (GeV) [11] with accelerating gradients GeV/m. This technique is useful for developing the solution of relativistic Newton-Lorentz force equation of motion theoretically. An intense, tightly-focused, ultra-short laser pulse fulfills the aim because of generation of an intense electric field. We can achieve high energy electron beam from such pulse directly in vacuum with direct laser acceleration (DLA) mechanism [8, 9], laser wakefield acceleration (LWFA) [6,7] and in a plasma [116]. Cosh Gaussian (ChG) [114], Hermite Gaussian (HG) [131] and Hermite Cosh Gaussian (HChG) [160] laser profiles have been promising laser profiles in this field. In 1988, Hora [32] was the pioneer to invent vacuum acceleration by nonlinear mechanism. There are some advantages of vacuum over plasma: instabilities are vanished in vacuum, and electron injection technique in vacuum is easier than plasma. As a result, electron encounters

repeated phases of acceleration and deceleration regardless of their speed so the Lawson-Woodward theorem prohibits under the following conditions: (1) The laser field in vacuum has no boundary. (2) There are no static electric and magnetic fields. (3) The interaction region is endless. (4) The electron moves with speed of light (c) along the acceleration path. (5) Ponderomotive effects are neglected [33, 117]. So, Lawson-Woodward theorem gives the limit of laser vacuum acceleration. The first concept of electron acceleration came from Tajima and Dawson four decades ago [10]. Experimentally, Malka et al., [18] first ensured electron acceleration in vacuum and noted MeV energies. For their set up, they employed 10^{19} W/cm², 300 fs LP intense laser pulse. First, experimentally electron acceleration in the laser wakefield had been performed by Amiranoff et al., [77]. Polarization characteristics also play a crucial role in transferring energy on laser driven charged particle acceleration. Better trapping has been investigated in case of radially polarized (RP) laser pulse [118]. It has also been noticed that higher energy gain occurs when we employ CP laser pulse in comparison with others [119]. Tightly focused chirped pulse with magnetic field have also played a key role on acceleration scenario in vacuum. Kant et al., [120] also verified it. They showed that electron can enhance energy up to 5.78 GeV at intensity 1.38×10^{20} W/cm² and 8.5 MG optimum axial magnetic field. It had also been seen chirp and magnetic field both the parameters can boost up energy and achieve maximum energy gain ~ GeV and retain for larger distances [121]. Since 20th century, electron acceleration with chirped pulse amplification (CPA) technique [13] has spread worldwide and a large number of scientists have focused as an eye bird due to wide-ranging application such as: induced fusion, wakefield accelerators, industries, biology, medical sciences etc. Because chirp destroys the symmetry of phase, as a result electron accelerates and enhances its energy. It has been seen that the frequency chirp gives us a successful interaction between chirp and electron [50-52]. Singh (2005) showed that chirped pulse enhanced electron energy in vacuum [53]. In 2014, Salamin and Jisrawi showed that the absolute maximum energy was almost twice for a linear chirp than a quadratic chirp [54]. It was reported that periodic chirp enhances interaction time between electron and laser and hence, betatron resonance sustains for longer distances as a result

periodic chirp enhanced near about 2.5 folds energy gain than the liner chirp [55]. When frequency chirped laser pulse is employed with wiggler magnetic field, electron enhances energy up to 10.5 GeV in vacuum [122]. So polarization, magnetic field and chirp are the key characteristics for enhancing high energy gain. Different electron scenario has been noticed by employing different laser envelopes [54, 123, 124]. It has been studied about wakefield amplitude [125] by studying 3 districts laser envelope. Most of the authors prefer Gaussian laser pulse envelope due to its symmetry in shape. There is no skewness in the shape of Gaussian envelope. Kuri has shown that skew also affects the acceleration process [128]. Application of frequency chirp and external magnetic field have given us a lots of information time to time by several authors in their work [44, 58, 120 121].

In this chapter I have used Sin^4 , Cos^2 , trapezoidal laser pulse. I have compared Sin^4 with trapezoidal laser pulse. Sin^4 with trapezoidal laser pulse were used earlier (54) in single manner but a comparison was needed to us because more study will be required on that one. That's why I have studied trapezoidal and Cos^2 laser pulses in detail. In both these paper I have studied the role of frequency chirp and external magnetic (axial) field on these profile and I have noticed a remarkable result.

4.1.1 Comparison of different laser pulse envelopes with frequency chirp

4.1.1.1 Electromagnetic fields and electron dynamics

In a recent model for a laser pulse, the term $(\omega_0 t - k_0 z)$ has been replaced by a new term η , where ω_0 is initial frequency and k_0 is wave number. The power chirp will be written in following form: $\eta \rightarrow \eta + \alpha \eta^{n+1}$

Where, b is the dimensionless chirp parameter,

$n = 1$ gives linear chirp and $n = 2$ gives quadratic chirp and so on.

The above equation will valid when $|b\eta| < 1$.

Because chirp creates the asymmetry in the phase so Lawson-Woodward theorem is valid and as a result electron accelerates and enhances its energy.

In this study, we have considered two linearly polarized laser pulse envelopes. One is Sin^4 and another is trapezoidal pulse envelope. The transverse electric field ($\vec{E} = \hat{x}E_x$) equations of Sin^4 pulse envelope are given below:

$$\vec{E}(\eta) = \hat{x}E_0 \sin(\phi_0 + \eta) \sin^4\left(\frac{\eta}{2M}\right) \quad (4.1)$$

$$\vec{B}(\eta) = \hat{y}\frac{E_0}{c} \sin(\phi_0 + \eta) \sin^4\left(\frac{\eta}{2M}\right) \quad (4.2)$$

Where, $\phi_0 =$ Initial phase

$E_0 =$ Constant amplitude

$\eta = \omega_0 t - k_0 z$

$M =$ an integer chosen to ensure that the fields vanish at $\eta = 0$ and $\eta = 2M\pi$

The momentum and energy equations for the respective pulse envelope are given below:

$$\frac{dp_x}{dt} = -eE_x + v_z eB_y \quad (4.3)$$

$$\frac{dp_y}{dt} = 0 \quad (4.4)$$

$$\frac{dp_z}{dt} = -v_x eB_y \quad (4.5)$$

$$\frac{d\gamma}{dt} = -eE_x v_x \quad (4.6)$$

Field equation of trapezoidal pulse envelope are given below:

$$\vec{E} = \hat{x}E_0 fg \quad (4.7)$$

$$\vec{B} = \hat{y}\frac{E_0}{c} fg \quad (4.8)$$

Where, g denotes an appropriate pulse shape function, f depends on $(\omega_0 t - k_0 z)$ where

$$k_0 = \frac{\omega_0}{c}$$

For trapezoidal pulse envelope the turn-on and turn-off parameter is defined as:

$$\begin{aligned}
g(\eta) &= \frac{\eta}{5\pi} & 0 \leq \eta \leq 5\pi \\
&= 1 & 5\pi \leq \eta \leq 25\pi \\
&= -\frac{\eta}{5\pi} + 6 & 25\pi \leq \eta \leq 30\pi
\end{aligned}$$

$$\eta = \omega_0 t - k_0 z$$

$$f = \sin(\phi_0 + \eta)$$

The momentum and energy equations for the respective pulse envelope are given below:

$$\frac{dp_x}{dt} = -eE_x + v_z eB_y \quad (4.9)$$

$$\frac{dp_y}{dt} = 0 \quad (4.10)$$

$$\frac{dp_z}{dt} = -v_x eB_y \quad (4.11)$$

$$\frac{dy}{dt} = -eE_x v_x \quad (4.12)$$

$P_x = \gamma m_0 v_x$, $P_y = \gamma m_0 v_y$ and $P_z = \gamma m_0 v_z$. (v_x, v_y, v_z) are the (x, y, z) components of velocity, $\gamma^2 = 1 + (p_x^2 + p_y^2 + p_z^2)/m^2 c^2$. The all parameters have been normalized as: $a_0 = \frac{eE_0}{m\omega_0 c}$, $t' = \omega_0 t$, $r'_0 = \frac{\omega_0 r_0}{c}$, $x' = \frac{\omega_0 x}{c}$, $y' = \frac{\omega_0 y}{c}$, $z' = \frac{\omega_0 z}{c}$, $v'_x = \frac{v_x}{c}$, $v'_y = \frac{v_y}{c}$, $v'_z = \frac{v_z}{c}$, $p'_x = \frac{p_x}{mc}$, $p'_y = \frac{p_y}{mc}$, $p'_z = \frac{p_z}{mc}$, and $\gamma' = \frac{\gamma}{mc^2}$.

4.1.1.2 Results and discussion

In this analytical and numerical simulations, we have assumed the different parameters in the following way: intensity parameter $a_0 = 3$ (corresponding intensity $\sim 1.23 \times 10^{19} \text{ W/cm}^2$), with laser wavelength $\lambda = 1\mu\text{m}$ and phase varies from 0 to 2π . Figure 4.1 exhibits the relationship between enhanced energy and different initial phase of electron for trapezoidal pulse envelope as enhance energy depends on initial phase

of electron. The graph includes without chirp (black line) and chirping effect (red line). In both cases, with and without chirp, $\pi/6$ is the optimum phase. Here electron undergoes up and down phase for both the pulse shape. So, for the execution of successful resonance between electron and test pulses, initial electron phase plays a vital role. Figure 4.2 has been drawn as we apply linear frequency chirp on trapezoidal pulse envelope. This graph shows variation between maximum energy gains with dimensionless chirp parameter (b). From this graph we have obtained an optimum chirp parameter i.e 0.009. At this value of chirp parameter, we obtained maximum energy gain up to 2.697 GeV which is 1.94 times greater than without chirp. As frequency chirp breaks the symmetry of pulse, so as a result significant enhancement is obtained in electron energy gain.

5

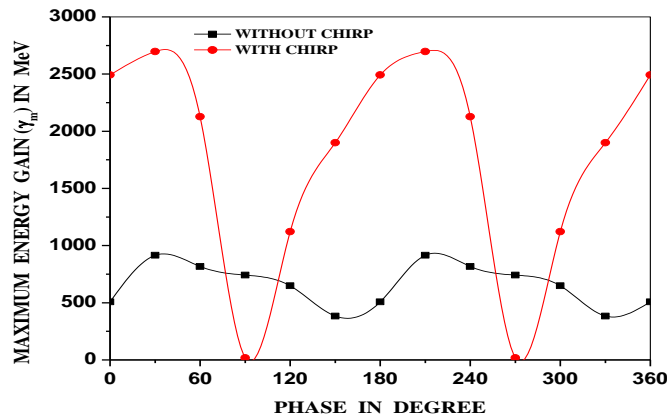


Figure 4.1. Maximum energy gain with different phase for without chirp and with chirp at intensity parameter $a_0 = 3$, for trapezoidal laser pulse envelope.

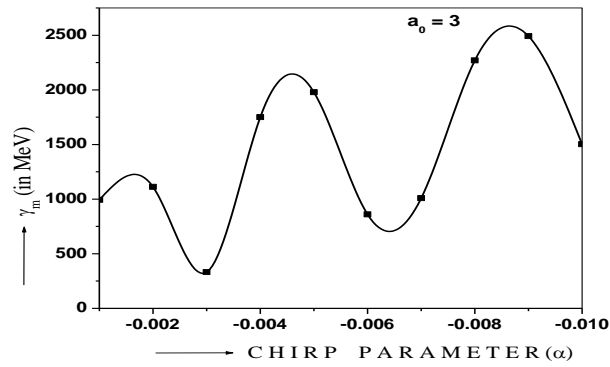


Figure 4. 2. Maximum energy gain with different chirp parameter (α) at $a_0 = 3$, for trapezoidal laser pulse envelope.

Figure 4.3 has been drawn for Sin^4 pulse envelope at intensity parameter $a_0 = 3$. It exhibits how maximum energy gain changes with chirp parameter (b). For Sin^4 pulse envelope we have taken $M = 3, 4$ and 5 . For $M = 4$ and 5 cases the optimum chirp parameter is -0.008 and for $M = 3$ it is -0.005 . As earlier discussed for trapezoidal pulse envelope chirp plays an important role on electron acceleration, we have got maximum energy gain 1.037 GeV (for $M = 3$), 1.319 GeV (for $M = 4$) and 1.095 GeV (for $M = 5$) at optimum chirp parameter. From figure 4.4, we can find out the optimum initial phase of electron for Sin^4 pulse. 0° is

the optimum phase of electron for $M = 4$ and 5 and $\pi/3$ is the optimum phase for $M = 3$ when no chirp has been employed. Results have been drawn in figure 4.5 where linear chirp has been employed. From Fig. 4.5, we have analyzed that 0° is the optimum phase for $M = 3$ and $2\pi/6$ is the optimum phase for $M = 4$ and 5 .

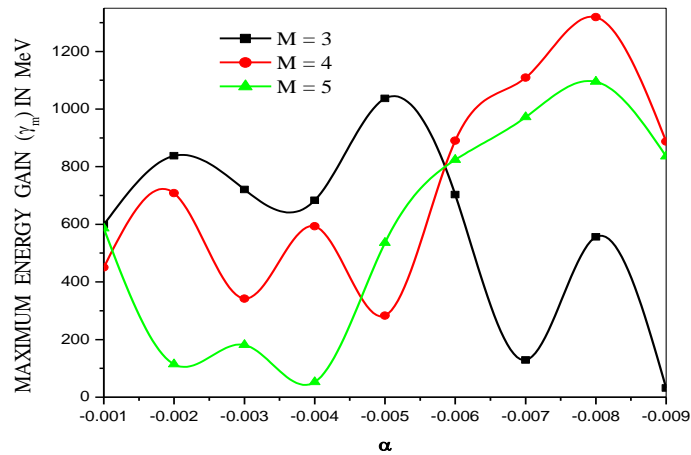


Figure 4.3. Maximum energy gain with different chirp parameter (α) at $a_0 = 3$, for Sin^4 laser pulse envelope.

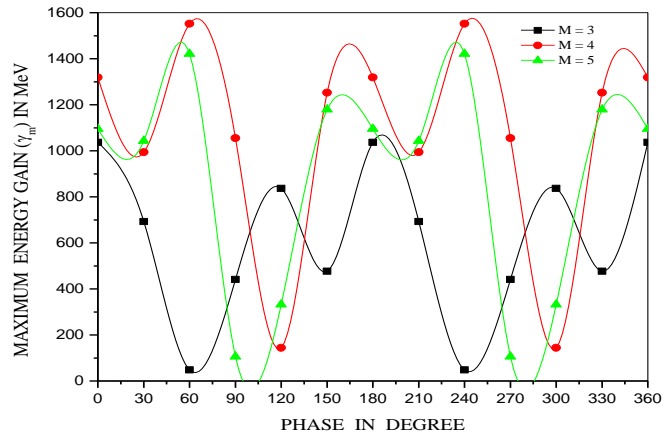


Figure 4.4. Maximum energy gain with different phases for without chirp at $a_0 = 3$ for Sin^4 laser pulse envelope.

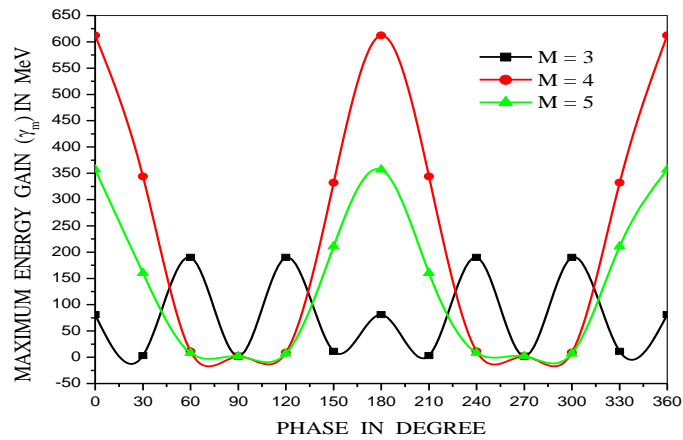


Figure 4.5. Maximum energy gain with different phases with chirp at $a_0 = 3$ for Sin^4 laser pulse envelope.

4.1.1.3 Conclusion

In this investigation, we have perused the scenario of electron acceleration by using trapezoidal pulse shape envelope and Sin^4 pulse shape envelope. For both the cases, we have considered linear frequency chirp effect at intensity parameter $a_0 = 3$. We have analyzed that for case of trapezoidal pulse envelope electron enhances its maximum energy ≈ 2.697 GeV and for Sin^4 pulse envelope electron enhances its maximum energy ≈ 1.552 GeV ($M=4$) for same conditions. Our conclusion can be summarized as follows: under optimum conditions, from the interaction between trapezoidal and Sin^4 pulse shape envelope, in both the cases, we have observed GeV order energy gain. My conclusion is that trapezoidal envelope is superior than Sin^4 envelope.

4.1.2 Combined effect of frequency chirp and axial magnetic by trapezoidal laser pulse envelope

4.1.2.1 Electron dynamics

In a recent model for a laser pulse, the term $(\omega_0 t - k_0 z)$ has been replaced by a new term η [28], where ω_0 is initial frequency and k_0 is laser wave number. The power chirp will be written in following form: $\eta \rightarrow \eta + \alpha \eta^{n+1}$

Where, α is the chirp parameter.

$n = 1$ gives linear chirp.

The above equation will be valid when $|\alpha\eta| < 1$.

Because chirp creates the asymmetry of the phase, so the Lawson-Woodward theorem is valid and as a result electron accelerates and enhances its energy.

In this study, we have assumed linearly polarized trapezoidal laser pulse envelope. The transverse electric field ($\vec{E} = \hat{x}E_x$) equations of trapezoidal pulse envelope are given below:

$$\vec{E} = \hat{x}E_0fg \quad (4.13)$$

$$\vec{B} = \hat{y}\frac{E_0}{c}fg \quad (4.14)$$

Where, g denotes an appropriate pulse shape function, f depends on $(\omega_0t - k_0z)$ where, $k_0 = \frac{\omega_0}{c}$.

For trapezoidal pulse envelope the turn-on and turn-off parameter is fixed as:

$$\begin{aligned} g(\eta) &= \frac{\eta}{5\pi} & 0 \leq \eta \leq 5\pi \\ &= 1 & 5\pi \leq \eta \leq 25\pi \\ &= -\frac{\eta}{5\pi} + 6 & 25\pi \leq \eta \leq 30\pi \end{aligned}$$

$$\eta = \omega_0t - k_0z$$

$$f = \sin(\phi_0 + \eta)$$

The z-direction external axial magnetic field along is written as: $\vec{B}_s = \hat{z}B_0$

Where, B_0 is the maximum value.

The momentum and energy equations for the respective pulse envelope are given below:

$$\frac{dp_x}{dt} = -eE_x - ev_yB_0 + ev_zB_y \quad (4.15)$$

$$\frac{dp_y}{dt} = ev_x B_0 \quad (4.16)$$

$$\frac{dp_z}{dt} = -ev_x B_y \quad (4.17)$$

$$\frac{dy}{dt} = -ev_x E_x \quad (4.18)$$

Where, $P_x = \gamma m_0 v_x$, $P_y = \gamma m_0 v_y$ and $P_z = \gamma m_0 v_z$. $\gamma^2 = 1 + (p_x^2 + p_y^2 + p_z^2)/m^2 c^2$. The normalized parameters were set as: $a_0 = \frac{eE_0}{m\omega_0 c}$, $b_0 = \frac{eB_0}{m\omega_0 c}$, $t' = \omega_0 t$, $r'_0 = \frac{\omega_0 r_0}{c}$, $x' = \frac{\omega_0 x}{c}$, $y' = \frac{\omega_0 y}{c}$, $z' = \frac{\omega_0 z}{c}$, $v'_x = \frac{v_x}{c}$, $v'_y = \frac{y}{c}$, $v'_z = \frac{v_z}{c}$, $p'_x = \frac{p_x}{mc}$, $p'_y = \frac{p_y}{mc}$, $p'_z = \frac{p_z}{mc}$, and $\gamma' = \frac{\gamma}{mc^2}$.

4.1.2.2 Result and Discussion

In this analytical and numerical calculations we have assumed the different parameters in the following way: normalized intensity parameter $a_0 = 3$ (corresponding intensity $I \sim 1.23 \times 10^{19} \text{ W cm}^{-2}$) by using the formula $I \left(\frac{W}{\text{cm}^2} \right) = 1.36817 \times 10^{18} \left[\frac{a_0}{\lambda(\mu\text{m})} \right]^2$, with laser wavelength $\lambda = 1 \mu\text{m}$ and phase varies from 0 to 2π . Figure 4.6 (a) represents the variation between maximum energy gain with dimensionless chirp parameter (α) which is responsible for efficient energy transfer. From this graph, we can say that the optimum value of chirp parameter is -0.02 . At this value laser pulse transfers maximum energy to electron. 4.6 (b) shows the relationship between maximum energy gain and intensity parameter $a_0 = 3$ and chirp parameter $\alpha = -0.02$. From this graph we may conclude that at this chirp parameter electron's energy gain is near about to be saturated. Figure 4.7 exhibits the relationship between enhanced electron energy and different initial phases of trapezoidal pulse envelope with (red line) and without (black line) linear chirp as enhanced energy depends on initial phase of laser. The observed optimum phase is $5\pi/6$ for using chirp and without chirp is $\pi/6$. Here, the electron undergoes acceleration and deceleration

phase for the pulse shape. For $0-30\pi$, in the presence of suitable chirp, the optimum phases are observed as $(5\pi)/6, (11\pi)/6, (17\pi)/6, \dots$ and can be generalized as, $(n - 1/6)\pi, n = 1, 2, 3, \dots$, whereas without frequency chirp, the optimum phases for maximum energy are found to be $\pi/6, (7\pi)/6, (13\pi)/6, \dots$ and can be generalized as, $(n - 1/6)\pi, n = 0, 1, 2, \dots$. So, for the execution of successful resonance between electron and test pulse, initial phase of laser plays a vital role. At this value of optimum chirp parameter and optimum phase we have got maximum energy gain 5.288 GeV which is 4.77 times greater than without chirp. Because chirp breaks the symmetry of pulse, as a result electron interacts several times with laser pulses for longer duration. Hence electron enhances its energy.

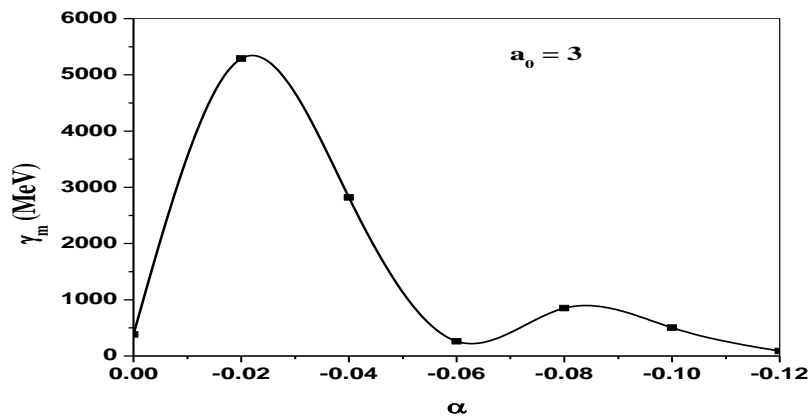


Figure 4.6 (a). Maximum energy gain with different chirp parameter (α) at intensity parameter $a_0 = 3$ for trapezoidal laser pulse envelope.

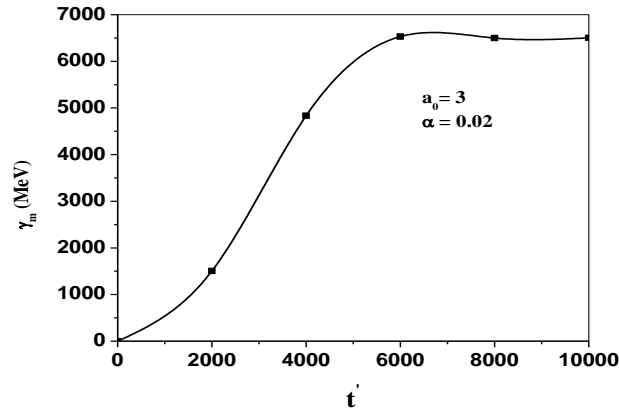


Figure 4.6 (b). Maximum energy gain with normalized time at intensity parameter $a_0 = 3$, chirp parameter $\alpha = -0.02$ for trapezoidal laser pulse envelope.

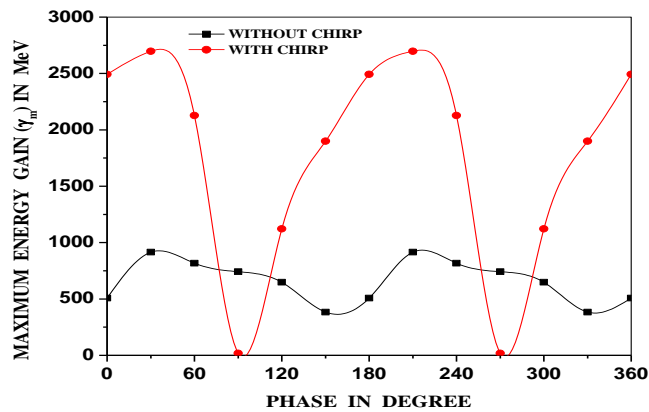


Figure 4.7. Maximum energy gain with different phases for with chirp and without chirp at intensity parameter $a_0 = 3$ for trapezoidal laser pulse envelope.

Figure 4.8 exhibits the relationship between energy gain and different values of magnetic field along with optimum phase and optimum chirp parameter. For that purpose, the optimum external axial magnetic field is $b_0 = 0.0008$ (corresponding to a magnetic field of 86 KG). I have noticed energy gain up to 6.504 GeV with effects. Magnetic field

increases $\vec{v} \times \vec{B}$ for betatron resonance, interaction time between electron and laser pulse increases. Hence electron enhances its energy and keeps the maximum energy for longer time and corridor.

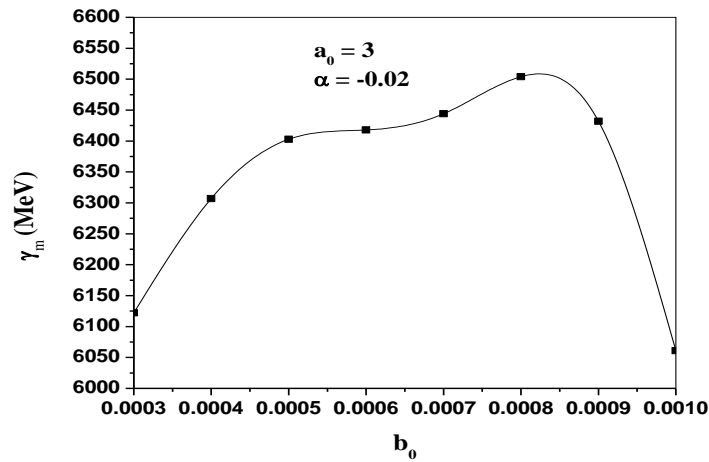


Fig. 4.8. Maximum energy gain with b_0 at intensity parameter $a_0 = 3$ and chirp parameter ($\alpha = -0.02$) for trapezoidal laser pulse envelope.

Fig. 4.9 exhibits the relationship between energy gain and normalized time at intensity parameter $a_0 = 3$ with optimum phase, chirp parameter, and magnetic field. Due to the unique shape of trapezoidal laser pulse, the interaction time increases. So, electron enhances its energy and retains the same for longer corridor. We have observed the enhanced energy in Giga electron volt.

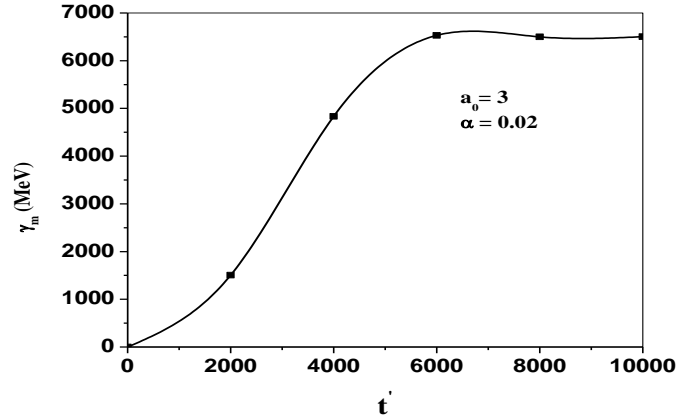


Figure 4.9. Maximum energy gain with normalized time at $a_0 = 3$, chirp parameter $\alpha = -0.02$, $b_0 = 0.0008$ for trapezoidal laser pulse envelope.

4.1.2.3 Conclusion

In this chapter, I have analyzed electron acceleration scenario by employing trapezoidal envelope in vacuum. I have also analyzed the chirping and axial magnetic field effect on acceleration process. My conclusion can be summarized as follows: under optimum conditions from the interaction between test envelope (trapezoidal) and electron, electron enhances its energy up to 5.288 GeV in vacuum under the effect of linear chirp at intensity parameter $a_0 = 3$ (Intensity $I \sim 1.23 \times 10^{19} \text{ Wcm}^{-2}$) and optimizing phase = $5\pi/6$. When both effect employed electron enhances its energy up to 6.504 GeV. Here, the frequency chirp enhances the interaction time and retains the maximum energy gain at resonance, whereas, the applied magnetic field enables the betatron resonance to attain maximum energy gain.

4.1.3 Influence of frequency chirp and axial magnetic field on electron acceleration by employing Cos^2 laser pulse envelope

4.1.3.1 Electron Dynamics:

Single electron dynamics along z direction has been studied in this chapter. In a recent model for a laser pulse, the term $(\omega_0 t - k_0 z)$ has been replaced by a new term η , where ω_0 is initial frequency and k_0 is wave number. The power chirp will be written in following form: $\eta \rightarrow \eta + \alpha \eta^{n+1}$, where, α is the dimensionless chirp parameter, $n = 1$ depicts the linear chirp and $n = 2$ represents quadratic chirp and so on.

The equation $\eta \rightarrow \eta + \alpha \eta^{n+1}$ will be legal when $|\alpha \eta| < 1$.

The chirp destroys the symmetry in the phase so Lawson-Woodward theorem is valid and as a result electron gears up and gains its energy.

In this study, we have taken a LP Cos^2 laser pulse envelope [34]. The transverse electric field ($\vec{E} = \hat{x}E_x$) equation for this purpose is given below:

$$\vec{E}(\eta) = \hat{x}E_0 \sin(\phi_0 + \eta + \alpha \eta^2) \cos^2\left(\frac{\pi}{\tau\omega_0}(\eta - \bar{\eta})\right) \quad (4.19)$$

$$\vec{B}(\eta) = \hat{y}\frac{E_0}{c} \sin(\phi_0 + \eta + \alpha \eta^2) \cos^2\left(\frac{\pi}{\tau\omega_0}(\eta - \bar{\eta})\right) \quad (4.20)$$

$$\eta = \omega_0 t - k_0 z$$

$$\bar{\eta} = 15\pi$$

$$\text{Temporal width, } \tau = 50 \text{ fs}$$

$$c \text{ is the speed of light in free space} = 3 \times 10^8 \text{ m/s}$$

The external axial magnetic field is as: $\vec{B}_s = \hat{z}B_0$

The momentum and energy equations for the respective pulse envelope are given below:

$$\frac{dp_x}{dt} = -eE_0 \sin(\phi_0 + \eta + \alpha \eta^2) \cos^2 \left(\frac{\pi}{\tau\omega_0} (\eta - \bar{\eta}) \right) - v_y e B_0 + v_z e \frac{E_0}{c} \sin(\phi_0 + \eta + \alpha \eta^2) \cos^2 \left(\frac{\pi}{\tau\omega_0} (\eta - \bar{\eta}) \right) \quad (4.21)$$

$$\frac{dp_y}{dt} = v_x e B_0 \quad (4.22)$$

$$\frac{dp_z}{dt} = -v_x e \frac{E_0}{c} \sin(\phi_0 + \eta + \alpha \eta^2) \cos^2 \left(\frac{\pi}{\tau\omega_0} (\eta - \bar{\eta}) \right) \quad (4.23)$$

We have written the equations (3), (4), and (5) in terms of velocity as:

$$\frac{dv'_x}{dt'} = \frac{1}{c_1} \left[-a_0 \sin(\phi_0 + \eta + \alpha \eta^2) \cos^2 \left(\frac{\pi}{\tau\omega_0} (\eta - \bar{\eta}) \right) \right] - b_0 v'_y + a_0 v'_z \sin(\phi_0 + \eta + \alpha \eta^2) \cos^2 \left(\frac{\pi}{\tau\omega_0} (\eta - \bar{\eta}) \right) \quad (4.24)$$

$$\frac{dv'_y}{dt'} = \frac{b_0}{c_2} v'_x \quad (4.25)$$

$$\frac{dv'_z}{dt'} = -\frac{a_0}{c_3} v'_x \sin(\phi_0 + \eta + \alpha \eta^2) \cos^2 \left(\frac{\pi}{\tau\omega_0} (\eta - \bar{\eta}) \right) \quad (4.26)$$

$$\frac{dy'}{dt} = -a_0 v'_x \sin(\phi_0 + \eta + \alpha \eta^2) \cos^2 \left(\frac{\pi}{\tau\omega_0} (\eta - \bar{\eta}) \right) \quad (4.27)$$

We have optimized the parameters by numerical simulation. $P_x = \gamma m_0 v_x$, $P_y = \gamma m_0 v_y$ and

$P_z = \gamma m_0 v_z$, $\gamma^2 = 1 + (p_x^2 + p_y^2 + p_z^2)/m^2 c^2$. The normalized parameters are as follows:

$$a_0 = \frac{eE_0}{m\omega_0 c}, t' = \omega_0 t, r'_0 = \frac{\omega_0 r_0}{c}, x' = \frac{\omega_0 x}{c}, y' = \frac{\omega_0 y}{c}, z' = \frac{\omega_0 z}{c}, v'_x = \frac{v_x}{c}, v'_y = \frac{v_y}{c}, v'_z =$$

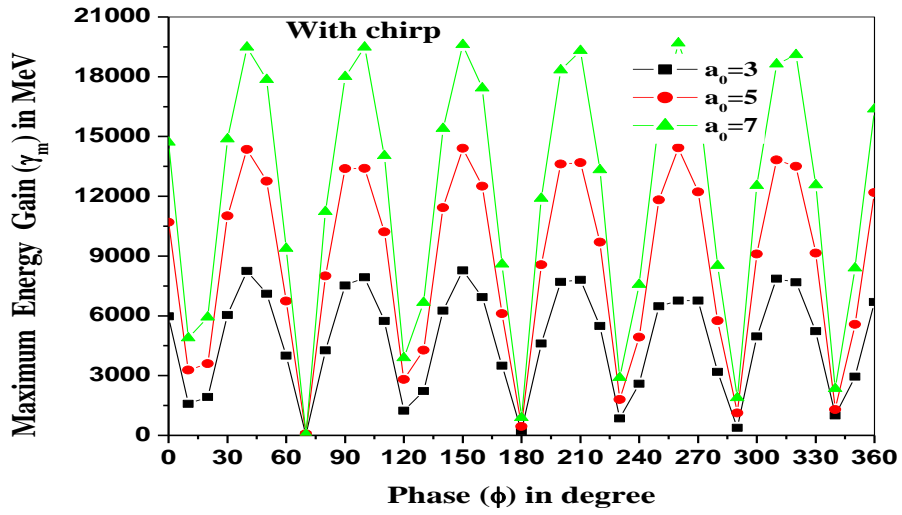
$$\frac{v_z}{c}, p'_x = \frac{p_x}{mc}, p'_y = \frac{p_y}{mc}, p'_z = \frac{p_z}{mc}, \text{ and } \gamma' = \frac{\gamma}{mc^2}, c_1 = \frac{1}{(1-v_x'^2)^{1/2}} + \frac{v_x'^2}{(1-v_x'^2)^{3/2}}, c_2 =$$

$$\frac{1}{(1-v_y'^2)^{1/2}} + \frac{v_y'^2}{(1-v_y'^2)^{3/2}}, \text{ and } c_3 = \frac{1}{(1-v_z'^2)^{1/2}} + \frac{v_z'^2}{(1-v_z'^2)^{3/2}}$$

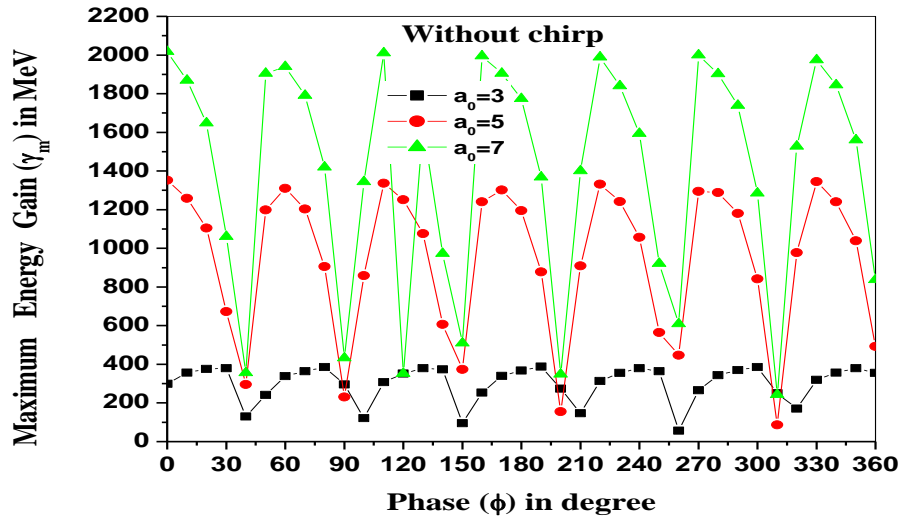
4.1.3.2 Results and discussion

In this theoretical calculations, we have assumed the different parameters in the following way: intensity parameter $a_0 = 3$ (corresponding intensity $\sim 1.23 \times 10^{19} \text{ W/cm}^2$), $a_0 = 5$ (corresponding intensity $\sim 3.42 \times 10^{19} \text{ W/cm}^2$), and $a_0 = 7$ (corresponding intensity $\sim 6.7 \times 10^{19} \text{ W/cm}^2$), by using the formula $I\left(\frac{\text{W}}{\text{cm}^2}\right) = 1.36817 \times 10^{18} \left[\frac{a_0}{\lambda(\mu\text{m})}\right]^2$, with laser wavelength $\lambda = 1\mu\text{m}$ by varying phase from 0 to 2π . We have taken here temporal width $\tau = 50 \text{ fs}$.

Figure 8.1(a) shows the relation between electron energy and initial phases (degree) of Cos^2 pulse envelope at frequency chirp $\alpha = -0.02$ for different intensities $a_0 = 3, 5, \text{ and } 7$. From this study, we have noticed that the optimum phases are $190^\circ, 0^\circ, \text{ and } 0^\circ$ for $a_0 = 3, 5, \text{ and } 7$ respectively. In this case, electron boots its energy $\sim 0.299 \text{ GeV}, 1.352 \text{ GeV}, \text{ and } 2.018 \text{ GeV}$ respectively. When we employ the frequency chirp, the optimum phases also change. After struggling at $150^\circ, 260^\circ, \text{ and } 260^\circ$, electron is able to match its phase with laser's phase for $a_0 = 3, 5, \text{ and } 7$ respectively. Here, the electron undergoes acceleration and deceleration phase for the pulse shape. So, for the execution of successful resonance between electron and test pulse, initial phase of laser plays a vital role. At this value of optimum chirp parameter and optimum phase, we have got maximum energy gain up to $8.274 \text{ GeV}, 14.437 \text{ GeV}, \text{ and } 19.678 \text{ GeV}$, which is several times greater than without chirp. This is due to the fact that chirp creates the asymmetry of pulse, and finally, a number of interaction between the electron and laser pulses happens for longer time period. Hence electron gains its energy significantly.



4.10 (a)



4.10 (b)

Figure 4.10. Maximum energy gain with different phases 4.10 (a) with chirp ($\alpha = -0.02$), 4.10 (b) without chirp at intensity parameter $a_0 = 3, 5$, and 7 for \cos^2 laser pulse envelope.

Successful energy transfer from laser pulse to electron depends on chirp parameter. In this study the value of suitable chirp parameter is -0.02 for effective energy gain. Figure 4.11 exhibits the relationship between maximum energy gain and normalized time at $a_0 =$

3, 5, and 7 and chirp parameter $\alpha = -0.02$ for each intensity parameter. From this graph, it is clear that gaining energy is almost close to constant for this optimum chirp parameter. In the manuscript, a optimum frequency chirp is required to transfer efficient energy between laser and electron as it increases their interaction duration. In this situation, we observe the dominant nature of frequency chirp on pre-accelerated electron. Electron with sufficient energy has a chance to retain the maximum energy. And it can be seen throughout the manuscript that frequency chirp takes aprt a dominant role in retaining the electron energy over several Rayleigh lengths.

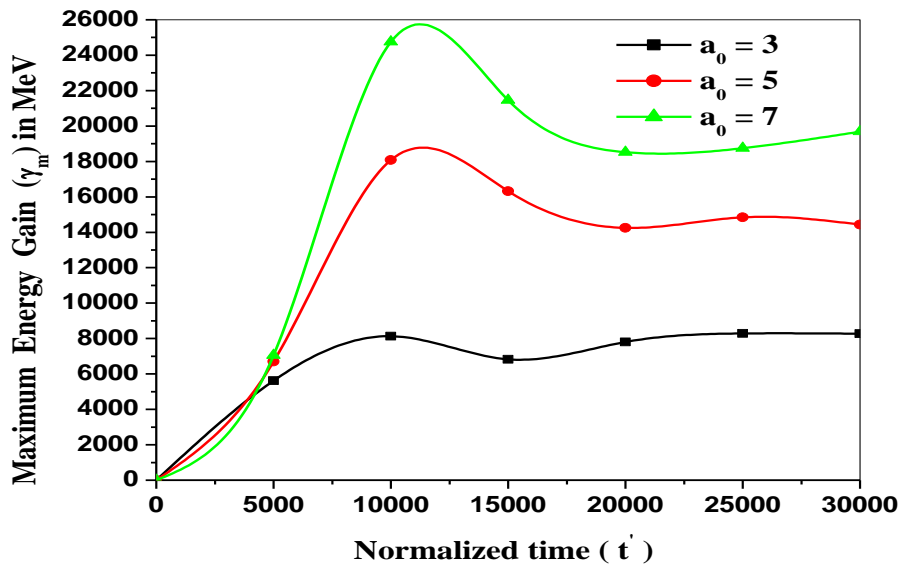
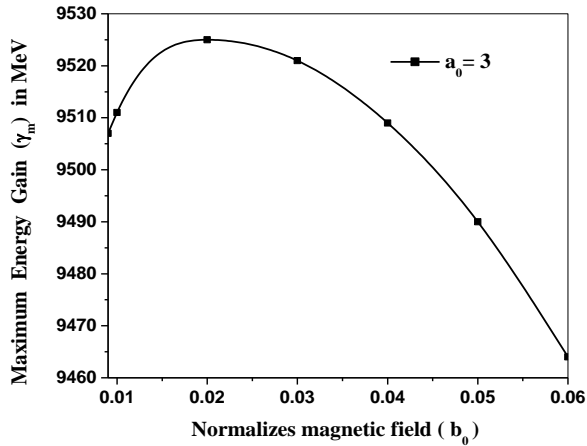


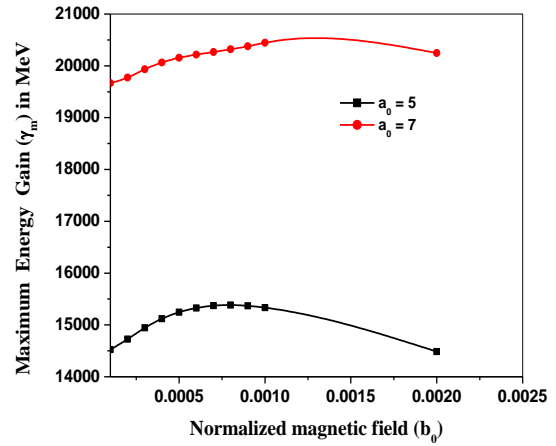
Figure 4.11. Maximum energy gain with normalized time at $a_0 = 3, 5,$ and 7 with $\alpha = -0.02$ for \cos^2 laser pulse envelope.

Figure 4.12 displays the interconnection between energy gain and magnetic field for the test pulse shape with optimum value of phase and chirp parameter. For such energy gain, the optimum external axial magnetic field is $b_0 = 0.02$ (corresponding to a magnetic field of 2.1 MG), $b_0 = 0.0008$ (corresponding to a magnetic field of 86 KG) for $a_0 = 5,$

and $b_0 = 0.001$ (corresponding to a magnetic field of 107 KG) $a_0 = 5$. With both effect I have noticed that electron enhances its energy up to 9.525 GeV, 15.382 GeV, and 20.447 GeV respectively. At optimum magnetic field laser trapped electron. Magnetic field rises $\vec{v} \times \vec{B}$ force and because of betatron resonance, interaction time between electron and laser pulse rises. In such cases acceleration process fulfill its purpose.



4.12(a)



4.12 (b)

Figure 4.12 Maximum energy gain with normalized magnetic field (b_0) $a_0 = 3$ in 4.12 (a) and $a_0 = 5, 7$ in 4.12 (b) with optimum chirp parameter ($\alpha = -0.02$) for \cos^2 laser pulse envelope.

In figure 4.13 I have drawn the graph between energy gain and normalized time at intensity parameter $a_0 = 3, 5,$ and 7 with optimum phase, chirp parameter and magnetic field. \cos^2 pulse envelope has a unique shape, the interaction time increases. So electron gains its energy and conserves the maximum energy for longer corridor.

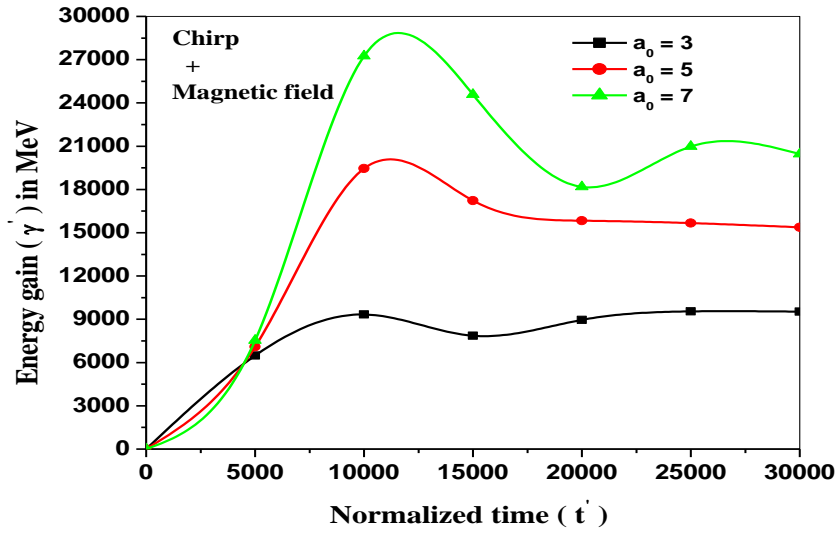


Figure 4.13 Energy gain with normalized time at intensity parameter $a_0 = 3, 5,$ and 7 chirp parameter $\alpha = -0.02$, normalized magnetic field $b_0 = 0.0008$ for trapezoidal laser pulse envelope.

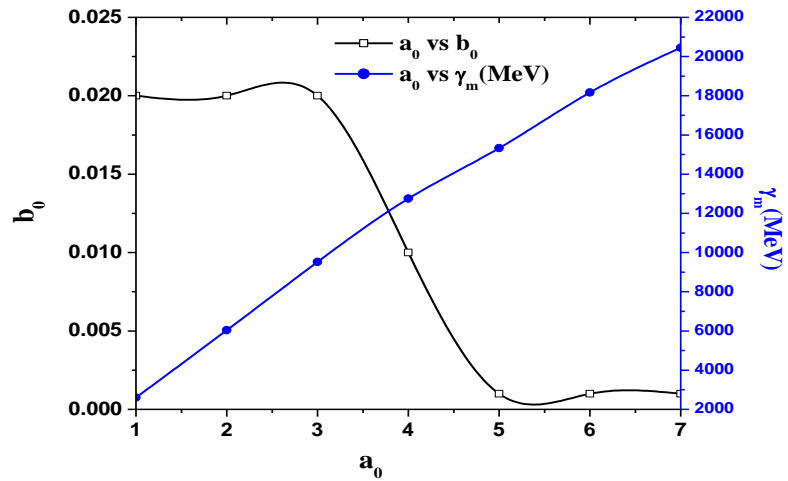


Figure 4.14 shows the variation of normalized magnetic field (b_0) and maximum energy gain (γ_m) with respect to intensity parameter (a_0).

Figure 4.14 shows the calibration curve between a_0 vs b_0 and a_0 vs γ_m together. From this graph, it is clear that γ_m is a function of a_0 and they are directly proportional to each other. When a_0 increases, γ_m also increases. Here, we have taken laser pulse duration $\tau = 50\text{fs}$, linear frequency chirp parameter $\alpha = -0.02$. With an rise in the value of a_0 , electron travels longer distance and interaction takes part for longer duration. This signifies that an increase in a_0 , compress focal spot, which strongly enriches the energy gain. In the same graph, it is clear that normalized magnetic field (b_0) is inversely proportional to a_0 . As a_0 increases, b_0 decreases. That means at minimum magnetic field, electron enhances more rapidly, provided the frequency chirp parameter is optimized. Due to intensity distribution in the axial direction increases, betatron resonance maintains at lower value of magnetic field.

4.1.3.3 Conclusion:

In this chapter, we have made analytical and numerical simulation scenario by using LP \cos^2 laser pulse envelope for efficient electron acceleration in vacuum. Role of linear chirp as well as axial magnetic field have been studied to assure high energy gain. Electron's energy gain (γ) and maximum energy gain (γ_m) were observed by optimizing different parameters such as: phase (φ), laser intensity parameter (a_0), normalized magnetic field (b_0). We have also observed the variation between γ_m and b_0 with a_0 . γ_m is directly proportional to a_0 , where as b_0 is inversely proportional to a_0 . This work is the extension of Salamin's work [35], where they employed frequency chirp only. But in this chapter, we have employed additionally external axial magnetic field. Major energy gain has been done by employing only linear frequency chirp as it destroys the symmetry of laser pulse, so the electron transacts a number of times with laser pulse for longer duration. By employing external axial magnetic field with frequency chirp, we have observed a minor energy gain on the previous case. The results presented in the present study are beneficial for future research, where huge amount of energy is required for various applications such as: cancer treatment, hard X-ray generation etc.

CHAPTER-5

Efficient electron acceleration by radially polarized Hermite-Cosh-Gaussian laser beam in an ion channel

5.1 Introduction:

The scientific development of short pulse laser is now under our control. It is efficient to generate petawatt power. The evolution of femtosecond laser has a great importance on charged particle acceleration in vacuum and plasma also [126, 17, 163-165]. Day by day high power laser is showing its greater interest by performing in scientific research. Short pulse lasers have the ability to produce femtoseconds (fs) pulses which accelerates electron in relativistic manner. The intense laser-plasma interaction process is offering the scope of wide range of new applications. More than 40 years ago Tajima and Dawson [10] first accelerate electron by ponderomotive force which excite wakefield of relativistic speed of light (c). If electron with adequate energy impulse into wakefield, it will trap electrons. As a result the electrons accelerate and makes itself strong. This scenario is familiarly termed as wakefield scenario. Their idea was experimentally proved by Amiranoff et al.,[77] in 1998. They observed 1.6 MeV energy gain and also noticed 1.5 GeV/m longitudinal electric field. In 1997 experimental verification was performed by Malka et al.,[18]. In vacuum and plasma it was a challenged to accelerate electron without scattering, independence of medium's effect. Faure et al.,[152] produced good quality-low spreading mono-energetic electron beam by producing plasma bubble which trapes electron and accelerates plasma electron effectively. Any accelerator schemes need either self-focused laser pulse or drive over longer distance (Rayleigh lengths). Ion density channel in plasma [1, 166 - 168] is suited for the above purpose. Laser ablation [1], capillary discharges [169], and laser induced plasma [92, 170-173] are the performing plasma channel mechanism for efficient laser guiding. The first plasma channel was created

by hydrodynamic expansion of a plasma column. In this approach, a laser pulse having energy 100 mill joule (mJ) and length 100 picosecond (ps) was focused. The plasma channel thus formed is not fully ionized by this method. Presently high intensity femtoseconds laser pulse is used. Through a long complicated process it creates an ion channel. Plasma ion channel is also used as an effective medium of acceleration process. Ion channel is used for compressing and transferring higher energetic electron beam as a focusing and guiding device and it is replaced in place of focusing magnet. Electron acceleration has been analyzed experimentally in ion channel [93-96]. In such cases energy gain is much greater in plasma ion channel than in vacuum by employing same laser intensity. Rajput and Kant [143] analyzed electron energy with axicon Gaussian RP laser pulse in ion channel. They recorded 2.02 GeV energy gain at intensity $3.1 \times 10^{20} \text{Wcm}^{-2}$ with normalized ion density 0.0003. Ghotra¹⁸ employed plasma ion channel to study electron acceleration by employing Cos-Gaussian radially polarized laser pulse. Electrons energy had been investigated by changing different parameters like ion density, laser intensity, initial phase of laser etc. Under optimum condition author noticed GeV order energy gain. We are the pioneer of HChG laser beam which has been employed to study electron acceleration [160]. Electric field of ion density channel takes part an important role in enhancing electron energy while laser pulse interacts with plasma. Also many explanation we have received from several mechanism [97-100] for gaining electron energy. Channel depth is an important factor in plasma density profile. When laser pulse propagates under specified condition, then channel depth and critical value of ion density Δn_c [101] must be same. The propagation characteristics of the laser pulse depends on pulse length variation and presence of wakefield [102].

In this chapter, I will discuss the efficient electron acceleration in an ion density channel by employing a RP HChG laser beam. Salient features of HChG laser beam are: 1. HChG beam is not a new laser beam profile. We can generate it by the superposition of Hermite Gaussian (HG) beams and Cosh-Gaussian (ChG) beam [174]. 2. Effectiveness of HChG laser beam depends on time of focus. 3. Mode indices and the decentered parameter have a great impact on self-focusing of HChG laser beam [175, 176]. As cylindrical

symmetry was found in RP laser pulse's which is critical for better electron entrapment [131]. Also RP laser has its own property of narrow divergence and low spread power in comparison with LP and CP laser pulses. That's why RP radiation is easy to focus. The combined effect of radial polarization and ion density channel on electron acceleration has been theoretically analyzed by Kaur and Gupta [103]. By employing RP ChG laser pulse electron acceleration has been studied in ion channel [104]. They successfully analyzed the different parameters related to laser pulse on electron acceleration. The order of this chapter is assembled like: section 2 describes governing equations. Numerical calculations and discussion in the section 3. Conclusion has been drawn in the final section 4 as usual.

Ion channel is a promising medium. Earlier I have indicated that we are the pioneer of electron acceleration by employing HChG laser beam in ion channel also. I have studied the role of intensity parameter, spot size, ion density, decentered parameter, velocity of electron on electron acceleration. Previous authors worked on Gaussian [177] and ChG [178] in ion channel. Near about same type of result I have also noticed but my profile was new.

5.1.1 Effect of intensity parameter on RP HChG laser beam

5.1.1.1 Electromagnetic fields and electron dynamics

When a highly intense laser ($a_0 > 1$) interacts with plasma, it creates a narrow channel of ionized gas or plasma, called an ion channel. The intense electric field of laser pulse creates a region of lower density or vacuum in the center of plasma. This is "bubble regime". The ion channel can be used in applications such as guiding and accelerating charged particle, generating THz radiation etc.

In this chapter, I have employed RP-HChG laser pulse envelope along the z direction in vacuum. The transverse and radial component of this laser beam are written as:

$$\vec{E}_r = \hat{r}E_0H_S\left(\frac{\sqrt{2}r}{r_0}\right)\cosh\left(\frac{br}{r_0}\right)e^{-\left(r^2/r_0^2\right)}e^{i(kz-\omega t)} \quad (5.1)$$

$$\vec{E}_z = -\hat{z} \frac{i}{kr} E_r \left[1 + 2S\sqrt{2} \frac{r}{r_0} \frac{H_{s-1}\left(\sqrt{2}\frac{r}{r_0}\right)}{H_s\left(\sqrt{2}\frac{r}{r_0}\right)} + b \frac{r}{r_0} \tanh\left(b \frac{r}{r_0}\right) - 2 \frac{r^2}{r_0^2} \right] \quad (5.2)$$

here, E_0 is the amplitude, r_0 is the beam waist width, r is the radiated distance, s is Hermite order and b is the decentered parameter.

Hence, The Newton-Lorentz force equation will be in the form

$$\frac{\partial \vec{p}}{\partial t} = -e [\vec{E} + (\vec{v} \times \vec{B})] \quad (5.3)$$

Cicchitelli et al. (34) worked on RP Gaussian laser beam and they noted that RP laser beam has both component: longitudinal and transverse. In this case, longitudinal field is dominant. There will be no longitudinal component of magnetic of magnetic field. When a laser beam propagates through a plasma, it can produce a plasma channel because electron density decrease towards the laser axis. If we use intense laser, electrons from axial direction of laser beam expelled as a strong radial ponderomotive force is there due to laser field. The radial electric field for ion channel impacts the electron dynamics. Let us consider an electrostatics force which generates ion channel [35] written in the following form:

$$\vec{E}_c = \frac{n_i e r}{2\epsilon_0} \hat{r} \quad (5.4)$$

In the above relation (4) n_i denotes the ion density.

By using eq. (1-4), the electron energy gain is as follows

$$\frac{d\gamma'}{dt'} = a_0 H_s \left(\frac{\sqrt{2}r'}{r_0} \right) \cosh \left(\frac{br'}{r_0} \right) e^{-\left(r'^2/r_0'^2\right)} e^{i(k'z' - t')} \left[v_z' \frac{i}{k'r'} \left[1 + 2S\sqrt{2} \frac{r'}{r_0} \frac{H_{s-1}\left(\sqrt{2}\frac{r'}{r_0}\right)}{H_s\left(\sqrt{2}\frac{r'}{r_0}\right)} + b \frac{r'}{r_0} \tanh\left(b \frac{r'}{r_0}\right) - 2 \frac{r'^2}{r_0'^2} \right] - v_r' \right] - \frac{n_i r' v_r'}{2} \quad (5.5)$$

5.1.1.2 Result and discussion

In this chapter, we have set up the different parameters such as: normalized intensity parameter $a_0 = 5$ (corresponding intensity $\sim 3.42 \times 10^{19} \text{ Wcm}^{-2}$), $a_0 = 7$ (corresponding intensity $\sim 6.7 \times 10^{19} \text{ Wcm}^{-2}$) $a_0 = 10$ (corresponding intensity $\sim 1.36 \times 10^{20} \text{ Wcm}^{-2}$), $a_0 = 12$ (corresponding intensity $\sim 1.97 \times 10^{20} \text{ Wcm}^{-2}$), by using the formula $I \left(\frac{\text{W}}{\text{cm}^2} \right) = 1.36817 \times 10^{18} \left[\frac{a_0}{\lambda(\mu\text{m})} \right]^2$ and the prescribed value of laser

wavelength λ is $1\mu\text{m}$. The angular frequency of laser beam is $\omega_0 = 1.88 \times 10^{15} \text{ rad/s}$. 1.42 MeV has been used as an initial energy of electron. If we presume pre-accelerated electron at $t = 0$, then we have noticed that laser effectively transfer its energy to electron so that it can gain GeV order energy which has been reflected in this investigation. We have selected the normalized ion density parameters as $n_i = 0, n_i = 0.0001, 0.0003, 0.0006, 0.0009, 0.00001, 0.00003, 0.00006, 0.00009$ are considered. (\sim ion density range $3.3 \times 10^{23} \text{ Wcm}^{-2} - 9.9 \times 10^{22} \text{ W.m}^{-3}$)

A lot of study can be done by employing ion channel on electron acceleration. Here I have investigated the role of laser intensity on electron acceleration. We have discussed and drawn a graph between energy gain and normalized time for a fixed parameter $r'_0 = 20, b = 1, s = 1$, and $n_i = 0.00001$ by changing intensity parameter $a_0 = 5, 7$, and 10 . We have observed that electron travels longitudinally with larger duration. This is the cause of energy gain. We have noticed 0.179 GeV , 0.206 GeV , and 0.212 GeV for $a_0 = 5, 7$, and 10 respectively. We have also noticed that in the front line of the laser pulse electrons energy increases and in the trailing edge its energy remains constant.

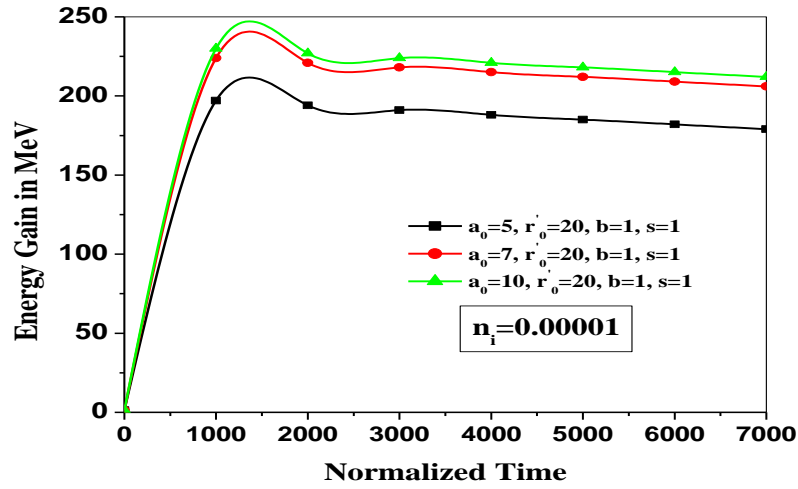


Figure 5.1: Energy gain vs normalized time for $b = 1.0$ for $a_0 = 5, 7,$ and 10 , $r'_0 = 20, s = 1$, ion density $n_i = 0.00001$.

5.1.1.3 Conclusion

I have employed RP HChG laser beam in a plasma ion channel. Here, I have investigated the role of intensity parameter (a_0) on electron acceleration and noticed a significant result. The main observation is that ion channel is very much sensitive that's why we need to optimize laser parameter properly.

5.1.2 The combined effect of RP-HChG laser beam and ion channel on electron acceleration scenario

5.1.2.1 Governing equations

In this study, I have considered radially polarized Hermite Cosh Gaussian (HChG) laser pulse envelope which propagates along z direction in vacuum. The field is given by

$$\vec{E} = \hat{r}E_r + \hat{z}E_z \quad (5.6)$$

The transverse component is expressed as

$$\vec{E}_r = \hat{r}E_0 H_S \left(\frac{\sqrt{2}r}{r_0} \right) \cosh \left(\frac{br}{r_0} \right) e^{-\left(r^2/r_0^2\right)} e^{i(kz-\omega t)} \quad (5.7)$$

The longitudinal component is represented as

$$\vec{E}_z = -\hat{z} \frac{i}{kr} E_r \left[1 + 2S\sqrt{2} \frac{r}{r_0} \frac{H_{S-1}\left(\frac{\sqrt{2}r}{r_0}\right)}{H_S\left(\frac{\sqrt{2}r}{r_0}\right)} + b \frac{r}{r_0} \tanh \left(b \frac{r}{r_0} \right) - 2 \frac{r^2}{r_0^2} \right] \quad (5.8)$$

Hence, The Lorentz force equation will be written in the following form

$$\vec{F} = \frac{\partial \vec{p}}{\partial t} = -e [\vec{E} + (\vec{v} \times \vec{B})] \quad (5.9)$$

Cicchitelli et al. [22] worked on RP Gaussian laser beam and they noted that RP laser beam has both longitudinal and transverse component. In this case longitudinal field plays a crucial role. It accelerates electron in the longitudinal direction. By using Maxwell equation

$\vec{\nabla} \times \vec{E} = -\partial \vec{B} / \partial t$ we can find out the magnetic field which is azimuthal component $B_\theta = \frac{E_r}{c}$. There will be no longitudinal component of magnetic of magnetic field. When a laser

beam propagates through a plasma, it can produce a plasma channel because electron density decrease towards the laser axis. Intense laser solves the above drawback. Let us consider an electrostatics force which generates ion channel [179] written in the following form:

$$\vec{E}_c = \frac{n_i e r}{2 \epsilon_0} \hat{r} \quad (5.10)$$

Where, n_i denotes ion density.

Now the Lorentz force equation will be changed as:

$$\vec{F} = \frac{\partial \vec{p}}{\partial t} = -e [\vec{E} + \vec{E}_c + (\vec{v} \times \vec{B})] \quad (5.11)$$

Where, B is the Laser's magnetic field and $B = \frac{E_r}{c}$

By using eq. (6), the momentum, energy and velocity equations are written as

$$\frac{dp_r'}{dt'} = a_0 H_S \left(\frac{\sqrt{2} r'}{r_0'} \right) \cosh \left(\frac{b r'}{r_0'} \right) e^{-\left(r'^2 / r_0'^2 \right)} e^{i(k' z' - t')} (v_z' - 1) - \frac{n_i r'}{2} \quad (5.12)$$

$$\begin{aligned} \frac{dp_z'}{dt'} = a_0 H_S \left(\frac{\sqrt{2} r'}{r_0'} \right) \cosh \left(\frac{b r'}{r_0'} \right) e^{-\left(r'^2 / r_0'^2 \right)} e^{i(k' z' - t')} & \left[\frac{i}{k' r'} \left[1 + 2S\sqrt{2} \frac{r'}{r_0'} \frac{H_{S-1} \left(\frac{\sqrt{2} r'}{r_0'} \right)}{H_S \left(\frac{\sqrt{2} r'}{r_0'} \right)} + \right. \right. \\ & \left. \left. b \frac{r'}{r_0'} \tanh \left(b \frac{r'}{r_0'} \right) - 2 \frac{r'^2}{r_0'^2} \right] - v_r' \right] \quad (5.13) \end{aligned}$$

$$\begin{aligned} \frac{dv_r'}{dt'} = a_0 H_S \left(\frac{\sqrt{2} r'}{r_0'} \right) \cosh \left(\frac{b r'}{r_0'} \right) e^{-\left(r'^2 / r_0'^2 \right)} e^{i(k' z' - t')} & \left[v_z' \frac{i}{k' r'} \left[1 + 2S\sqrt{2} \frac{r'}{r_0'} \frac{H_{S-1} \left(\frac{\sqrt{2} r'}{r_0'} \right)}{H_S \left(\frac{\sqrt{2} r'}{r_0'} \right)} + \right. \right. \\ & \left. \left. b \frac{r'}{r_0'} \tanh \left(b \frac{r'}{r_0'} \right) - 2 \frac{r'^2}{r_0'^2} \right] - v_r' \right] - \frac{n_i r' v_r'}{2} \quad (5.14) \end{aligned}$$

$$\frac{dv_z'}{dt'} = \frac{a_0}{c_1} H_S \left(\frac{\sqrt{2} r'}{r_0'} \right) \cosh \left(\frac{b r'}{r_0'} \right) e^{-\left(r'^2 / r_0'^2 \right)} e^{i(k' z' - t')} (v_z' - 1) - \frac{n_i r'}{2} \quad (5.15)$$

$$\frac{dv'_z}{dt'} = \frac{a_0}{c_2} H_S \left(\frac{\sqrt{2}r'}{r'_0} \right) \cosh \left(\frac{br'}{r'_0} \right) e^{-\left(r'^2 / r_0'^2 \right)} e^{i(k'z' - t')} \left[\frac{i}{k'r'} \left[1 + 2S\sqrt{2} \frac{r'}{r'_0} \frac{H_{S-1} \left(\frac{\sqrt{2}r'}{r'_0} \right)}{H_S \left(\frac{\sqrt{2}r'}{r'_0} \right)} + \right. \right. \\ \left. \left. b \frac{r'}{r'_0} \tanh \left(b \frac{r'}{r'_0} \right) - 2 \frac{r'^2}{r_0'^2} \right] - v'_r \right] \quad (5.16)$$

Here, (p_r, p_z) are the (r, z) components of the momentum, $\vec{p} = \gamma m \vec{v}$, $\gamma^2 = 1 + (p_r^2 + p_z^2)/m^2 c^2$. The normalized parameters are as follows: $a_0 = \frac{eE_0}{m\omega_0 c}$, $t' = \omega_0 t$, $r'_0 = \frac{\omega_0 r_0}{c}$, $r' = \frac{\omega_0 r}{c}$, $z' = \frac{\omega_0 z}{c}$, $v'_r = \frac{v_r}{c}$, $v'_z = \frac{v_z}{c}$, $p'_r = \frac{p_r}{mc}$, $p'_z = \frac{p_z}{mc}$, $\gamma' = \frac{\gamma}{mc^2}$, $k' = \frac{kc}{\omega_0}$, $c_1 = \frac{1}{(1-v_r'^2)^{1/2}} + \frac{v_r'^2}{(1-v_r'^2)^{3/2}}$, and $c_2 = \frac{1}{(1-v_z'^2)^{1/2}} + \frac{v_z'^2}{(1-v_z'^2)^{3/2}}$

5.1.2.2 Numerical calculation and discussions:

In this manuscript, we have arranged the different parameters like as: normalized intensity parameter $a_0 = 5$ (corresponding intensity $\sim 3.42 \times 10^{19} \text{ Wcm}^{-2}$), $a_0 = 7$ (corresponding intensity $\sim 6.7 \times 10^{19} \text{ Wcm}^{-2}$), $a_0 = 10$ (corresponding intensity $\sim 1.36 \times 10^{20} \text{ Wcm}^{-2}$), $a_0 = 12$ (corresponding intensity $\sim 1.97 \times 10^{20} \text{ Wcm}^{-2}$), by using the formula $I \left(\frac{\text{W}}{\text{cm}^2} \right) = 1.36817 \times 10^{18} \left[\frac{a_0}{\lambda(\mu\text{m})} \right]^2$ and the prescribed value of laser wavelength λ is $1\mu\text{m}$. The angular frequency of laser beam is $\omega_0 = 1.88 \times 10^{15} \text{ rad/s}$. 1.42 MeV is the initial energy of electron. If we presume pre-accelerated electron at $t = 0$, then we have noticed that laser effectively transfer its energy to electron. As a result electron enhances its energy to GeV order which has been reflected in this study. I have selected the normalized ion density parameters as $n_i = 0$, $n_i = 0.0001$ (corresponding to ion density $1.1 \times 10^{23} \text{ m}^{-3}$), $n_i = 0.0003$ (corresponding to ion density $3.3 \times 10^{23} \text{ m}^{-3}$), $n_i = 0.0006$ (corresponding to ion density $6.6 \times 10^{23} \text{ m}^{-3}$), $n_i = 0.0009$ (corresponding to ion density $9.9 \times 10^{23} \text{ m}^{-3}$), $n_i = 0.00001$ (corresponding to ion density $1.1 \times 10^{22} \text{ m}^{-3}$), $n_i = 0.00003$ (corresponding to ion density $3.3 \times 10^{22} \text{ m}^{-3}$), $n_i = 0.00006$

(corresponding to ion density $6.6 \times 10^{22} \text{m}^{-3}$), and $n_i = 0.00009$ (corresponding to ion density $9.9 \times 10^{22} \text{m}^{-3}$).

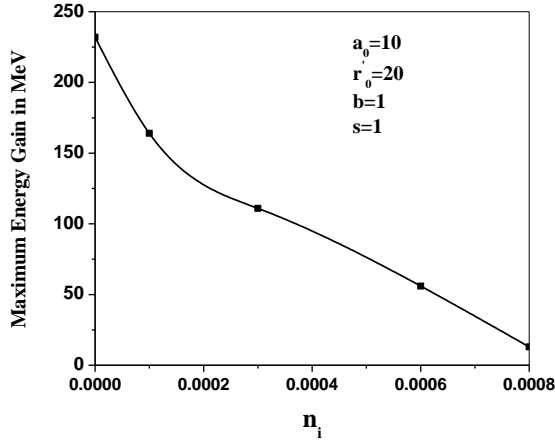


Fig. 5.2 (a)

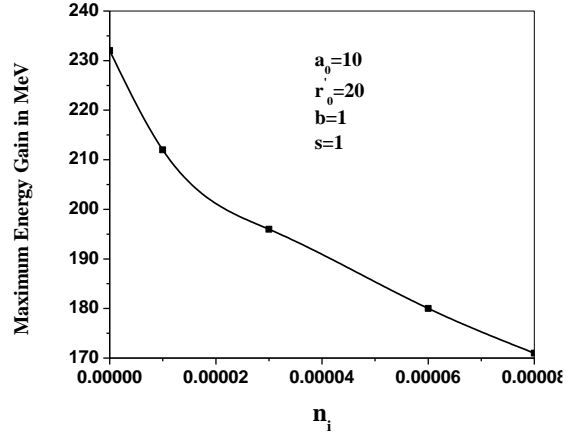


Fig. 5.2 (b)

Figure 5.2. Maximum energy gain with ion density at fixed value of laser spot size $r'_0 = 20$, intensity parameter $a_0 = 10$, decentered parameter $b = 1$, hermite order $s = 1$. Figure 5.2 (a) is for $n_i = 0, 0.0001, 0.0003, 0.0006, 0.0008$ and Figure 5.2 (b) is for $n_i = 0, 0.00001, 0.00003, 0.00006, 0.00008$ respectively.

Figure 5.2 (a) and 5.2 (b) have been plotted the value of maximum energy gain by changing ion density (n_i). This plot shows, increase in ion density decreases the energy gain. From this graph it is clear that ion density plays a key role on increasing energy gain. A significant energy changed have been noticed as small change in ion density. Maximum energy gain decays with increase in ion density due to large restoring force. I have noted energy gain at ion density $n_i = 0, 0.00001, 0.00003, 0.00006$ and 0.00009 are 0.697 GeV , 0.678 GeV , 0.667 GeV , 0.660 GeV , and 0.656 GeV at $a_0 = 10, r'_0 = 20, b = 1$, and $s = 1$, and $v_r[0] = 0.5c$ and $v_z[0] = 0.85c$ respectively.

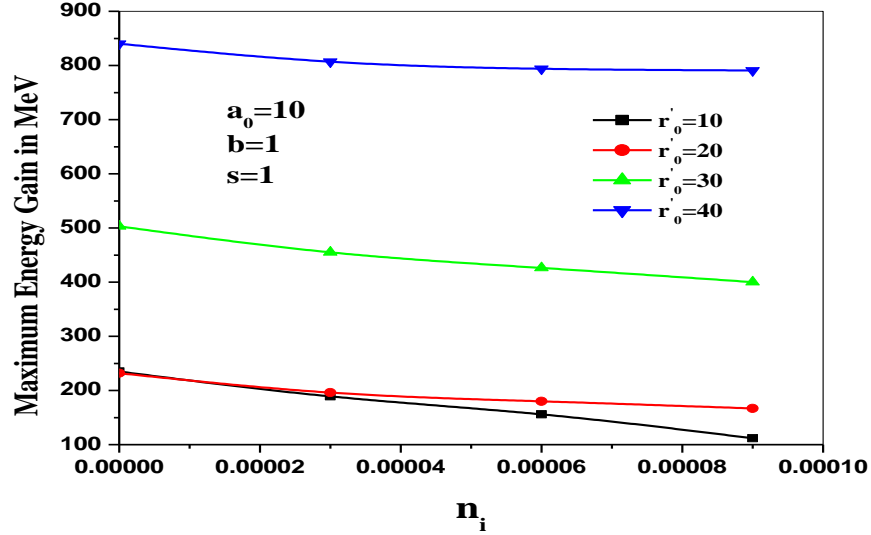


Figure 5.3. Maximum energy gain with ion density by varying laser spot size $r'_0 = 10, 20, 30,$ and 40 for decentered parameter $b = 1,$ hermite order $s = 1,$ and intensity parameter $a_0 = 10.$

Figure 5.3 depicts the change in maximum energy gain with ion density (n_i) for various beam width $r'_0 = 10, 20, 30,$ and 40 at a fixed value of intensity $a_0 = 10,$ $b = 1$ and $s = 1$. From this observation it is clear that we laser spot size and beam waist play a key role on enhanced energy. We all know that small beam waist aligned across a short distance. I noticed an energy gain of 0.235 GeV at $r'_0 = 10$ and $n_i = 0$ which increases to 0.840 GeV at $r'_0 = 40$ and $n_i = 0$. In the similar case energy gain is 0.112 at $r'_0 = 10$ and $n_i = 0.00009$ which increases to 0.791 GeV at $r'_0 = 40$ and $n_i = 0.00009$. The transverse momentum and longitudinal momentum are proportional to longitudinal force $\vec{v} \times \vec{B}$. The same funda will be used in case of energy gain also. I noticed that divergence of the laser beam is inversely proportional to the beam waist, resulting in increased energy gain. The laser beam's intensity was sustained up to several Rayleigh lengths.

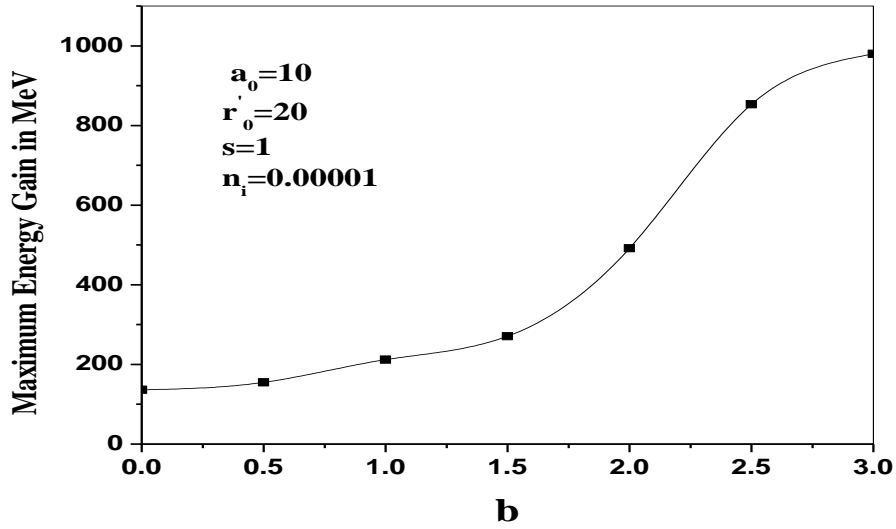


Figure 5.4. Maximum energy gain with decentered parameter $b = 0.5, 1.0, 1.5, 2.0, 2.5,$ and 3.0 for $a_0 = 10, r'_0 = 20, s = 1,$ and $n_i = 0.00001.$

Figure 5.4 depicts the relationship of γ_m with b . In this particular case I have used the parameter as $a_0 = 10, r'_0 = 20, s = 1,$ and $n_i = 0.00001.$ I have varied b from 0 to 3 as an interval of 0.5. Increase in b increases the axial intensity distribution. As a whole electron enhances more and more energy. In this case, at the rising part of laser pulse electron gains its energy significantly and at the trailing part energy saturates. Plots are obtained for $b = 0, 1.0, 1.5, 2.0, 2.5,$ and 3. It is obvious that the enhanced energy is strongly influenced by the b of the HChG laser beam. It has been shown in the earlier chapter [160]. An energy gain of 0.136 GeV is noticed for $b = 0,$ which rises to 0.98 GeV for $b = 3.0.$

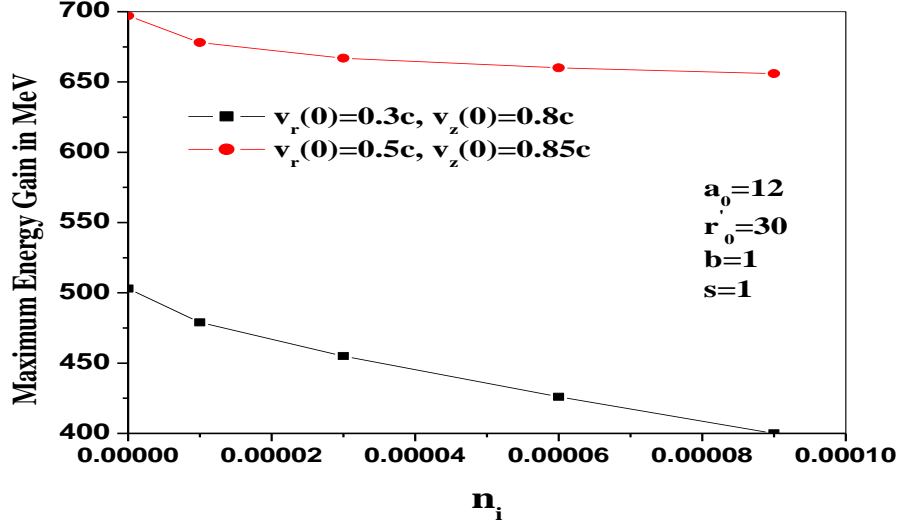


Figure 5.5. Maximum energy gain with ion density by varying initial velocity of electron at $v_r[0] = 0.3c, v_z[0] = 0.8c$ (black line) and $v_r[0] = 0.5c, v_z[0] = 0.85c$ (red line) at fixed laser spot size $r'_0 = 30$, decentered parameter $b = 1$, hermite order $s = 1$, and intensity parameter $a_0 = 12$.

It is well known to us that if radial and axial velocity of electron changes, electron can be accelerated with more energies. It has been shown in figure 5.5. The electron's energy which is a function of ion density (n_i) has been calculated here with initial radial velocity $v_r[0] = 0.3c$ and an axial velocity $v_z[0] = 0.8c$. In the second case, we have selected the above parameters as $v_r[0] = 0.5c$ and $v_z[0] = 0.85c$. It is discovered that electrons travelling at near to the speed of light interact with laser pulse for a long time period, since less scattering is noticed in these cases. Finally, we observe higher energy gain in comparison with lower radial and axial velocity. Because the Lorentz factors couple transverse motion of electron and longitudinal electric field at optimum values of radial and axial velocity in the plasma ion channel. As a result we noticed the enhancement of

energy by electrons. With increasing radial and axial velocity electron prefers efficient acceleration. In such cases ponderomotive scattering reduces in ion channel and electron travels for longer distances with higher energies.

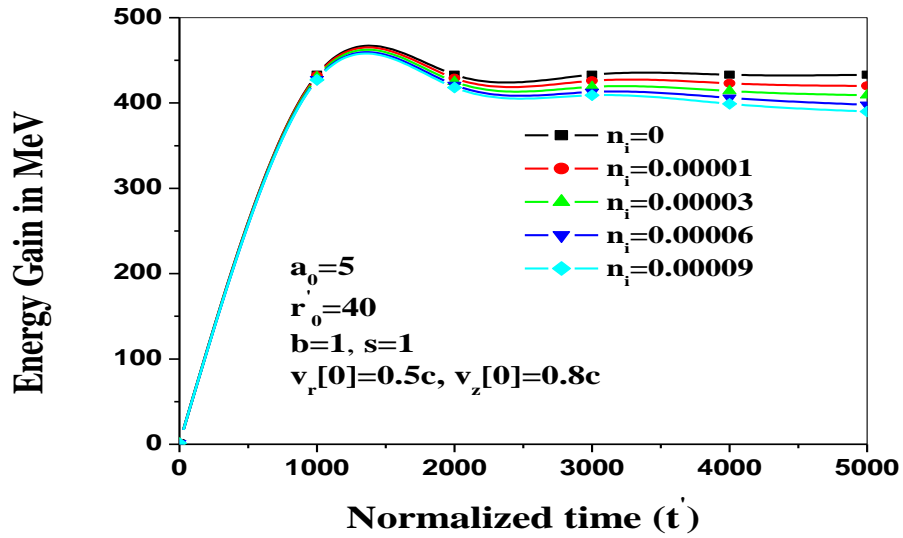


Figure 5.6. Electron's energy gain with normalized time for ion density $n_i = 0, 0.00001, 0.00003, 0.00006,$ and 0.00009 at specific values of $b = 1.0, a_0 = 5, r'_0 = 40, s = 1, v_r[0] = 0.5c,$ and $v_z[0] = 0.8c.$

Figure 5.6. depicts the change in energy gain with normalized time by varying ion density $n_i = 0, 0.00001, 0.00003, 0.00006,$ and 0.00009 at a fixed $a_0 = 5r'_0 = 40, b = 1,$ and $s = 1, v_r[0] = 0.5c,$ and $v_z = 0.8c.$ From this figure it is clearly seen that increase in ion density decreases the energy gain. Because when we increase ion density a large amount of restoring force created which decays the energy gain. As a result we notice less amount of energy gain as we increase ion density. Here, we have noticed 0.433 GeV energy gain at $n_i = 0$ and 0.390 GeV energy gain at $n_i = 0.00009.$ Due to leading edge of laser pulse energy gain increases and due to trailing edge of laser pulse energy remains constant.

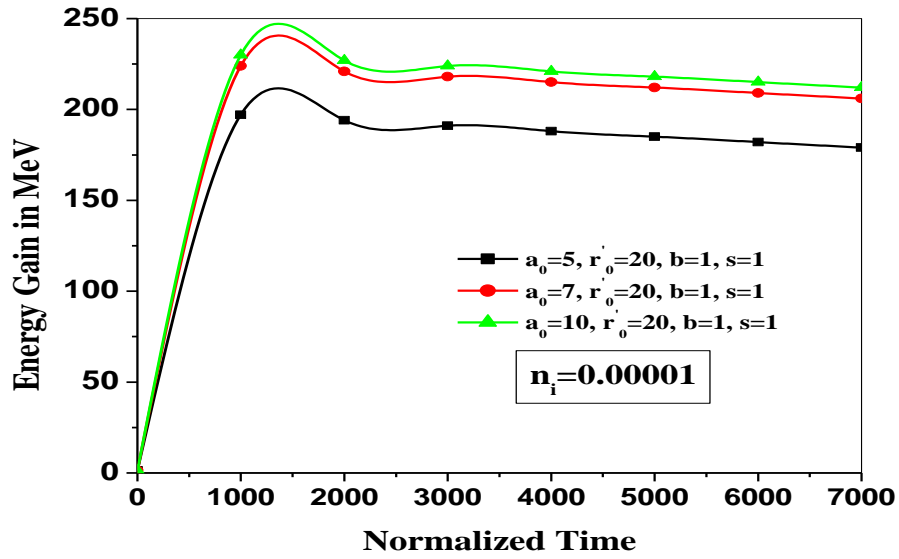


Figure 5.7 Electron's energy gain with normalized time for specific values of $b = 1.0$ for $a_0 = 5, 7,$ and 10 , $r'_0 = 20, s = 1$, ion density $n_i = 0.00001$.

The change of energy gain has been studied in figure 6 with normalized time by changing $a_0 = 5, 7,$ and 10 , $r'_0 = 20$, $b = 1$, $s = 1$, and $n_i = 0.00001$. It is carefully noticed that along the beam propagation direction electrons energy has been increased as I increase laser's intensity. For $a_0 = 5, 7,$ and 10 maximum energy gain has been observed as 0.179 GeV, 0.206 GeV and 0.212 GeV respectively. It is well known to us that longitudinal distance will be increased by electron when intensity of the laser beam increases, which has been reflected in this study also. The ponderomotive force is determined by the electric field's intensity distribution. Electrons were captured and accelerated with high energies when they interacted with the increasing part of the laser pulse. In the other situation, electrons interact with the laser pulse's trailing edge, and their energy gain is nearly saturated.

5.1.2.3 Conclusion:

The RP-HChG laser beam has been demonstrated analytically as an electron acceleration in ion channel successfully. We have highlighted the role of intensity parameter (a_0), laser spot size (r'_0), decentered parameter (b), ion density (n_i) in this chapter to secure high electron energy gain. Because of the early focus of the HChG laser beam, it is remarkably better designed than other laser beams for gaining GeV order energy over short time period. The teamwork between better trapping laser light (RP) and electrostatic field of ion density channel encloses the electron to traverse a considerable distance and attains higher energy along longitudinal direction. It is clearly noticed that HChG laser beam is very much sensitive in ion channel. So our observation prescribed that while handling this profile we must properly optimize the laser parameters with ion channel.

CHAPTER-6

SUMMARY AND FUTURE SCOPE

This research work is fully dedicated to the analysis of “Efficient electron acceleration by short pulse laser” in vacuum and plasma. Out of the two fundamental mechanisms of charged particle acceleration process: Wakefield acceleration and Direct Laser Acceleration (DLA). The Direct Laser Acceleration has been investigated theoretically and numerically in this study. In the DLA scheme, the electron is accelerated by subjecting it to a focused laser field. For a fused laser, there is asymmetry in configuration of electric as well as magnetic fields, which are found to be the strongest near the focal point and grows weaker while moving away from it. As a result of this asymmetrical nature, the weaker laser field which is far from the focus, is not able to extract back electron energy transferred to the electron by the laser closer to the focus and hence, a net energy is gained by the electron along the propagation of laser. These fundamental mechanisms are based on “Captured and Acceleration Scenario” simply “CAS”. In CAS, the core of the laser propagation path captures and accelerates electrons to relativistic energy in the order of GeV with accelerating gradients GeV/m. “CAS” mainly depends on laser profile. Under optimum conditions, laser effectively hands over its energy to electron. Enhanced electron energy can be calculated by solving Newton-Lorentz force equation.

I have concentrated ourselves to enhance electrons energy numerically and analytically by employing:

- Different laser profile like: Sin^4 , Trapezoidal, Hermite-Cosh-Gaussian, Cos^2 .
- Frequency chirp
- External magnetic field
- Vacuum medium, plasma ion channel
- Polarization effect

Chapter 3 is devoted to the electron acceleration by a new laser profile named Hermite-Cosh-Gaussian (HChG) laser profile. In laboratory, this laser profile can be created by superposition of HG and ChG beams. The specialty of HChG laser beam is that two parameters: decentered parameter and hermite order are connected with this profile which manage better trapping and control self-focusing phenomena. If we increase the value of decentered parameter, the intensity distribution increases. It also increases the focal depth of laser pulse. As a result, electron can enhance its energy. Moreover, higher order of Hermite function imposes a better trapping of electron. As a result, an improved acceleration process has been noticed in this chapter. The divergence of the laser beam is inversely proportional to the beam waist and increase in laser intensity increases the interaction duration between laser and electron, as a result electron travels a longer distance. Finally, a remarkable energy gain by electron has been noted in this chapter.

A linear and circular polarization of Hermite-Cosh-Gaussian (HChG) laser pulse were used to analyze electron acceleration in a vacuum in chapter 3. Electron energy gain has been studied with laser intensity and beam waist width which are same as discussed in chapter 5. Polarization plays a key role on electron acceleration. Due to axial symmetry of CP laser pulse, electron gains more energy in comparison with LP laser pulse. This analytical work may have valuable concept of applications in remote sensing and many others field.

I have also discussed the role of linear chirp as well as axial magnetic field on acceleration scenario by employing HChG laser beam in vacuum in chapter 3. In this theoretical and analytical research, radial polarized (RP) HChG laser beam has been employed. The energy gain and maximum energy gain have been shown by varying different parameters such as: a_0 , r'_0 , b_0 , b , and α . It is clear that chirp parameter (α) dominates on other parameters. As a result, at lowest value of chirp parameter, I have noticed maximum energy gain without magnetic field. This study may minimize the cost of future accelerator and help to medical science for better radiation treatment & also reduce the expense of radiation treatment.

Chapter 4 deals with the comparative study of Sin^4 and Trapezoidal laser profile with linear chirp for efficient electron acceleration. Here we have used Sin^4 and Trapezoidal laser pulse with negative linear frequency chirp. By optimizing all parameters I have noticed GeV order energy gain. I have noticed that under the same condition electron achieved more energy gain for trapezoidal envelope than Sin^4 envelope. Since trapezoidal laser pulse possesses a special shape. It also deals with an analytical work of acceleration scenario by employing linearly polarized (LP) unchirped and chirped trapezoidal envelope in vacuum. Additionally, an external axial magnetic field has been employed to study electron acceleration. In this chapter, the maximum energy gain has been investigated by changing linear frequency chirp parameter, laser phase varying from 0 to 30π , normalized time and normalized axial magnetic field. The time period of interaction between electron and laser pulse increases due to frequency chirp and retains the maximum energy gain till resonance, while, the applied magnetic field enables the betatron resonance to attain maximum energy gain. Here I have made analytical and numerical simulation scenario by using LP \cos^2 laser pulse envelope for efficient electron acceleration in vacuum. Role of linear frequency chirp and external axial magnetic field have been studied to assure high energy gain. Electron's energy gain (γ) and maximum energy gain (γ_m) were observed by optimizing different parameters such as: phase (φ), laser intensity parameter (a_0), normalized magnetic field (b_0). Major energy gain has been noticed by employing frequency chirp. Here negative frequency chirp has been used. As frequency chirp destroys symmetry of the laser pulse, so electron transacts a number of times with laser pulse for longer duration. This is the main cause of enhancement of electron's energy. Also, an additional energy gain has been noticed when an external axial magnetic is employed with frequency chirp. This result presented in this chapter 4 may be beneficial for future research, where huge amount of energy is required for various applications such as: cancer treatment, hard x-ray generation etc.

Chapter 5 dedicates the efficient electron acceleration in a plasma ion channel. For this purpose I have employed RP HChG laser beam. It is very much needed to control the propagation of intense laser pulse and propagate several Rayleigh Length. For guiding laser

pulse over several Rayleigh Length plasma ion channel is very much effective process. Plasma ion channel not only guide and control laser beam but also stabilize some problems like FRS etc. To fulfill such purpose energy gain has been investigated by changing different parameters: a_0 , r'_0 , b , and n' . The collaboration between better trapping laser light (RP) and electrostatic field generated by ion density channel ensures longer distance and attains higher energy along longitudinal direction. It is clearly noticed that HChG laser beam is very much sensitive in ion channel. So my observation prescribed that while handling this profile, we must properly optimize the laser parameters with ion channel.

The Noble Prize in Physics 2005 was divided: one half awarded to Roy J. Glauber "for his contribution to the quantum theory of optical coherence", the other half jointly to John L. Hall and Theodor W. Hänsch "for their contributions to the development of laser-based precision spectroscopy, including the optical frequency comb technique". The Noble Prize in Physics 2013 was awarded jointly to François Englert and Peter W. Higgs "for the theoretical discovery of a mechanism that contributes to our understanding of the origin of mass of subatomic particles, and which recently was confirmed through the discovery of the predicted fundamental particle, by the ATLAS and CMS experiments at CERN's Large Hadron Collider". The 2018 Noble Prize in Physics was awarded "for groundbreaking inventions in the field of laser physics" with one half to Arthur Ashkin "for the optical tweezers and their application to biological systems", the remaining half jointly to Gérard Mourou and Donna Strickland "for their method of generating high-intensity, ultra-short optical pulses".

FUTURE SCOPE

I have focused on laser driven electron acceleration in vacuum and plasma medium by direct laser acceleration (DLA) mechanism and in plasma micro channel. We have accelerated electron by employing different conditions like: polarization, frequency chirp, laser profile, external magnetic field etc. In 2005, the Noble prize was awarded due to the discovery of laser-based precision spectroscopy, including the optical frequency comb technique". Due to lack of experimental evidence, the theory was unexplored. But in 2012,

when experiment in CERN attested the theory by experimentally, the highest award came in 2013. On the basis of CPA technique (discovered in 1985) the highest civilization award in Physics came in 2018 due to its application in Optical Tweezer. A very few percentage of our Universe has been explored. To explore our Universe, accelerator is very key equipment. Without accelerator research in basic science is impossible. So, various groups of researchers from different country have developed themselves for the modification of acceleration process so that our understanding may be cleared. So acceleration process is taking a key role and also will take key role in future research.

The high charge and short pulse behavior of accelerated electron bunches has interesting applications in the generation of coherent THz radiation due to femto second electron bunches interacting with the plasma. These THz radiations so generated further employed in various applications in non-linear THz spectroscopy, topography, material characterization, remote sensing, security identification etc. Also the femto-second X-ray pulse generation is another important application of electron acceleration. These fs X-ray pulses are produced by the betatron radiation due to the electron beam propagation in the plasma.

REFERENCES

- [1] Kitagawa Y et al. 2004 Phys. Rev. Lett., **92** 5002-5005.
- [2] Sari A H et al. 2005 Laser Part. Beams **23** 467-473.
- [3] Mangles S P D et al. 2006 Laser Part. Beams **24** 185-190.
- [4] Salamin Y I et al. 2008 Phys. Rev. Lett., **100** 1-4.
- [5] Harman Z 2011 Phys. Rev. A **84** 3814-3820.
- [6] Sprangle P 1988 AIP Conference Proceedings **175** 231-239.
- [7] Joshi C and Katsouleas T 2003 Physics Today **56** 47-53.
- [8] Salamin Y I 2010 Phys. Lett. A **3** 4950-4953.
- [9] Wong L J et al. 2017 Sci. Rep. **7** 1159-1167.
- [10] Tajima T and Dawson J 1979 Phys. Rev. **43** 267-270.
- [11] Ghotra H S and Kant N 2015 Phys. B **120** 141-147.
- [12] Ghotra H S and Kant N 2016 Phys. Plasmas **23** 053115.
- [13] Strickland D and Mourou G 1985 Opt. Commun. **56** 219- 221.
- [14] Shimoda K 1962 Appl. Opt. **1** 33.
- [15] Scully M O and Zubairy S 1991 Phys. Rev. A **44** 2656.
- [16] Hauser T et al. 1994 Phys. Lett. A **186** 189.
- [17] Sprangle P et al. 1996 Phys. Plasmas **3** 2183.
- [18] Malka G et al. 1997 Phys. Rev. Lett. **78** 3314.
- [19] Mora P and Quesnel B 1998 Phys. Rev. Lett. **80** 1351.
- [20] Bulanov S V and Prohorov A M 2006 Plasma Physics and Controlled Fusion B **48** 29.
- [21] Sinha U 2012 Phys. Plasmas **19** 043104.
- [22] Cicchitelli L et al. 1990 Phys. Rev. A **41** 3727-3732.
- [23] Wang J X 1998 Phys. Rev. E **58** 6575-6577.
- [24] Hora H 2000 Laser Part. Beams **18** 135-144.
- [25] Stupakov G V and Zolotarev M S 2001 Phys. Rev. Lett. **86** 5274-5277.
- [26] Xu J J 2005 J. Appl. Phys. **98** 6105-6108.

- [27] Rau B et al. 1997 Phys. Rev. Lett. **78** 3310-3313.
- [28] Faure J 2001 Phys. Rev. E **63** 5401-5404.
- [29] Leemans W P 2002 Phys. Rev. Lett. **89** 4802-4805.
- [30] Courant E D et al. 1985 Phys. Rev. A **32** 2813-2823.
- [31] Kimura W D et al. 2001 Phys. Rev. Lett. **86** 4041-4043.
- [32] Hora H 1988 Nature **333** 337- 338.
- [33] Esarey E et al. 1995 Phys. Rev. E Stat. Phys. Plasmas Fluids Relat. Interdiscip. Top. **52** 5443-5453.
- [34] Hartemann F V 1995 Phys. Rev. E Stat. Phys. Plasmas Fluids Relat. Interdiscip. Top. **51** 4833-4843.
- [35] Quesnel B and Mora P 1998 Phys. Rev. E Stat. Phys. Plasmas Fluids Relat. Interdiscip. Top. **58** 3719-3732.
- [36] Wang P X 2001 Appl. Phys. Lett. **78** 2253.
- [37] Salamin Y I and Keitel C H 2002 Phys. Rev. Lett. **88** 095005.
- [38] Hu S X and Starace A F 2002 Phys. Rev. Lett. **88** 245003.
- [39] Plettner T 2005 Phys. Rev. Lett. **95** 134801.
- [40] Esarey E et al. 2009 Rev. Mod. Phys. **81** 1229-1285.
- [41] C S Liu and Tripathi V K 2005 Phys. Plasmas **12** 3103- 3110.
- [42] Singh K P 2006 J. Opt. Soc. Amer. B, Opt. Phys. **23** 1650-1654.
- [43] Sepke S M and Umstadter D P 2006 Opt. Lett. **31** 2589- 2591.
- [44] Gupta D N and Ryu C M 2005 Phys. Plasmas **12** 3103 -3107.
- [45] Varin C 2013 et al. Appl. Sci. **3** 70-93.
- [46] Marceau V et al. 2012 Opt. Lett. **37** 2442-2444.
- [47] Karmakar A and Pukhov A 2007 Laser Particle Beams **25** 371-377.
- [48] Mourou G et al. 1998 Phys. Today **51** 22.
- [49] Perry M D et al. 1999 Opt. Lett. **24** 160.
- [50] Singh K P 2005 App. Phys. Lett. **87** 254102.
- [51] Khachatryan A G et al. 2004 Phys. Rev. E **70** 067601.
- [52] Singh K P and Malik H K 2008 Laser Part. Beams **26** 363.

- [53] Forslund D W et al. 1985 Phys. Rev. Lett. **54** 558-61.
- [54] Salamin Y I and Jisrawi N M 2014 J. Phys. B: At. Mol. Opt. Phys. **47** 025601.
- [55] Ghotra H S and Kant N 2016 Laser Phys. Lett. **13** 5402-5408.
- [56] Singh R et al. 2019 Atomic, Molecular, Condensate & Nano Phys. **6** 81-91.
- [57] Kant N et al. 2018 High En. Den. Phys. **26** 16-22.
- [58] Lindl J D 1998 AIP-Press.
- [59] Borghesi M 2001 Plasma Phys. Control. Fusion **43** A267.
- [60] Roth M 2001 Phys. Rev. Lett. **86** 436.
- [61] Esarey E et al. 1996 IEEE Trans. Plasma Sci. **24** 252.
- [62] Milchberg H M et al. 1995 Phys. Rev. Lett. **75** 2494.
- [63] Tabak M et al. 1994 Phys. Plasmas **1** 1626.
- [64] Eder D C et al. 1994 Phys. Plasmas **1** 1744.
- [65] Spence N et al. 2001 Phys. Plasmas **8** 4995.
- [66] Sheng Z M et al. 2005 Phys. Rev. Lett. **94** 095003.
- [67] Adak A et al. 2015 Phys. Rev. Lett. **114** 115001.
- [68] Jha P et al. 2011 Euro Phys. Lett. **94** 15001.
- [69] Gorbunov L and Kirsanov V 1987 Sov. Phys. JETP **66** 290-294.
- [70] Hamster H et al. 1993 Phys. Rev. Lett. **71** 2725-2728.
- [71] Rosenbluth M N and Liu C S 1972 Phys. Rev. Lett. **29** 701-705.
- [72] Mourou G and Umstadter D 1992 Physics of Fluids B: Plasma Physics **4** 2315-2325.
- [73] Perry M D and Mourou G 1994 Science **264** 917-924.
- [74] Joshi C 2007 Physics of Plasmas **14** 055501.
- [75] Clayton C E et al. 1985 Phys. Rev. Lett. **54** 2343-2346.
- [76] Clayton C E et al. 1993 Phys. Rev. Lett. **70** 37-40.
- [77] Amiranoff F et al. 1998 Phys. Rev. Lett. **81** 995-998.
- [78] Joshi C et al. 1981 Phys. Rev. Lett. **47** 1285-1288.
- [79] Sprangle P et al. 1992 Phys. Rev. Lett. **69** 2200-2203.
- [80] Nakajima K et al. 1995 Phys. Rev. Lett. **74** 4428-4431.

- [81] Esarey E et al. 2009 Rev. Mod. Phys. **81** 1229-1285.
- [82] Krall J et al. 1993 Phys. Rev. E **48** 2157-2161.
- [83] Coverdale C A et al. 1995 Phys. Rev. Lett. **74** 4659-4662.
- [84] Modena A et al. 1995 Nature **377** 606.
- [85] Mangles S P et al. 2004 Nature **431** 535.
- [86] Geddes C et al. 2004 Nature **431** 538.
- [87] Faure J et al. 2006 Nature **444** 737.
- [88] Clayton C E et al. 2007 Nature **445** 741.
- [89] Mizuta Y et al. 2012 Phys. Rev. ST Accel. Beams **15** 121301.
- [90] Wachulak P W et al. 2014 Phys. Plasmas **21** 103106.
- [91] Wachulak P W et al. 2015 Laser and Part. Beams **33** 293.
- [92] Durfee C G and Milchberg H M 1993 Phys. Rev. Lett. **71** 2409.
- [93] Kneip S et al. 2008 Phys. Rev. Lett. **100** 105006.
- [94] Kneip S at 2009 Proc. SPIE **7359** 73590.
- [95] Gahn C et al. 2002 Phys. Plasmas **9** 987.
- [96] Walton B R et al. 2006 Phys. Plasmas **13** 113103.
- [97] Pukhov A et al. 1999 Phys. Plasmas **6** 2847.
- [98] Arefiev A V et al. 2012 Phys. Rev. Lett. **108** 145004.
- [99] Robinson A P L et al. 2013 Phys. Rev. Lett. **111** 065002.
- [100] Naseri N et al. 2012 Phys. Rev. Lett. **108** 105001.
- [101] Esarey E et al. 1997 IEEE J. Quan. Electr. **33** 1879-1914.
- [102] Upadhyay A K et al. 2009 Plasma Phys. Contr. Fusion **51** 105011.
- [103] Kaur M and Gupta D N 2017 IEEE Trans. Plasma. Sci. **45** 2841.
- [104] Singh J et al. 2022 Commun. Theor. Phys. **73** 095502.
- [105] Mora P and Thomas M. Antonsen Jr. 1996 Phys. Rev. E., **53** 2068.
- [106] Chen L M et al. 2013 Scientific Reports **3** 1912.
- [107] Kneip S et al. 2011 Nat. Phys. **7** 867.
- [108] Cipiccia S et al. 2011 Nat. Phys. **7** 867.
- [109] Corde et al. 2013 Rev. Mod. Phys. **85** 1.

- [110] Huang T W et al. 2016 Phys. Rev. E. **93** 063203.
- [111] Gahn C et al. 1999 Phys. Rev. Lett. **83** 4772.
- [112] Mangles S P D et al. 2005 Phys. Rev. Lett. **94** 245001.
- [113] Bussolino G et al. 2013 J. Phys. D: Appl. Phys. **46** 245501.
- [114] Fukuda Y et al. 2007 Physics Letters A **363** 130.
- [115] Piazza A Di et al. 2012 Rev. Mod. Phys. **84** 1177.
- [116] Hu R et al. 2015 Sci. Rep. **5** 15499.
- [117] Woodward P M 1946 J. Inst. Electr. Eng. Part IIIA **93** 1554.
- [118] Ghotra H S and Kant N 2016 Phys. Plasmas **23** 013101.
- [119] Ghotra H S and Kant N 2016 Opt. Commun. **365** 231.
- [120] Kant N et al. 2020 Eur.Phys. J.D **74** 142.
- [121] Singh A et al. 2017 Laser Phys. **27** 110001.
- [122] Rajput J et al. 2017 AIP Conference Proceeding **1860** 020005.
- [123] Salamin Y I and Carbajo S 2019 Front. Phys. **7** 2.
- [124] Salamin Y I 2012 Phys. Lett. A **376** 2442-2445.
- [125] Jokar F and Eslami E 2012 Optik. **123** 1947-1951.
- [126] Hora H et al. 1999 Laser Part. Beams **18** 135-144.
- [127] Singh J et al. 2020 J. Phys. **1531** 2027-2030.
- [128] Kuri D K 2020 Phys. Plasmas **27** 3102-3107.
- [129] Tovar A A and Casperson L W 1998 J. Opt. Am. A **15** 2425.
- [130] Casperson L W and Tovar A A 1998 J. Opt. Am. A **15** 954.
- [131] Ghotra H S et al. 2018 Laser Part. Beams **36** 154.
- [132] Zhang X P et al. 2008 Opt. Commun. **281** 4103.
- [133] Zhao Z and Lu B 2008 Opt. Quantum Electron **40** 615.
- [134] Gill T S et al. 2011 Phys. Plasmas **18** 3110.
- [135] Patil S D et al. 2012 Opt. Laser Technol. **44** 314.
- [136] Nanda V et al. 2018 Optik **156** 191.
- [137] Thakur V and Kant N 2019 Optik **183** 912.
- [138] Caperson L W et al. 1997 J. Opt. Soc. Am. A **14** 3341.

- [139] Ghotra H S and Kant N 2016 Laser Part. Beams **34** 385.
- [140] Varghese B et al. 2013 Opt. Exp. **21** 18304.
- [141] Sprangle P et al. 2000 Phys. Rev. Lett. **85** 5110-5113.
- [142] Geddes C G R et al. 2004 Nature **737** 521-527.
- [143] Rajput J and Kant N 2021 Optik **225** 5836.
- [144] Nuter R et al. 2020 Phys. Rev. E **101** 3202-3211.
- [145] Carbajo S et al. 2016 Phys. Rev. Accel. Beams **19** 1303-1309.
- [146] Zhao Z et al. 2008 Journal of the Optical Society of America B **25** 434-442.
- [147] Sun Y et al. 2019 Physical Review Letters **123** 3901-3906.
- [148] Kant N and Wani M A 2012 Optics Communications **285** 4483-4487.
- [149] Nanda V and Kant N 2014 Physics Plasmas **21** 2101-2106.
- [150] Erikson W L and Singh S 1994 Phys. Rev. E **49** 5778-5785.
- [151] Omer F S et al. 2020 Opt. Communications **458** 4735-4739.
- [152] Faure J 2004 Nature **431** 541-544.
- [153] Liu H et al. 2005 Appl. Phys. B, Lasers Opt. **82** 93-97.
- [154] Palmer R B 1988 Frontiers of Particle Beams **296** 607-635.
- [155] Gupta D N et al. 2020 Phys. Plasmas **27** 3105-3113.
- [156] Ghotra H S and Kant N 2015 Opt. Rev. **22** 539-543.
- [157] Gupta D N et al. 2019 Laser Phys. **29** 5301-5305.
- [158] Hashemian S H and Akou H 2019 Optik **163** 708-715.
- [159] Pramanik A K et al. 2021 IOP Conference Proceedings RAFAS **2267** 012013.
- [160] Pramanik A K et al. 2022 Laser Phys. Lett. **19** 075301.
- [161] Sohbatzadeh F and Aku H 2011 J Plasma Phys. **77** 3950.
- [162] Jisrawi N M et al. 2008 Laser and Particle Beams **32** 671.
- [163] Malka V et al. 2008 Nature Phys. **4** 447.
- [164] Leemans W and Esarey E 2009 Phys. Today **62** 44 .
- [165] Pukhov A and Meyer-ter-Vehn J 2002 Appl. Phys. B, Lasers Opt. **74** 355.
- [166] Ehrlich Y et al. 1996 Phys. Rev. Lett. **77** 4186.
- [167] Sprangle P et al. 2000 Phys. Rev. E **61** 4381-4393.

- [168] Hafizi B et al. 2003 Phys. Plasmas **10** 1483-1492.
- [169] Kameshima T et al. 2009 Phys. Plasmas **16** 093101.
- [170] Hosokai T et al. 2010 Appl. Phys. Lett. **96** 121501.
- [171] Clark T R and Milchberg H M 2000 Phys. Rev. E **61** 1954.
- [172] Krushelnick K et al. 1997 Phys. Rev. Lett. **78** 4047.
- [173] Giulietti A et al. 2006 Phys. Plasmas **13** 093103.
- [174] Belafhal A and Ibnchaikh M 2000 Optics Communications **186** 269.
- [175] Patil S et al. 2008 J. Mod. Opt. **55** 3529.
- [176] Patil S D et al. 2010 Laser Particle Beams **28** 343.
- [177] Gupta D N 2017 IEEE Trans. Plasma Sci. **45** 2841.
- [178] Ghotra H S 2022 Laser Phys. Lett. **19** 096002.
- [179] Tripathi V K et al. 2005 Phys. Plasmas **12** 043106.

PUBLICATIONS

- [1] Comparison of different laser pulse envelopes with frequency chirp for efficient electron acceleration in vacuum, A K Pramanik , H S Ghotra , N Kant and J Rajput, RAFAS-2021, *Journal of Physics: Conference Series* 2267 012013, 2022, [doi:10.1088/1742-6596/2267/1/01201](https://doi.org/10.1088/1742-6596/2267/1/01201)
- [2] GeV electron acceleration by Trapezoidal laser pulse envelope under combined effect of frequency chirp and axial magnetic field in vacuum, A K Pramanik, N Kant, J. Rajput, *IEEE Trans. On Plasma Science*, 50 3303, 2022, [doi:10.1109/TPS.2022.3195745](https://doi.org/10.1109/TPS.2022.3195745)
- [3] Efficient electron acceleration by using Hermite-Cosh-Gaussian laser beam in vacuum, A K Pramanik, H S Ghotra, N Kant, and J Rajput, *Laser Phys. Lett.*, **19** 075301 2022, [doi: 10.1088/1612-202X/ac7132](https://doi.org/10.1088/1612-202X/ac7132)
- [4] Comparative study of electron acceleration by linearly and circularly polarized Hermite-Cosh-Gaussian laser pulse in vacuum, J Rajput, A K Pramanik, P Kumar, S S Gaur, R Singh, N Kant, *Journal of Optics*, **52** 642-647 2022, <https://doi.org/10.1007/s12596-022-01000-0>
- [5] Efficient Electron Acceleration by Radially Polarized Hermite-Cosh-Gaussian Laser Beam in an Ion Channel , A K Pramanik, H S Ghotra, and J Rajput, *The European Physical Journal D*, **77** 161, 2023, <https://doi.org/10.1140/epjd/s10053-023-00740-3>

COMMUNICATIONS

- [1] Combined influence of linear chirp and axial magnetic field for enhance electron acceleration due to Hermite-Cosh-Gaussian laser beam in vacuum (A K Pramanik, H S Ghotra, and J Rajput)
- [2] Influence of frequency chirp and axial magnetic field on electron acceleration by employing Cos^2 laser pulse envelope in vacuum (A K Pramanik and J Rajput) (Accepted in Journal of Applied Spectroscopy)
- [3] Ion channel assisted electron acceleration due to a radially polarized Hermite-Cosh-Gaussian laser beam (A K Pramanik and J Rajput) (Successfully presented this paper in the conference RAFAS 2023 organized by Lovely Professional University, Phagwara, Punjab).

LIST OF PUBLISHED WORK

4/10/23, 6:08 PM

Comparison of different laser pulse envelopes with frequency chirp for efficient electron acceleration in vacuum - IOPscience

IOPscience

PAPER • OPEN ACCESS

Comparison of different laser pulse envelopes with frequency chirp for efficient electron acceleration in vacuum

A K Pramanik¹, H S Ghotra², N Kant¹ and J Rajput¹

Published under licence by IOP Publishing Ltd

Journal of Physics: Conference Series, Volume 2267, 3rd International Conference on Recent Advances in Fundamental and Applied Sciences (RAFAS 2021) 24/06/2021 - 26/06/2021 Online

Citation A K Pramanik *et al* 2022 *J. Phys.: Conf. Ser.* **2267** 012013


DOI 10.1088/1742-6596/2267/1/012013

[jyoti_physics@yahoo.co.in](mailto: jyoti_physics@yahoo.co.in)

¹ Department of Physics, Lovely Professional University, G.T Road, Phagwara 144411, Punjab, India

² Extreme Light Infrastructure - Nuclear Physics (ELI-NP), "Horia Hulubei" National Institute for Physics and Nuclear Engineering, 30 Reactorului Street, RO-077125 Magurele, Jud. Ilfov, Romania

Buy this article in print

 Journal RSS

[Sign up for new issue notifications](#)

[Create citation alert](#)

[PDF](#)

[Help](#)

Abstract

In the present manuscript, we have investigated the effect of chirped laser pulse envelope to study electron acceleration in vacuum. For this purpose, we have chosen two different pulse shapes, i.e trapezoidal pulse envelope and Sin4 pulse envelope. Electron has been injected axially to the front of the tested envelopes. In all calculations, the front end of each pulse is presumed to have caught up with the electron at $t = 0$ at the coordinate origin. The relativistic Newton-Lorentz equations of motion of electron in the field of the laser pulse have been analytically and numerically solved. By optimizing laser and frequency chirp parameters, the energy gain of the order of GeV is obtained, and it has been

<https://iopscience.iop.org/article/10.1088/1742-6596/2267/1/012013/meta>

1/3

Ashok Kumar Pramanik



All



ADVANCED SEARCH

Journals & Magazines > IEEE Transactions on Plasma S... > Volume: 50 Issue: 9

GeV Electron Acceleration by Trapezoidal Laser Pulse Envelope Under Combined Effect of Frequency Chirp and Axial Magnetic Field in Vacuum

Publisher: IEEE [Cite This](#) [PDF](#)

Ashok Kumar Pramanik ; Niti Kant ; Jyoti Rajput All Authors

57 Full Text Views



Alerts

Manage Content Alerts Add to Citation Alerts

Abstract



Document Sections

- I. Introduction
- II. Electron Dynamics
- III. Results and Discussion
- IV. Conclusion

Abstract:In the present article, we have investigated efficient electron acceleration by employing trapezoidal laser pulse envelope under the combined effect of linear chirp and e... [View more](#)

► Metadata

Abstract: In the present article, we have investigated efficient electron acceleration by employing trapezoidal laser pulse envelope under the combined effect of linear chirp and external axial magnetic field in vacuum. In this envelope, the electric signal linearly rises to a certain level, stay there, and then falls back to its initial level. So, there will be an opportunity to increase the interaction time between laser pulse and electron for efficient energy transfer, which has been reflected in this study. A few megaelectronvolt electrons have been injected axially to the front of a trapezoidal short laser pulse. In all calculations, the front end of each laser pulse captures electron at $t = 0$. The dynamics arise from analytical and numerical solutions of Newton-Lorentz force equations of motion. Electron energy gain has been calculated for initial laser phase varying from 0 to 2π . For the optimum set of laser parameters, we have observed electro's energy gain of the order of GeV.

Published in: IEEE Transactions on Plasma Science (Volume: 50 , Issue: 9, September 2022)

Page(s): 3303 - 3307

INSPEC Accession Number: 22135888

Date of Publication: 17 August 2022

DOI: 10.1109/TPS.2022.3195745

Ashok Kumar Pramanik

LETTER

Efficient electron acceleration by using Hermite-cosh-Gaussian laser beam in vacuum

Ashok Kumar Pramanik¹, Harjit Singh Ghotra^{1,2}, Niti Kant¹ and Jyoti Rajput^{3,1}

Published 27 May 2022 • © 2022 Astro Ltd

Laser Physics Letters, Volume 19, Number 7

Citation Ashok Kumar Pramanik *et al* 2022 *Laser Phys. Lett.* **19** 075301

DOI 10.1088/1612-202X/ac7132

jyoti_physics@yahoo.co.in

¹ Department of Physics, Lovely Professional University, G.T. Road, Phagwara 144411, Punjab, India

² Central Instrumentation Facility (CIF), Division of Research and Development (DRD), Lovely Professional University, G.T. Road, Phagwara 144411, Punjab, India

³ Author to whom any correspondence should be addressed.

1. Received 10 February 2022
2. Accepted 13 May 2022
3. Published 27 May 2022



Buy this article in print

Journal RSS

Sign up for new issue notifications

Create citation alert

Abstract

The electron acceleration in vacuum has been studied theoretically using a radially polarized (RP) Hermite-cosh-Gaussian (HChG) laser beam. Even if the laser's power is low, the RP HChG laser beam

This site uses cookies. By continuing to use this site you agree to our use of cookies. To find out more, see our Privacy and Cookies policy.

Ashok Kumar Pramanik

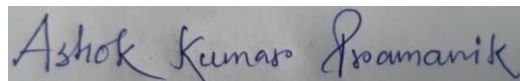
[Home](#) > [Journal of Optics](#) > ArticleResearch Article | [Published: 08 November 2022](#)

Comparative study of electron acceleration by linearly and circularly polarized Hermite-cosh-Gaussian laser pulse in a vacuum

[Jyoti Rajput](#), [Ashok Kumar Pramanik](#), [Prמוד Kumar](#), [Shiv Shankar Gaur](#), [Ravindra Singh](#) & [Niti Kant](#) [Journal of Optics](#) (2022)74 Accesses | [Metrics](#)

Abstract

Comparative study of electron acceleration by linearly polarized (LP) and circularly polarized (CP) Hermite-cosh-Gaussian lasers in vacuum has been analyzed. Hermite-cosh-Gaussian profile is a special kind of Gaussian profile whose decentered parameter (b) plays a crucial role in the electron acceleration. It has been observed that the electron energy enhancement for CP laser pulse is much higher as compared to LP laser pulse for optimized values of laser parameters like laser intensity parameter (a_0), laser spot size (r_0), etc. It is seen from the results that maximum electron energy gain increases rapidly with the increase in the value of decentered parameter for



Efficient electron acceleration by X +

link.springer.com/article/10.1140/epjd/s10053-023-00740-3

Home > The European Physical Journal D > Article

Regular Article – Ultraintense and Ultrashort Laser Fields | Published: 22 August 2023

Efficient electron acceleration by radially polarized Hermite-Cosh-Gaussian laser beam in an ion channel

Ashok Kumar Pramanik, Harjit Singh Ghotra & Jyoti Rajput

The European Physical Journal D 77, Article number: 161 (2023) | Cite this article

55 Accesses | Metrics

Abstract

Radially polarized (RP) Hermite-Cosh-Gaussian (HChG) laser beam has been employed to study electron acceleration in an ion channel. As RP-HChG laser beam focus earlier, depending on this property electron acquires high order energy over short periods of time. The ion channel generates an electric field that prevents electrons from escaping from the interaction zone and maintains betatron resonance. Electron's energy gain has been analyzed by varying different parameters like: intensity parameter (a_0), laser spot size (r_0), decentered parameter (b), ion density (n_1). The combined effect of RP-HChG laser beam and ion channel

Access via your institution

Access options

Buy article PDF

39,95 €

Price includes VAT (India)

Instant access to the full article PDF.

Rent this article via DeepDyve.

Learn more about Institutional subscriptions

Type here to search

6:28 PM 9/15/2023

Ashok Kumar Pramanik

CONFERENCE CERTIFICATES

Certificate No. 225271



LOVELY
PROFESSIONAL
UNIVERSITY
Transforming Education Transforming India



Certificate of Participation

This is to certify that Mr. Ashok Kumar Pramanik
of Lovely Professional University Phagwara Punjab
has given oral presentation on Comparison of different laser pulse envelope for efficient electron acceleration in vacuum
in the International Conference on "Recent Advances in Fundamental and Applied Sciences" (RAFAS 2021) held on June 25-26, 2021, organized by School of Chemical Engineering and Physical Sciences, Lovely Faculty of Technology and Sciences, Lovely Professional University, Punjab.

Date of Issue : 15-07-2021
Place of Issue: Phagwara (India)



Prepared by
(Administrative Officer-Records)

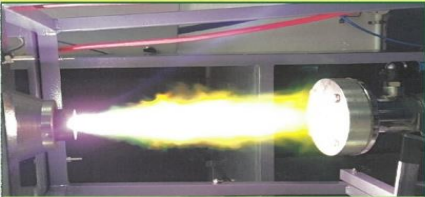



Organizing Secretary
(RAFAS 2021)





Convener
(RAFAS 2021)

**SECOND INTERNATIONAL CONFERENCE ON
ADVANCES IN
PLASMA SCIENCE
AND TECHNOLOGY
(ICAPST-21)**






SRI SHAKTHI
INSTITUTE OF ENGINEERING AND TECHNOLOGY
Approved by AICTE, New Delhi • Affiliated to Anna University, Chennai
Accredited by NAAC with 'A' Grade




This is to certify that

A.k. Pramanik, Lovely Professional Univ
has participated / presented the paper titled
Efficient electron acceleration in vacuum
by using trapezoidal laser pulse envelope
in the
SECOND INTERNATIONAL CONFERENCE ON ADVANCES IN PLASMA SCIENCE AND TECHNOLOGY (ICAPST-21)
conducted during 27-29 May 2021



Convener



Principal

"Sri Shakthi Nagar", L&T By-Pass, Coimbatore - 641 062. Web : www.siet.ac.in
Ph : 0422 - 2369900 E-mail : principal@siet.ac.in

Ashok Kumar Pramanik



LOVELY
PROFESSIONAL
UNIVERSITY

Transforming Education Transforming India



Certificate No. 263615

Certificate of Participation

This is to certify that **Dr./Mr./Ms. Ashok Kumar Pramanik** of **Lovely Professional University** has given oral presentation on **Ion Channel Assisted Electron Acceleration Due To A Radially Polarized Hermite-Cosh-Gaussian Laser Beam** in the 4th International Conference on “Recent Advances in Fundamental and Applied Sciences” (RAFAS 2023) held on March 24-25, 2023, organized by School of Chemical Engineering and Physical Sciences, Lovely Faculty of Technology and Sciences, Lovely Professional University, Punjab.

Date of Issue: 12-04-2023
Place: Phawara (Punjab), India

Prepared by
(Administrative Officer-Records)

Organizing Secretary
(RAFAS 2023)

Convener
(RAFAS 2023)

Ashok Kumar Pramanik

BIO-DATA

MR. ASHOK KUMAR PRAMANIK

M.Sc. Physics, B.Ed.

akphmp@gmail.com, 79ashok32@gmail.com



6294049126, 9434990537

Ashok Kumar Pramanik was born in West Bengal, India in 1979. He has received B.Sc. HONS. Degree in Physics in 1999 from Vidyasagar University, India. He has also received the master's degree in Physics from CSJMU, Kanpur, India in 2002.

In 2004, he joined in a Government-Sponsored Higher Secondary School as a Physics Teacher and he is working till now. Presently, he has concentrated in theoretical research work in the field of "Laser driven electron acceleration in vacuum and plasma" under the guidance of Dr. Jyoti Rajput, Associate Professor, LPU, Punjab, India.

PERSONAL DETAIL:

Date of Birth: 7th day of October 1979

Parents : Mr. Madhusudan Pramanik

: Smt. Prativa Pramanik

Language Known: Bengali, Hindi, English

Google Scholar: A K Pramanik (Author)

ORCID ids: <https://orcid.org/0009-0009-6393-2095>

ResearchGate: akphmp@gmail.com

EDUCATIONAL QUALIFICATION: B.Sc. HONS. in PHYSICS [1999]

M.Sc. in PHYSICS [2002]

B.Ed. [2008]

Technical Skills: Windows, Excel, Power Point

Software: MATHEMATICA, ORIGIN

PROFESSION: Ashok Kumar Pramanik is an Assistant Teacher of a GOVT. SPONSORED Intermediate School in PGT Scale in West Bengal since 2004. He has 19⁺ years teaching experience.

RESEARCH INTEREST: ELECTRON ACCELERATION IN VACUUM & PLASMA MEDIUM.